FACOLTÀ DI INGEGNERIA CIVILE ED INDUSTRIALE

DIPARTIMENTO INGEGNERIA CHIMICA, MATERIALI ED AMBIENTE

DOTTORATO DI RICERCA IN INGEGNERIA CHIMICA E DEI PROCESSI

XXVII CICLO

INNOVATIVE MATERIALS FOR HEAVY METALS AND HYDROCARBONS REMOVAL FROM WASTEWATER OF OIL INDUSTRY

TUTOR:

PROF. MARCO PETRANGELI PAPINI

CANDIDATO:

DOTT. MORENO MARETTO

BACKGROUND AND AIM OF THESIS 8
CHAPTER 1 12
WATER AND PETROCHEMICAL ACTIVITIES 12
1.1 Extraction water 12
1.2 Process water 14
1.3 Production water characteristics 15
1.4 Management of produced water 17
1.5 Remediation technologies of produced water 18
1.5.1 Physical-chemical treatment 18
1.5.2 Adsorption of dissolved organics 19
1.5.3 Membrane filtration 22
1.5.4 Gravity separation 24
1.5.5 Retention ponds/Storage pits 24
1.5.6 API separator 24
1.5.7 Skimmer tanks and vessels 26
1.5.8 Plate coalescence 26
1.5.9 Enhanced coalescence 28
1.5.10 Mare's Tail 28
1.5.11 Enhanced gravity separation 29
1.5.12 Hydrocyclones 30
1.5.13 Centrifuges 31
1.5.14 C-tour process 32
1.6 Chemical treatment 34
1.6.1. Chemical precipitation 34
1.6.2. Chemical oxidation 35
1.6.3 Electrochemical process 35
1.6.4 Photocatalytic treatment 36

1.6.5. Fenton process 37
1.6.6. Treatment with ozone 38
1.7 Biological treatment 38
1.8 References 43
Chapter 2 50
THE ADSORPTION PROCESS 50
2.1 Thermodynamic point of view 52
2.2 Relevant adsorption model 55
2.3 Kinetic point of view 59
2.5 References 63
CHAPTER 3 65
ZEOLITE AND RELATED MATERIALS 65
3.1 Activated carbon 66
3.2 Alumina 69
3.3 Silica gel 70
3.4 Polymeric resin 72
3.4.1 Purolite® S910 resin 74
3.5 Zeolite 78
3.5.1 Structure and composition 79
3.5.2. Clinoptilolite 82
3.6 Mesoporous material 86
3.6.1 MCM-41 88
3.6.2. MSA 91
3.6.3 Zeolite Y 93
3.6.4 SBA-15 94
3.7 References 97
CHAPTER 4 104
NEW MATERIAL FOR HEAVY METALS REMOVAL: BATCH TESTS 104

4.1 Materials 104
4.2 Methods 105
4.3 Data evaluation 106
4.3.1 Kinetic and thermodynamic models 106
4.4 Results and discussion 109
4.4.1 Adsorption kinetics: heavy metals 109
4.4.2 Heavy metal adsorption isotherms: clinoptilolite and Purolite® S910 Resin 112
4.4.3 Effect of ionic strength 115
4.4.4 Effect of co-contamination: organic compounds 118
4.4.5 Heavy metal adsorption isotherms: MSA 122
4.5 Conclusion 123
4.6 References 125
CHAPTER 5 135
NEW MATERIAL FOR AROMATIC HYDROCARBONS REMOVAL: BATCH TESTS 135
5.1 Materials and methods 136
5.2 Data evaluation: Kinetic and thermodynamic models 138
5.3 Results and discussion 141
5.3.1 Pore distribution study 141
5.3.2 Kinetic study 145
5.3.3 Isotherm study 152
5.3.4 Regeneration study 161
5.4 Conclusion 164
5.5 References 166
CHAPTER 6 169
NEW MATERIAL FOR HYDROCARBONS AND HEAVY METALS REMOVAL: 169
STRUCTURAL CHARACTERIZATION. 169
6.1 Experimental section 170
6.1.1 Materials 170

6.1.2 Adsorption tests....171
6.1.3 SEM....172
6.1.4 XRD....172
6.1.5 FTIR....173
6.1.6 Acidity Measurement....173
6.1.7 TGA....174
6.2 Result and discussion....174
6.2.1 SEM....174
6.2.2 XRD....178
6.2.3 FT-IR....185
6.2.4 TGA....191
6.3 Conclusions....195
6.4 References....197
CHAPTER 7....199
CONCLUSIONS AND FINAL EVALUATIONS....199

BACKGROUND AND AIM OF THESIS

Recovery of waste water is one of the most important challenges for our future due to the endemic scarcity of this resource in many parts of the world. Wastewaters derived from petrochemical activities represent a large share of water linked to human activities. This is due to the centrality of oil for global economy and the great water consumption for all the linked activities that goes from extraction to refinery. In the last decays the sensibility towards this topic arose due to the great world population growth that requires more and more water for drinking usage, agricultural and industrial purposes. From this point of view the sustainability of all those process that involved water consumption has to be guaranteed. Oil extraction and refining is one of those processes that involves huge amount of water that has to be recovered. Dispersed and dissolved hydrocarbons (at high concentration), presence of heavy metals and inorganic ions make very difficult the recovery of oilfield water. Oil wastewater can be divided into two categories: production water linked to phase of oil extraction and process water linked to the refinery's operations.

During the oil extraction phase, a large amount of waste water is produced. It is naturally present in the deposit rock and extracted with the oil, forming an emulsion. This wastewater is very rich in insoluble and soluble hydrocarbons such as short chain ketones, aldehydes and/or phenols. It is also characterized by high salinity and by the presence of heavy metal ions such as Pb^{2+}, Cd^{2+}, Ni^{2+}, $Cr_2O_7^{2-}$ and VO_3^{+}, typical of the geochemistry of the deposit rock and of the chemical composition of the ancestral organic matter. Several primary treatments, including oil separation, coagulation,

flocculation, flotation and filtration have been successfully used to remove oil and suspended solids from produced water. Biological treatments, also known as secondary treatments, should also be considered when these effluents are discharged into natural receiving bodies. For instance, approximately 145 million cubic meters of water were utilized in 2005 in the Canadian state of Alberta for the extraction of oil from oil shale, and in the USA refining operations use approximately 16 million liters of water per year. Concerning this data, it is needful to reuse this waste water at least for the same activities. In addition to the extraction water, another large amount of water is used during the refining activities, the so called process water. This water might be rich in hydrocarbons if it is used in a steam reforming unit or distillation tower, or rich in inorganic and heavy metal ions if it is used in a desalting unit.

The presence of the refineries is linked to the contamination of the groundwater by heavy and light hydrocarbons and sometimes heavy metals. In addition to this, the oil refineries are in many cases located along the coasts, and high salinity of seawater may represent a further problem in the remediation of the contaminated groundwater. Currently the large use of hydrofracking technology is spreading, especially in the USA. This kind of technology is based on the fracturing of the deposit rock to release and collect gas and oil; this is easier than by the traditional methods. Fracking cannot be classified as a "green" process and usually causes the contamination of the groundwater adjacent to the deposit rocks. The use of adsorption technologies to recover waste water for all the petrochemical activities is a very useful technology, especially by using active carbon as the adsorbent material. Active carbon is the traditional adsorbent used for water remediation and can be produced from several vegetable sources, such as coconut shells or cellulosic waste, or more traditional sources, such as carbon and wood. However, its usage has important disadvantages in terms of selectivity and regeneration.

The first is a consequence of the aqueous medium in which active carbon has to operate. Water molecules are strong competitors for the active sites of the active carbon, such as the alcoholic and carboxylic ones, and water has the particular ability to drench the carbon pore, preventing the adsorption of contaminants. Regarding selectivity, major problems might be encountered in the remediation of groundwater which can be relatively rich with humic substances. These substances are formidable interfering agents because they are able to interact strongly with the adsorption sites of the activated carbon. Regeneration problems may take place, especially in cases where very high regeneration temperatures are used. In these cases, the high temperature might promote sintering of the material, condensation of the active sites, collapse of the internal structure and consequently a decreasing of the subsurface area with loss of material by burning. Furthermore, if carbon is used with high salinity water, this kind of regeneration does not guarantee the elimination of the adsorbed inorganic ions. To overcome these disadvantages, in the last decades different materials have been developed such as synthetic zeolite, mesoporous materials and the newest MOFs. In particular, the zeolite materials are more stable at high temperature and more selective; moreover, they can be modified with specific ligands to increase selectivity and stability. A process for treatment of wastewater contaminated by organic compounds by adsorption on hydrophobic (siliceous) zeolites has been recently reported. Quite good results have been described in case of dissolved hydrocarbons, while reduced effectiveness has been noticed in presence of oil droplets due to pore clogging. In particular, the mesoporous materials seem to be very effective for hydrocarbon removal both in emulsion and in solution. Their large pore size is more suitable to host large organic molecules, allowing the functionalization of the material with a wide variety of

hindered ligands and improving their chemical and physical stability as well as adsorption performances.

From this point of view adsorption technologies providing zeolite materials, both microporous and mesoporous, present a good choice for water remediation due to their simplicity, effectiveness, long term stability and adaptability.

The development of new materials for adsorption technology is the main goal of this thesis. In particular some microporous materials for heavy metals uptake and several mesoporous material for hydrocarbons confinement have been characterized from structural and process point of view. Kinetic and thermodynamic (adsorption isotherms) behaviour of all material with different organic and inorganic pollutants is deeply investigated. Mathematical models to describe adsorption kinetics and isotherms have also been developed in order to obtain important parameter useful for the transaction from bench-scale to the next pilot scale. Structural characterization has been carried out to understand which changes occurred in material structure after adsorption of contaminants, the host-guest interactions and thermal stability of materials. This double characterization work was planned to screen a set of known materials and compare their performances to those of a new mesoporous amorphous material: the mesoporous silica-alumina or MSA. Indeed, the ultimate aim is to use MSA as multitalented material for simultaneous removal of heavy metals and hydrocarbons from wastewater derived from oil extraction, oil refining or oil contamination.

CHAPTER 1

WATER AND PETROCHEMICAL ACTIVITIES

This chapter describes the relationship between water and petrochemical activities, from the extraction phase until the refining of gas and oil. The production water involved in the petrochemical activities can be divided into production water and process water and it represents the largest byproduct of oil production. Because of the importance of water resources on a global scale, water recovery represents nowadays a challenge for future generations.

1.1 Extraction water

The extraction water is the wastewater produced during the extraction of oil from reservoirs. The most is naturally present in the oilfield and its composition is strictly linked to the geological composition of the rocks (also called formation water) (Sauer et al., 1997). Usually, in the underground reservoirs light hydrocarbons are stratified upon the water level and the heavy hydrocarbons are on the bottom, in a way that a mixture of oil and water is present at equilibrium (Viel et al., 2004). The composition of this mixture is function of the inherent solubility of hydrocarbons but a small amount of hydrocarbons is also dispersed in the water as stable oil droplets. Moreover the extraction water has a saline content greater than seawater and a large content of heavy metals, typical of the rock geological composition. Instead, very volatile hydrocarbons form the gas phase in which water vapor could be present. During the extraction phase

this vapor can condensate in the pipelines forming a secondary kind of extraction water richer in soluble and volatile hydrocarbons (Ray and Engelhardt, 1992).

The use of water is also increasing exponentially in the recovery of oil from oil sands. Nowadays the relative high cost of crude oil deriving from traditional reservoir makes economically competitive the extraction from sands, even if this latter technique costs a large consumption of water used to extract oil in soil flushing process. The oil extraction from sands is widely used in the Canadian state of Alberta, in which the greater oil sand reservoirs of the world have been estimated (www.api.org). In the neighboring United states of America the largely used technology is the hydrofracking (www.eia.gov). This kind of technology is based on the fracturing of the deposit rock to release and collect gas and oil; this is easier than the traditional technologies but it is not a friendly environmental process because it causes the contamination of the groundwater adjacent to the deposit rocks (EPA report). Rocks are fractured by using pressurized water, often modified by adding chemicals agent to facilitate the rock cracking and the oil lift. Some of these chemicals are very toxic and it is necessary to remove them using specific treatments. In this category of water we can also consider the water used for maintaining the adequate pressure in the wells to facilitate the oil lift. The volume of water used to hold the pressure at high level increases at end of the well life (Stephenson, 1992).

1.2 Process water

The process water derives from all the processes that take place to transform the crude oil into refined products, such as fuels, fine chemicals or plastics. In this case the chemical composition of water depends on the specific process in which it is involved.

The most large use of water during the transformation of crude oil into fuel or other chemicals is due to the refinery operations (table 1.1). At first, the distillation of crude oil into different fractions requires a lot of water at the top of the distillation column to cool down the outgoing fluids. In addition, water is also required at the bottom of the column to heat at the same time the outgoing fluids. The largest amount of water is spent in this operations and it proportionally increases with the plant dimensions. Water, as cooling or heating fluids, is also used in other operations such as cracking, isomerization, alkylation or reforming. Each of these industrial transformations occur by a catalyst and water is often used to regenerate the catalytic bed; water from this process is characterized by a large amount of hydrocarbons. Also, water is mixed with crude oil in specific units called desalination unit to selectively extract ions from oil. This kind of water is rich of salts and heavy metal cations. However, during the desalination process light and soluble hydrocarbons are also extracted, determining a more diversified water contamination.

Process	Liters of water/BBL oil
Distillation	98,410
FCC Fluid Catalitic Craking	56,780
Catalityc Reforming	22,710
Alkylation	9,840
desalting	7,950
Visbreaking	7,570
Hydrocraking	7,570
Coking	3,79
Isomerization	3,79
Hydrotreating	3,79
Merox Process	Little or none

Table 1.1 Main refinery's operations and their water consumption.

1.3 Production water characteristics

As mentioned above production water includes both extraction and process water so its chemical and physical characteristics change, depending on its origin. However it is possible to individuate some common features. The presence of oil droplets is essentially due to the high weight hydrocarbon (both aromatic and aliphatic) and their stability is correlated to the superficial tension between water and oil, which depends on

the ionic strength, temperature and pH of the aqueous medium (Veil et al, 2004). Generally, the solubility of the organic compounds decreases at the increasing of molecular weight. As a consequence, the soluble organic fraction of produced water is composed only by the low weight compounds: BTEX (benzene, toluene, ethyl-benzene and xylene), alcohols (phenols and methanol), aldheydes and ketons (acetone) and carboxylic acids (volatile fatty acids). Medium weight hydrocarbons (C6 to C15) instead are present only at low concentration. Besides the organic species, also inorganic constituents are present, alkaline cations such as Li^+, Na^+, K^+, Ca^{2+}, Mg^{2+}, Ba^{2+}, Sr^{2+} and anion like Cl^- , SO_4^{2-}, CO_3^{2-}, HCO_3^-. Their distribution in water reflects the chemical composition of the deposit rocks and they are responsible for the high ionic strength of produced water. Indeed the salinity of produced water might be higher than seawater especially in terms of sodium and chloride concentrations, considering that the total saline concentration of produced water can reach 30.000 mg/l more than the saline concentration of marine environment. Moreover, produced water contains very often heavy metal cations, whose presence depends on the age of the wells and ,also in this case, on the geology of the deposit site. Thus produced water can contain nickel, cadmium, chromium, mercury, silver, copper, lead and zinc at trace levels concentration (Hansen and Davies, 1994). Finally, naturally occurring radioactive materials (NORM) are another constituents of these wastewaters and again their presence is due to the geological formation of the rocks. The most representative radioactive materials ions are radium and barium ions. Heavy metals and NORM are the most toxic constituents of produced water and their removal is difficult to realize, because of the impossibility to transform them in harmless compounds through chemical or physical processes. Production water may also contain solid particles, like sand and silt, that derive from the drilling operations and, in addition to them, some

chemical agents such as biocides, corrosion inhibitors, emulsion breakers, antifoam are added to prevent operational problems. All these constituents have to be removed from production water to waste it in accordance with the environmental laws but also to allow its reuse in other applications (Veil et al, 2004).

1.4 Management of produced water

Considering the massive consumption of water by petrochemical activities, its remediation for further purposes is strictly necessary in order to prevent an increasing of its scarcity. The oilfield water is an high contaminated wastewater and it has to be treated for its reuse and recycle or, in the worst condition, for discharging it without environmental contamination. Because of the oil wastewater can be considered like a waste, the same philosophy can be applied to its management. Indeed the reduction of fresh water in all the human activities should be promoted through its recycle in the same productive processes or its reuse in other productive fields. To this purpose the application of remediation technologies is required, in order to obtain the quality standard appropriate to the new use (reuse) or the same original use (recycle). Disposal represents the ultimate chance in a virtuous wastewater management and it can be applied if the known technologies are not able to treat water till the defined environmental standards.

1.5 Remediation technologies of produced water

Remediation of produced water is an essential option to realize a good wastewater management. The most important aim of remediation is to transform the potential danger of wastewater into a resource or into an harmless waste. The general activities of operators that treat produced water are as follows:

1. De-oiling: removing dispersed oil and grease,

2. Soluble organics removal,

3. Disinfection,

4. SS removal: removing of suspended particles and sand,

5. Dissolved gas removal: removing of light hydrocarbon gases, carbon dioxide, and hydrogen sulfide,

6. Desalination: removing dissolved salts,

7. Softening: removing excess water hardness,

8. Miscellaneous: removing NORM.

1.5.1 Physical-chemical treatment

This kind of treatments are based on the different physical properties of water and contaminants, i.e. density, solubility, dimension.

1.5.2 Adsorption of dissolved organics

This technology is a ripe and spread technologies especially in oilfield wastewater treatment. It involves a porous and sometimes reactive material that is able to adsorb onto both its great surface and its porous the “guest” molecules. Nowadays the most used adsorbent is the activated carbon but the use of other materials such as zeolite, polymers and organoclay materials are spreading (Ali and Gupta, 2007, Ranck J.M. et al., 2005).

Activated carbon can remove soluble BTEX but it has some disadvantages linked to its use in a real remediation context. This material suffers a lot of interferences from molecules that naturally are into the produced or groundwater such as cations or humic and fulvic acids. These substances can react with carboxylic and alcoholic groups on the carbon surface, preventing the adsorption of hydrocarbons contaminant. Another disadvantage occurs during the regeneration process: the wet air oxidation process is not able to guarantee a whole regeneration avoiding the sintering too.

Organoclay is formed by clay, montmorillonite modified with an organic compounds, often a cationic quaternary amine salt. The quaternary cation is exchanged with the natural exchangeable ions present on the negative charge sites of the clay surface. When all the natural ions are replaced by the quaternary ions an organophilic layer cover the clay surface. This layer interacts with the hydrocarbons molecules, removing them from water. Thanks to this characteristic, organoclay can remove also insoluble free hydrocarbons. When organoclay and activated carbon are used together the hydrocarbon concentration decreases below water quality standards (Doyle and Brown, 2000).

Polymeric resins are composite material composed of methylmethacrylate (MMA) or styrene and divinylbenzene (DVB) by suspension polymerization. Resins are used especially in heavy metal removal with the adding of chelating and/or exchange groups at the surface. The most common are sulfonic, acetic, amidoxime groups. These sites are not suitable for hydrocarbons adsorption but the co-polymeric matrix is sufficient to support the organic removal. Indeed these copolymers can reduce oil content of produced water to around 85% (Carvalho et al., 2002).

Zeolites can be described as inorganic polymer of tetrahedral SiO_4 and Al_2O_3. Natural zeolites, such as clinoptilolite, are characterized by ordered crystalline structure that form a channel system of micropores (average channel diameter below 2 nm). The co-presence of Si and Al in the lattice produces a charge imbalance on the zeolite surface. The oxygen atoms are the carrier of the negative charge and they represent the exchange site of the zeolite. The charge imbalance is counterbalanced by little ion as H^+, Na^+ Mg^{2+} and Ca^{2+}. Most of the known zeolites have natural origin, but in the last decades a number of new zeolites were synthesized. They are involved in the adsorption of heavy metal cations or ammonium ions in the water softening process. As concerns hydrocarbons adsorption, modified zeolites represent new emerging materials. These particular classes of zeolite are obtained by replacing the counterbalancing ions with big surfactant molecules or quaternary ammonium ions, such as the hexadecyltrimethylammonium (HDTMA) (Ranck J.M. et al., 2005). Surfactant modified zeolites are able to adsorb organic compounds using the interaction between the hydrophobic substituted surfactant and hydrocarbon,s as in the case of organaclays. Modified zeolites by tailoring the internal pore surface with alkyl chains are also successfully used to remove BTEX from saline produced water (Janks and Cadena 1992).

Mesoporous materials represent a new class of materials inspired by natural zeolites and synthesized for the first time by the Mobil Oil Corporation researchers in the early 90's (Charles et al., 1990). They synthesized a new material called M41S. These materials are also composed by silicon, aluminum and oxygen but, unlike zeolites, they can be crystalline or amorphous. In addition, their channel system is formed by pores bigger than the zeolite's ones. The average diameter of mesoporous materials is included between 2 and 50 nm. They were originally used as catalyst in alkylation, isomerization and cracking of hydrocarbons, thanks to their pore dimensions suitable to host large hydrocarbon molecules. Afterwards they were employed, on a laboratory and pilot scale, as adsorbents for the organic compounds uptake from gaseous and water effluents. Nowadays a lot of mesoporous materials are known and they differentiate each other by the use of different synthetic via and templates. Their family class can be identified with its own acronym:

- Hexagonal Mesoporous Silica (HMS);
- Michigan State University (MSU);
- Korea Advanced Institute of Science and Technology (KIT);
- Santa Barbara Amorphous (SBA);
- Porous Clay Heterostructure (FSM).

In general the adsorption performances of adsorbents is affected by:

• Temperature and pH,

• Suspended oil,

• Low heavy metal concentration and organic–metal complex,

• Dissolved contaminants (organic chemicals)

• High salinity (Hansen and Davies, 1994).

The use of adsorption technologies is quiet recent but it seems to have a good diffusion due to the simplicity of the equipments and their maintenance.

1.5.3 Membrane filtration

Membrane filtration is a technology which has been developed in the past 2 decades for water and waste water treatment. Membrane filtration systems can be subdivided into four classes: micro filtration (MF) , ultra filtration (UF), nanofiltration (NF) and reverse osmosis (RO), depending on the different dimension of the membrane pores. Micro filtration membranes have the largest pores, UF and NF separate smaller particles and droplets, while RO is able to retain dissolved matter as salts especially in the desalination operation. MF and UF are the most applied in waste water treatment while NF is very rarely applied. RO is used for production of drinking water or boiler feed water from salted water and its use in the waste water treatment is not so spread unless an extensive pre-treatment (MF and/or UF) is applied before RO. The use of NF and RO tout court in the waste water remediation is essentially due to their softness and high cost of maintenance. Indeed NF and RO membranes clog very easily.

Membranes are manufactured of various materials: polymers, such as naphion, cellulose, nylon, PTFE, or ceramics. They can be made of different configurations: tubular or spiral wound membranes or hollow fibers which are fitted in membrane modules. When a membrane is applied to wastewater treatments there is production of a permeate (or cleaned water) and a retentate (in which the contaminants are

concentrated). The retentate, which may still contain 98 - 99% water and the majority of pollutants, must be disposed of or treat by different methods. The retentate of a micro-filtration or ultra-filtration unit may constitute 5 - 10% of the waste water flow rate depending on both the type of membranes and composition of the wastewater. Although membrane filtration is able to reduce oil concentration in water up to 5 ppm or less, there is not a massive use of them in wastewater remediation and the development of membranes for these applications is still under investigation. Fouling and poor long term stability are the main problems that affect membrane systems. Indeed in full plant scale membranes must be replaced every 3 - 5 years with high cost of maintenance (Li et al., 2002) Some effective applications were reported by Bilstad and Espedal (Bilstad et al., 2004) comparing MF and UF membranes in pilot trial to treat the North Sea oilfield-produced water. Results showed that UF could reach up the effluent standards for total hydrocarbons, SS and dissolved constituents. Using UF membrane treatment with molecular weight cut-off (MWCO) between 100,000 and 200,000 Da, a reduction of total hydrocarbon concentration up to 2 mg/L from 50 mg/L (96% removal) was observed. Benzene, toluene and xylene (BTX) were reduced up to 54%, and some heavy metals like Cu, and Zn were removed to the extent of 95%. The indicated feed-water specifications for ideal performance of UF were oil and solids less than 50 and 15 ppm, respectively. Ceramic membranes are a new class of materials for the treatment of produced water, Shams Ashaghi et al [Ashaghi et al., 2007, Chen et al., 1991] tested the performances of them to separate oil, grease, and SS from produced water. Permeate quality of dispersed O&G (oil and grease) was 5 mg/L and of SS was less than 1mg/L. The combination system of membrane pretreatment and RO is an effective method for produced water treatment (Burnett, 2004). Xu et al. (Xu et al., 2008) investigated a two stage laboratory-scale membrane for treating gas field produced water from sandstone

aquifers. This system was composed of a pretreatment unit of NF followed by an ultra-low-pressure RO unit. It showed the ability to reach up the quality standards for potable and irrigation water and iodide concentration in brine.

1.5.4 Gravity separation

This kind of technologies are used especially to separate the oil droplet or emulsified oil from water using the different density of oil and water.

1.5.5 Retention ponds/Storage pits

By using this technology oil and water are separated into retention ponds/storage pits, where the oil moves up on the surface and the water goes down on the bottom of the ponds or pits. This is a long term operation but it is characterized by low cost maintenance. The oil is spill over the ponds into a near creek. The use of ponds and pits has been replaced by tank provided by a closed valve at the bottom of the tank. From the valve the separated water is spilled out leaving the oil into the tank.

1.5.6 API separator

The API (American Petroleum Institute) separator is one of most used type of oil-water separator in the petrochemical plants. It can remove up to 60 to 99% of the free oil in a waste stream. It works using the different of density between oil and water and the

eventual solids. It is constituted by a basin, frequently built of concrete, in which the waste stream is hold for the time necessary to the separation. During this time the lighter compounds go up till the surface where a device for floating scum picks them up out the basin. The heavier compounds and solids are deposited on the bottom where a scraping device removes them as sludge. The purified water and soluble compounds remain inside the basin (American Petroleum Institute) *Figure 1.1* shows the schematic of an API oil separator.

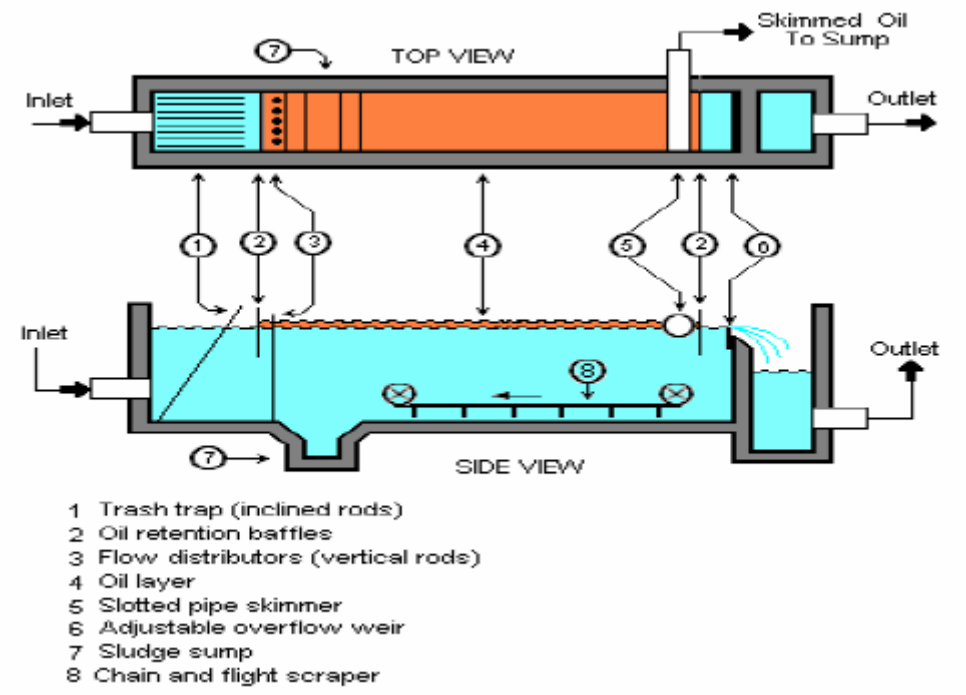

Figure 1.1 Schematic representation of API separator.

1.5.7 Skimmer tanks and vessels

The skim (clarifier) tank or vessel is the simplest form of primary treating equipment; showed in *Figure 1.2*. These items are suitable for long time residence operations in which wastewater is disposal and water and oil are left to separate by gravity and coalescence. Skim tanks can be used as atmospheric tanks, while pressure vessels and surge tanks are different configuration of the same equipment and they are usually employed ahead of other produced water treating equipment (Arnold and Stewart, 2004).

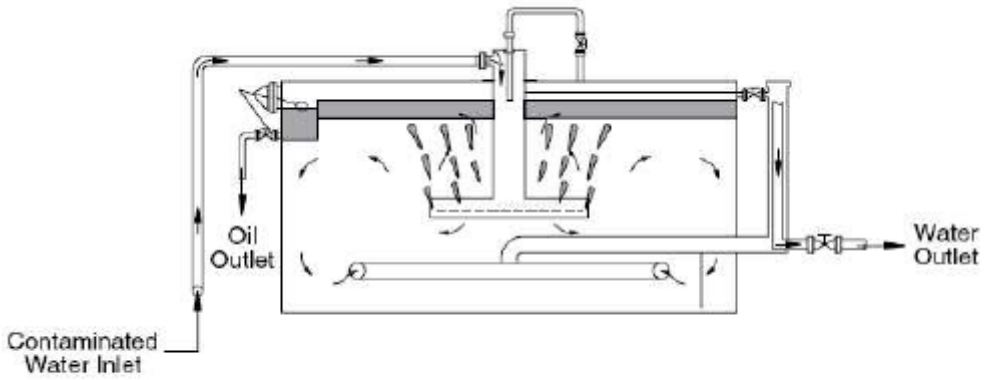

Figure 1.2 Schematic representation of Skimmer tanks and vessels

1.5.8 Plate coalescence

A lot of different types of equipments have been developed to promote, next to the separation by the solely gravity, the coalescence of small dispersed oil droplets. The double effect of gravity and coalescence improves the separation. By using this items is

possible to reach the performance of a skimmer in less space . There are various configurations of plate coalescers: parallel plate interceptors (PPI), corrugated plate interceptors (CPI) or cross-flow separators. They differentiate by the way of rising to a plate surface where coalescence and capture occur (American Petroleum institute). The motion of all the oil droplets that enter the space between two following plates is ruled by Stokes' law. Assuming that the oil droplet has a forward velocity equal to the bulk water velocity and solving for the vertical velocity needed by a particle entering at the bottom of the flow to reach the coalescing plate (at the top of the flow), it is possible to determine the droplet diameter. The most ancient type of plate is the parallel plate interceptors, while nowadays the most used in plant is the corrugated plate interceptors that is a modification of the former. *Figure 1.3* shows the flow pattern of a typical down-flow CPI design. In CPIs the parallel plates are corrugated (like roofing material), and the axes of the corrugations are parallel to the flow direction.

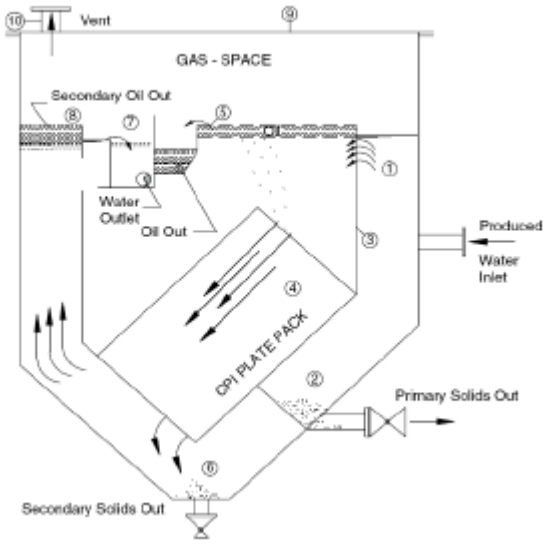

Figure 1.3 Schematic representation of Down-flow CPI design.

1.5.9 Enhanced coalescence

To enhance the coalescence of oil droplets a lot of devices have been developed, providing a pretreatment of the effluent to increase the drop dimension and facilitate the subsequential removal.

1.5.10 Mare's Tail

Tulloch (Tulloch, 2003) describes a pre-coalescer that is made of a bundle of oleophilic polypropylene fibers inside a cartridge set along a flow line just upstream of another separation device (e.g., hydrocyclone, filter). The hydrophobic fibers facilitate the aggregation of the smallest oil droplets for an easier removal during the successive operations. The coalescence occurs rapidly (within two seconds). The name "Mare's Tail" derives from the shape of this device that seems like a horse tail, due to the bundle of polypropylene fibers. Tulloch (Tulloch, 2003) shows that increasing the fiber length or their number in the cartridge the oil droplet growth enhances. *Figure 1.4* shows the principle of operation of a Mare's Tail pre-coalescer.

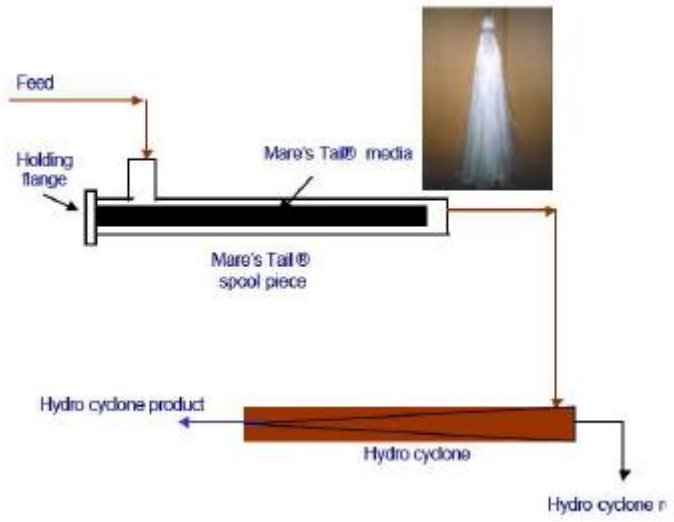

Figure 1.4 Principle of operation of a Mare's Tail pre-coalescer.

1.5.11 Enhanced gravity separation

To enhance the gravity separation a common way is to apply an external gravitational field to the effluent. In this way the particle deposition and aggregation rate can be greatly enhanced and also the smaller particles can be coalesced. The use of an external gravitational field has the main advantage to get smaller device than the classical ones and the same results can be obtained in shorter time. The two main categories of these technologies are described in the following sections.

1.5.12 Hydrocyclones

Hydrocyclones or Static oil-water separator is constituted by a cylindrical chamber in which concentric reducing and taper sections are set. Pressurized oily water enters tangentially through the inlet valve into this cylindrical chamber. At the same time the shape of the chamber and the heater pressure induce a centrifugal rotation motion of the fluid that amplify the effect of gravity during the separation. The centrifugal forces push the lighter oil droplets towards the center of the hydrocyclone where axial flow reversal occurs and the droplets can coalesce and the reject stream is recovered. The clean water instead moves to the wall chamber of the hydrocyclone and is discharged. The total residence time of the effluent in this device is only 2-3 seconds (Bradley, 1990). Hydrocyclones are particularly efficient if the system operates at high pressures by way of its static nature. On the contrary if the system works at low pressure, booster pumps are required for increasing the rate of the inlet effluent. The use of pumps can however induce a shearing action on the oil droplets reducing the system efficiency. Another disadvantage of Hydrocyclones, due to the high pressure, is the high and constant flow rates that are required for its optimum operation. If flow rates are low or variable, a recycle flow stream through a surge tank can be added (Canadian Association of Petroleum Prodducts, 2001). As shown in *Figure 1.5*, the liner consists of four sections: a cylindrical swirl chamber, a concentric reducing section, a fine tapered section, and a cylindrical tail section (American Petroleum institute).

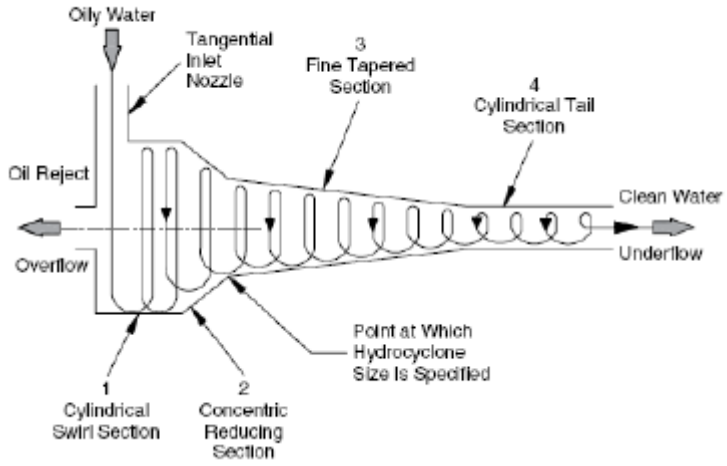

Figure 1. 5 Representation of Hydrocyclone and its main sections.

1.5.13 Centrifuges

Dynamic hydrocyclones are commonly known as centrifuges and they consist of a rotating cylinder chamber, two valves for the axial inlet and outlet, reject nozzle, and external motor (*Figure 1.6)*. The external motor is used to rotate the outer shell of the hydrocyclone in which the effluent is stoked. When the motor is switched, centrifugal rotation motion is transferred to the fluid and the applied rotation creates a "free vortex." The tangential speed is inversely proportional to the core distance of the cyclone, so that the lighter oil drops are collected in the center and separated from water. Centrifuges have found few applications relative to hydrocyclones because of poor cost–benefit ratio (American Petroleum institute).

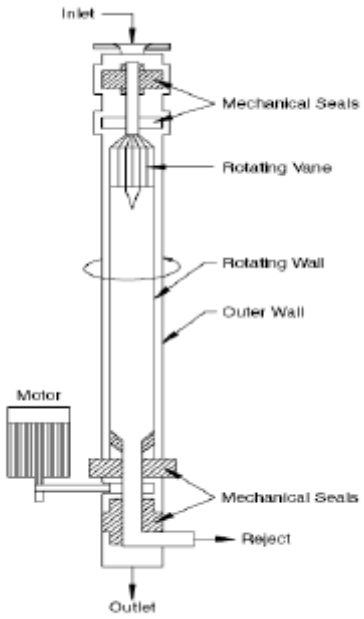

Figure 1.6 Representation of a typical centrifuge for oil-water separation.

1.5.14 C-tour process

The C-Tour Process was developed by AS company. The C-Tour technology is a liquid-liquid extraction process. In this process, a liquid condensate is the extract liquid suitable to remove the dissolved components in produced water. The condensate also helps the coalescing of dispersed oil with small oil droplets, promoting their removal from water. The C-Tour process is carried out through four steps:

- Harvest a suitable condensate stream from production;

- Inject condensate in liquid form into the produced water stream;

- Mix and disperse the condensate into the water;

- Allow adequate contact time between condensate and water;

- Separate the contaminated condensate from the water in a separation process

- Cycle the condensate, containing contaminants, back to the production stream.

It was estimated that this process can remove approximately 70% of dispersed oil and PAHs, as well as up to 70% of phenols (Knudsen et al., 2004). A flow diagram of C-tour processes is given in *Figure 11*.

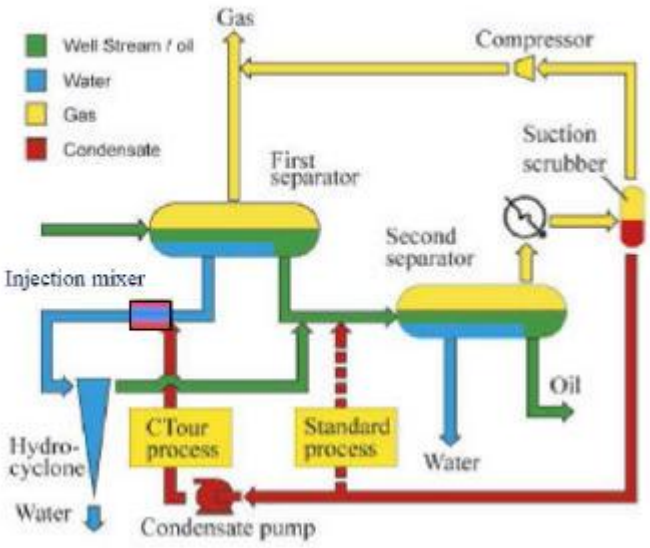

Figure 1.7 Flow diagram of the C-tour process.

1.6 Chemical treatment

1.6.1. Chemical precipitation

Gravity separation operations are usually used to remove suspended and colloidal particles, but are not suitable for removing dissolved compounds. Chemical precipitation instead is more suitable for removing these constituents and it requires the addiction of some chemicals to promote the decreasing of their solubility and consequently their precipitation. Lime softening, for example, is the common process for water softening. In the modified hot lime process, produced water containing 2000 ppm hardness, 500 ppm sulfides, 10,000 ppm TDS, and 200 ppm oil could be successfully converted into water with suitable standards for being employed in a boiler. Besides the use of lime, it is possible to add organic and inorganic polymers or polyelectrolyte, a kind of organic polymer that brings some charged center on its chain. Organic polymers, lime, metal hydroxide and salts are called flocculants agents and they have the peculiarity to act as bridge between the colloidal particle and suspended solids. For example FMA is an inorganic mixed metal (Fe, Mg, and Al) polynuclear polymer; it has good coagulation, de-oiling and scale inhibition properties, particularly in produced water with SS levels of 50–400 mg/L. Using FMA is possible to remove SS and oil to levels greater than 92% and 97%, respectively (Zhou et al., 2000). On the other hand, Houcine (Houcine, 2002) showed the high removal efficiency of heavy metals from produced water using a mix of spillsorb, calcite and lime. Moreover, a study concerning the treatment of produced water described the use of ferric ions as oxidant for removing arsenic and mercury, while flocculants were used to remove hydrocarbons. In this process, the oxidation–reduction potential of the wastewater was controlled by adding

the required amount of oxidant to allow the arsenic oxidation and the elemental form of mercury. Results showed low levels of contaminants: less than about 10 parts per billion (ppb) of mercury (calculated as Hg), less than about 250 ppb of arsenic (calculated as As), and less than about 40 ppm of TPH (Frankiewicz and Gerlach, 2000). The main disadvantages of the chemical precipitation processes are generation of sludge and the increasing concentration of metals (used as flocculants) in effluents.

1.6.2. Chemical oxidation

Chemical oxidation is the common method for decomposing refractory chemicals in wastewater using strong oxidant, catalysts, and irradiation (except ozone treatment) (Renou et al., 2002).

1.6.3 Electrochemical process

The electrochemical process for remediation of oilfield wastewater is still under study and only few laboratory tests have been performed in these last years. One of them is reported by (Ma et al., 2006) that showed a laboratory pilot-scale plant composed by double anodes with active metal, graphite and iron, and a noble metal content crystal with a large surface as cathode. Results showed the reduction of the COD and BOD of oilfield produced water by over 90% during the first 6 minutes of activity.

1.6.4 Photocatalytic treatment

Photocatalytic treatment born as a modification of the use of TiO_2 electrodes, usually employed for the photo-electrochemical decomposition of water to produced H_2 (Fujishima and Honda, 1972). There is not an industrial application of this device and only laboratory scale tests have been performed. This method can be used for different pollutants. The general process for organic pollutant treatment by photocatalytic method is :

$$\text{organic pollutant} + O_2 \xrightarrow{\text{semiconductor, } h\nu} CO_2 + H_2O + \text{mineral acids}$$

The interaction of light photon and TiO_2 semiconductor produces an electron streams that starts the oxidation reaction of organic pollutant with oxygen. The most proposed process for oilfield-produced water treatment by photocatalytic method includes a prior process of clarification by adding soda up to pH 11 and a successive filtration. The photocatalytic process is then applied to the clarified wastewater. Photocatalytic reaction was carried out in an open reactor to ensure the required amount of oxygen and the adequate amount of photcatalyst-TiO_2 is added. A high-pressure 250W mercury lamp illuminated the suspension at 298K starting the decomposition reaction. This method could reduce toxicity of produced water (Bessa et al., 2001). Li et al. (Li et al, 2006; Li et al., 2007) performed a study about the reduction of toxicity and COD removal efficiency, comparing the results to those of photo-catalysis and electrochemical oxidation. Results showed a COD removal by photoelectron-catalytic process much higher than by photo-catalytic or electrochemical oxidation. The same study showed that at equivalent doses, photoelectron-catalysis has the best performance

of reducing genotoxicity, whereas photo-catalysis is the least effective and do not lead significative change in mutagenicity. So the photoelectron-catalysis system seem to be the most effective technology for degradation of oilfield wastewater. In a similar study, (Adams et al. 2008) utilized a drum reactor with a single pass continuous-flow system for produced water effluents. In this reactor, titanium metal was used as substrate. The reactor drums were irradiated using sunlamp UV tubes. Results showed that hydrocarbon content could be reduced by more than 90% in 10 minutes.

1.6.5. Fenton process

Fenton process is a combined process in which flocculation, oxidation and adsorption occur in series reactors. The first phase is the flocculation in which poly-ferric sulfate was used as flocculant agent for a 30-minutes settling period. In the second reactor the oxidation reaction occurs at pH 3–4 by an oxidant aqueous solution of 30% H_2O_2 and 4% of Fe^{3+} for an oxidation time of 120 minutes. Finally, the third stage provides the use of active carbon as adsorbent in a batch process in which the active carbon is added up to the concentration of 4000–5000 mg/L and an adsorption time of 120 minutes is used (Yang and Zhang, 2005)

1.6.6. Treatment with ozone

This technology provides the use of ozone gas as oxidizing agent. In this case after the reaction the ozone becomes oxygen and this is the main advantage of this process: the absence of secondary toxic products. The use of ozonolysis is a very new technology and it is still in its laboratory research phase. However Morrow et al. (Morrow et al., 1999) proposed ozonolysis for decomposing dissolved organic compounds in produced water. Klasson et al. (Klasson et al., 2002) compared destruction of soluble organics by sono-chemical oxidation and ozonolysis using a sample of synthetic and real produced water. Sono-chemical oxidation could remove some compounds such as BTEX, but the combination of ozone and hydrogen peroxide did not improve the decomposition of organics to CO_2. Their experiment showed that the use of ozone is able to remove only the extractable organics within 3 days of working. This results underlined the low efficiency of this process and in addition the need to consider the high running costs due to the high demand of energy and chemicals.

1.7 Biological treatment

Biological treatment are characterized by the use of aerobic and anaerobic microorganisms. In aerobic treatment, activated sludge, trickling filters, sequencing batch reactors (SBRs), chemostate reactors, biological aerated filter (BAF), and lagoons are used. Four sources of microorganisms were studied and applied in biological treatment:

• Naturally occurring microorganisms,

• Commercial microorganisms,

• Specific groups of microorganisms,

• Acclimated sewage sludge.

Generally, activated sludge is the common method for treating wastewater. As other methods, biological treatments need to have a pretreated wastewater before operating the oil removal. For example, in a continuous-flow pilot plant an oil skimmer was set before the biological reactor to remove oil before treatment by activated sludge system. It was studied the operational efficiency of an activated sludge treatment unit that could maintain a total petroleum hydrocarbon (TPH) removal efficiency of 98–99% at a Solids Retention Time (SRT) of 20 days [3]. Freire et al. also (Freire et al., 2001) studied the ability of acclimated sewage sludge to remove COD from oilfield water using Sequencing Batch Reactor (SBR) with different percentages of produced water and sewage. In 45% and 35% (v/v) mixtures of wastewater, it was found a COD removal efficiency variable from 30% to 50%. Another study instead moved the attention from the COD to TOC removal using acclimated microorganisms in 180 mg/L NaCl. This study was carried out on three different biological systems including SBR, trickling filters and chemostate reactors and the operational conditions of each system was reported below:

• 2 L SBR with 24-h cycle (1 h for feed, 20 h for reaction, 2 h for settling, and 1 h for withdrawal).

• A trickling filter equipped with annular plastic supports with packing volume of 1.7 L and hydraulic load of 3 m^3/m^2 h.

• A 1L chemostate reactor with 8 days hydraulic retention time.

Even if SBR could cause a major loss of biomass, its removal efficiency (in terms of TOC) was higher than that of the trickling filter and of the chemostate (Baldoni et al., 2006).

Due to high salt concentration of wastewater it is possible to have depressive effect on the biomass activity. However Freire et al. found significant effect of only recalcitrant organic compounds on COD removal of mixed wastewater, while salinity seemed to not have affected biological treatment; also, Wei et al. (Wei et al., 2003) showed that inhibitory effect of the high salinity on composite microbial culture was negligible if Cl^- concentration was increased from 2000 to 36000 mg/L. Nevertheless, another study conducted by Dfaz et al. (Dfaz et al., 2000) showed that an increase of salinity up to 100,000 mg/L produced a dramatic decrease of biodegradation rate, because high concentration of sodium chloride causes environmental stress and microbial lysing effects (Tellez and Nirmalakhandan, 1992). In addition to this, salinity can lead both to a reduction of filamentous bacteria and the integrity of the flocks with a consequent increasing of the treated water turbidity (Lefebvre and Moletta, 2006) For improving biological treatment of effluent, membranes can be coupled to it Kang et al., 2003). Palmer et al. (Palmer et al., 1981) studied the treatment of oilfield-produced water using rotating surfaces covered of biofilm (biodisks). This biodisks were populated by bacterial sludge derived from sewage treatment plant. This kind of device is able to

remove BOD and O&G of 94% and 74%, respectively. Besides, immobilization of microorganisms can increase the treatment efficiency.

Li et al. (Li et al., 2005) studied the removal of COD of oilfield-produced water using *Bacillus* sp. (M-12) immobilized on polyvinyl alcohol (PVA). *Bacillus* sp. can achieved more than 90% efficiency of COD removal with initial COD of 2600 mg/L. Zhao et al. (Zhao et al., 2006) instead explored use of commercial microorganisms immobilized on poly-ammoniacum carriers. For this purpose a pair of BAF reactors was realized. Results showed that this microbial consortium can degrade TOC and oil of produced water of 78% and 94% respectively, with a hydraulic retention time of 4 hours and volumetric load 1.07 kg COD/(m^3day). Different microorganism such as, harmless bacteria, algae, fungi and protozoa, can convert through biological oxidation dissolved organics into water and CO_2, and ammonia into nitrates/nitrites (Palmer et al., 1981), but have no effect on TDS (Jackson et al., 2003). Beyer et al. (Beyer et al., 1979) studied a complex reactor composed of two-stage pilot lagoon of 80 m^3 placed in series and consisting of plastic-lined steel tanks, each filled with 60 m^3 of fluid. Each tank had a different task: the first was for oxidizing suspended oil and dissolved organics and the second lagoon was for oxidizing dissolved ammonia compounds

In biological treatment the mainly mechanism of dissolved hydrocarbon removal is the biodegradation, while dispersed hydrocarbons and particles are removed by a mechanism similar to bio-flocculation. Indeed, activated sludge can adsorb and occlude not only soluble but also insoluble materials. Bacteria can produce compounds such as surfactants (bio-surfactants) and emulsifiers (bio-emulsifiers) that are surface-active compounds able to enhance the solubility of hydrocarbons and thence improve their mass transfer from the bulk to the biodegrading bacteria (Hommel, 1990). Not all the organics and hydrocarbons are biodegradable, their biodegradability is directly

proportional to their structure simplicity, e.g., normal alkanes is easier than of branched and large molecules. The bio-recalcitrant molecules are removed along with sludge because they are adsorbed onto the bacterial surface or incorporated within the sludge flock. The mixture of hydrocarbons and microorganisms obtained after the biological treatment is classified as hazardous waste and it has to be disposed.

Aerobic biological treatment are not the only applicable biological treatment, especially when raw wastewater is concentrated in terms of organic compounds, anaerobic degradation of contaminants could be a good alternative to aerobic process (Metcalf, 2003) Gallagher (Gallagher, 2001) studied the bio-removal of organic acids in synthetic produced water in the presence of naphthenic acids under anaerobic conditions. The microbial consortium used for this experimentation derived from a sludge used in a anaerobic digester of a municipal treatment system. Results showed that anaerobic microorganism could not degrade naphthenic acids. Another study (Gurden and Cramwinckel, 2000) concerned the bioremediation approach to remove hydrocarbons and heavy metals from wastewater using an 800 m^2 reed bed with *Phragmites australis.* Results showed that more than 98% of hydrocarbons were biodegraded. Al Mahruki and Alloway (Al Mahruki and Alloway, 2006) studied a similar pilot plant, operating the reduction of total hydrocarbons and heavy metal concentration on 3000 m^3/day of produced water. The reduction of hydrocarbons was of 96% while metal concentration decreased up to 78% for Al, Ba, Cr, Cu, and Zn, up to 40% for Fe, Li, Mn, Pb, As, Cd, Co, Mo, Ni, Se, Tl, and V. Although this system is a cost-effective method, the effluent has to be refined and requires a lot of land.

1.8 References

Adams M. , Campbell I., Robertson P.K.J., Novel photocatalytic reactor development for removal of hydrocarbons from water, Int. J. Photoenergy (2008) 1–6,Art. No. 674537.

Al Mahruki A. , Alloway B., The use of reed-bed technology for treating oilproduction waters in the sultanate of Oman, in: SPE International Health, Safety & Environment Conference, Abu Dhabi, UAE, 2–4 April, 2006.

Ali Imran and Gupta V. K., Advances in water treatment by adsorption technology. Nature Protocols 1, 2661 - 2667 (2007)

American Petroleum Institute (API), 1990. Monographs on Refinery Environmental Control Management of Water Discharges (Design and Operation of Oil-Water Separators).Publication 421, First Edition.

Arnold, K.E. Stewart, M., Surface production operations-Design of Oil Handling Systems and Facilities, vol. 1, third ed., Gulf Publishing Co, Houston,Texas, 2008.

Arthur J.D. , Langhus B.G., Patel C., Technical Summary of Oil and Gas Produced Water Treatment Technologies, http://www.rrc.state.tx.us/commissioners/williams/environment/producedwatertrtmntTech.pdf,2005.

Baldoni-Andrey P. , Lesage N., Segues B., Pedenaud P., Dehaene P.L., Impact of high salinity of producedwater on the technical feasibility of biotreatment for E&P onshore applications, in: SPE International Health, Safety & Environment Conference, Abu Dhabi, UAE, 2–4 April, 2006.

Bessa E. , Sant'Anna G.L. Jr., Dezotti M., Photocatalytic/H_2O_2 treatment of oil field produced waters, Appl. Catal. B 29 (2001) 125–134.

Beyer A.H. , Palmer L.L., Stock J., Biological oxidation of dissolved compounds in oilfield-produced water by a pilot aerated lagoon, JPT J. Petrol. Technol. 31 (1979) 241–245.

Bilstad T. , Madland M., Espedal E.and Hanssen P. H., Membrane Separation of Raw and Anaerobically Digested Pig Manure Water Science & Technology Vol 25 No 10 pp 19–26 © IWA Publishing 1992

Bradley B.W., Produced water treatment technology assessment. Prepared for the American Petroleum Institute-Offshore effluent guidelines steering committee, Washington, DC, 1990.

Burnett, D.B., 2004. Potential for Beneficial Use of Oil and Gas Produced Water, http://www.rrc.state.tx.us/commissioners/williams/environment/ beneficialuses.pdf.

CAPP, 2001. Produced water waste management, Technical report, Canadian Association of Petroleum Products (CAPP), page 9.

Carvalho M.S. , Clarisse M.D., Lucas E.F., Barbosa C.C.R., Evaluation of the polymeric materials (DVB copolymers) for produced water treatment, in: SPE International Petroleum Exhibition and Conference, Abu Dhabi, UAE, 13–16 October, 2002.

Charles T. Kresge, Michael E. Leonowicz, Wieslaw J. Roth, James C. Vartuli Inorganic oxides as an absorbent and for catalytic conversion of inorganic and organic compounds US 5098684 A 1990

Chen, A.S.C., Flynn, J.T. , Cook, R.G. , Casaday, A.L.,1991.Removal of oil, grease,and suspended solids from produced water with ceramic crossflow microfiltration,SPE Prod. Eng. 6 (1991) 131–136.

Dfaz M.P. , Grigson S.J.W., Peppiat C.J., Burgess G., Isolation and characterization of novel hydrocarbon-degrading euryhaline consortia from crude oil and mangrove sediments, Mar. Biotechnol. 2 (2000) 522–532.

Doyle D.H. , Brown A.B., Produced Water treatment and hydrocarbon removal with organoclay, in: SPE Annual Technical Conference and Exhibition, Dallas, Texas, USA, 1–4 October, 2000.

Environment Canada Website www.ec.gc.ca/water/en/manage/use/e_wuse.htm

EPA report "The Potential Impacts of Hydraulic Fracturing on Drinking Water Resources". (2012)

Frankiewicz T.C., Gerlach J., Removal of hydrocarbons, mercury and arsenic from oil-field produced water, US Patent No. 6,117,333 (2000).

Freire D.D.C. , Cammarota M.C., Sant'Anna G.L., Biological treatment of oil field wastewater in a sequencing batch reactor, Environ. Technol. 22 (2001) 1125–1135.

Gallagher J.R., Anaerobic Biological Treatment Of Produced Water, http://www.energystorm.us/AnaerobicBiologicalTreatmentOfProducedWater-r54822.html, 2001.

Gurden C., Cramwinckel J., Application of reedbed technology in production water management, in: SPE International Conference on Health, Safety and Environment in Oil and Gas Exploration and Production, Stavanger, Norway, 26–28 June, 2000.

Hansen BR, Davies SR., Review of Potential Technologies for the Removal of Dissolved Components from Produced Chemical Engineering Research & Design, Vol.72, No.2, 176-188, 1994

Hommel R.K., Formation and physiological role of bio-surfactants produced by hydrocarbon-utilizing microorganisms, Biodegradation 1 (1990) 107–119.

Houcine M. , Solution for heavy metals decontamination in produced water/case study in southern Tunisia, in: International Conference on Health, Safety and Environment in Oil and Gas Exploration and Production, Kuala Lumpur, Malaysia, 20–22 March, 2002.

Jackson L.M. , Myers J.E., Design and construction of pilot wetlands for produced-water treatment, in: SPE Annual Technical Conference and Exhibition Denver, Colorado, USA, 5–8 October, 2003.

Janks J.S., Cadena F., Investigations into the use of modified zeolites for removing benzenes, toluene and xylene from saline produced water, in: J.P. Ray, F.R.Engelhardt (Eds.), Produced Water: Technological/Environmental Issues and Solutions, Plenum Publishing Corp., New York, 1992, pp. 473–488.

Kang I.J. , Lee C.H., Kim K.J., Characteristics of microfiltration membranes in a membrane coupled sequencing batch reactor system, Water Res. 37 (2003) 1192–1197.

Klasson K.T., Tsouris C., Jones S.A., Dinsmore M.D., Walker A.B., De Paoli D.W., Yiacoumi S., Vithayaveroj V., Counce R.M., Robinson S.M., Ozone Treatment of Soluble Organics in Produced Water, http://www.osti.gov/bridge, 2002.

Knudsen B.L., Hjelsvold M., Frost,T.K., Svarstad M.B.E., Grini, P.G., Willumsen C.F., Torvik, H. Meeting the zero discharge challenge for produced water. paper SPE 86671,

presented at the seventh SPE International Conference on Health, Safety, and Environment in Oil and Gas Exploration and Production held in Calgary, Alberta, Canada, 29–31 March 2004.

Lefebvre O. , Moletta R., Treatment of organic pollution in industrial saline wastewater: a literature review, Water Res. 40 (2006) 3671–3682.

Li Q. , Kang C., Zhang C., Waste water produced from an oilfield and continuous treatment with an oil-degrading bacterium, Process Biochem. 40 (2005) 873–877.

Li G., An T., Chen J., Sheng G., Fu J., Chen F., Zhang S., Zhao H., Photoelectrocatalytic decontamination of oilfield producedwastewater containing refractory organic pollutants in the presence of high concentration of chloride ions, J. Hazard. Mater. B138 (2006) 392–40

Li G., An T., Nie X., Sheng G., Zeng X., Fu J., Lin Z., Zeng E.Y., Mutagenicity assessment of produced water during photo-electro-catalytic degradation, Environ. Toxicol. Chem. 26 (2007) 416–423.

Li L.B. , Yan S., Zeng X.D., Lin D.Q., Analysis of organic compounds in oilfield produced water, Petrochem. Technol. 31 (2002) 472–475.

Ma H. , Wang B., Electrochemical pilot-scale plant for oil field produced wastewater by M/C/Fe electrodes for injection, J. Hazard. Mater. B132 (2006) 237–243.

Metcalf, Eddy, Wastewater Engineering: Treatment and Reuse, 4th ed., McGraw-Hill Inc., New York, 2003.

Morrow L.R. , Martir W.K., Aghazeynali H., Wright D.E., Process of treatingproduced water with ozone, US Patent No. 5,868,945 (1999).

Palmer L.L. , Beyer A.H., Stock J., Biological oxidation of dissolved compounds in oilfield produced water by a field pilot biodisk, J. Petrol. Technol. 8308-PA (1981) 1136–1140.

Ranck, J., Bowman, R., Weeber, J., Katz, L., and Sullivan, E. (2005). ”BTEX Removal from Produced Water Using Surfactant-Modified Zeolite.” J. Environ. Eng., 131(3), 434–442.

Ray J.P., Engelhardt F.R.,Produced Water–Technological/Environmental Issues and Solutions (1992)., Eds.;Plenum Press,New York & London.

Renou S., Givaudan J.G., Poulain S., Dirassouyan F., Moulin P., Landfill leachate treatment: review and opportunity, J. Hazard. Mater. 150 (2008) 468–493.

Sauer TC, Costa HJ, Brown J, Sand Ward TJ, (1997).Toxicity Identification Evaluations of Produced Water. Environmental Toxicology and Chemistry 16(10):2020 – 2028.

Shams Ashaghi, K., Ebrahimi, M., Czermak, P.,2007.Ceramic ultra- and nanofiltration membranes for oilfield produced water treatment: a mini review, Open Environ. J. 1 (2007) 1–8.

Stephenson MT (1992).Components of Produced Water:A Compilation of Industry Studies.Society of Petroleum Engineers May 1992:548–603.

Tellez G.T. , Nirmalakhandan N., Bioreclamation of oilfield produced wastewaters: characterization and feasibility study, in: J.P. Ray, F.R. Engelhardt (Eds.), ProducedWater: Technological/Environmental Issues and Solutions, Plenum Publishing Corp., New York, 1992, pp. 523–534.

Tulloch, S.J., 2003. "Development & Field Use of the Mare's Tail® Pre-Coalescer,"presented at the Produced Water Workshop, Aberdeen, Scotland, March 26-27.

US Energy Information administration: www.eia.gov

Veil J. , Puder M.G., Elcock D., Redweik R.J.J., A White Paper Describing Produced Water from Production of Crude Oil, Natural Gas and Coal BedMethane,2004.

Wei N. , Wang X.H., Li F.K., Y.J. Zhang, Guo Y., Treatment of high-salt oil field produced water by composite microbial culture, Urban Environ. Urban Ecol.16 (2003) 10–12.

Xu P., Drewes J.E., Heil D., Beneficial use of co-produced water through membrane treatment: technical-economic assessment, Desalination (2008) 225, pp.139–155.

Yang Z.G. , Zhang N.S., Treatment of produced wastewater by flocculation settlement-Fenton oxidation–adsorption method, Nat. Sci. Ed. 20 (2005) 50–53.

Zhao X., Wang Y., Z. Ye, Borthwick A.G.L., Ni J., Oil field wastewater treatment in biological aerated filter by immobilized microorganisms, Process Biochem. 41 (2006) 1475–1483.

Zhou F.S. , Zhao M.F., Ni W.X., Dang Y.S., Pu C.S., Lu F.J., Inorganic polymeric flocculent FMA for purifying oilfield produced water: preparation and uses, Oilfield Chem. 17 (2000) 256–259

Chapter 2

THE ADSORPTION PROCESS

The term “adsorption” refers to a physic-chemical phenomenon that occurs between gaseous or liquid molecules and the solid surface of a material. For gaseous compounds it is possible to distinguish between two different kind of adsorption, depending on the involved energy and the specificity of the mechanism: physisorption or chemisorption. Physisorption is a non-specific adsorption and it takes places between the material surface and fluid molecules. It is possible to imagine this kind of adsorption as the liquefaction of gaseous molecules onto the material surface (Oura et al., 2003). On the contrary, chemisorption involves the interactions between molecules and some specific points of the material surface called active sites. The adsorption proceeds with the break of the molecular bonds and the formation of new ones between the originated atoms and the superficial active sites (Oura et al., 2003). In particular, when the liquid compounds are considered, the classification of the adsorption process is done considering the typology of the interaction between adsorbate (liquid molecules) and adsorbent (solid material). For ionic species, electrostatic interactions occur among ions and the ionic exchangeable sites of the adsorbent. In this case a counter-ion desorbs from the site towards the external, leaving free its position for the adsorbing ion; this ionic exchange position takes place simultaneously. If the material surface is devoid of ionic exchange

sites but rich in other kind of sites, such as complexation or chelating sites, a superficial complexation between ions and these sites occurs. The most common complexation sites are hydroxyl, thiol and amino groups. Usually, different complexation groups can be joined in a unique group called chelating group (Fenglian and Qi, 2011). Chelating groups are typical of polymeric and, in general, of synthetic materials such as chelating resins and adsorbent polymers. Ionic exchange and surface complexation are typical adsorption mechanisms of inorganic ionic species. As concerns organic compounds instead, they are involved in different mechanisms of adsorption. The typical interactions between this class of compounds and material surface are Wan der Waals and London forces. The same interactions also occur between adsorbed molecules and free molecules promoting the adsorption of the latter (Parida et al., 2006)

Considerations about the typology of mechanism regulating the interactions between adsorbent and adsorbate are relevant to the microscopic environment.

Focusing the attention on the macroscopic level the selectivity of the adsorption process can be described by three distinct mechanisms: steric, equilibrium and kinetic. In the steric mechanism, the porous structure of the solid material operates a selection of molecules based on their different dimensions. Large molecules cannot enter the pores, because of their lack of a suitable diameter, while the smaller ones can penetrate pores and they are sieved from the bulk environment.

The equilibrium mechanism is based on the thermodynamic properties of solid surface to attract and bond the different species. In this way, the molecules that adsorbs with the strongest interactions are also the species preferentially removed by the solid. In other words, the affinity between adsorbate and adsorbent regulates the adsorption process.

From the kinetic point of view the adsorption process is controlled by the diffusivity of the species into the solid bulk and then into the porous framework of the sorbent. Molecules with high rate of diffusion are the most retained and, controlling contact time, it is possible to encourage the adsorption of the faster diffusing species.

These different mechanisms can act simultaneously or independently. For example it is possible a competition between different molecules characterized by similar dimension and diffusivity but different affinity, in this case the equilibrium mechanism is the determining step for adsorption.

Therefore, it is possible to characterize the adsorption processes of a chemical species by two points of view: Thermodynamic, that allows the knowledge of the maximum removal capacity and the application limits, and kinetic, focusing the attention on the rate of the overall adsorption process, on the fluid-dynamics parameters of the system and the material transfer process from liquid or gas phase to solid phase.

2.1 Thermodynamic point of view

Studying the adsorption process from a thermodynamic point of view means studying the process at equilibrium conditions, where the adsorption and the desorption of molecules from solid surface are balanced. This is the condition that the change of Gibbs free energy is equal to zero. The adsorption experiment can be performed under static or dynamic condition. In the first case we are dealing with batch configuration while in the second case with column configuration. Batch experiments can be made using two different approaches. The first-one provides the use of several solutions of a chemical compound at different concentration and each solution is kept in contact with

a fixed amount of adsorbent material. The concentration of the solution is determined before and after the contact with the material and the difference, normalized for the amount of the solid, represents the adsorbed amount of the considered compound. The second approach consists of a solution at unique starting concentration. This solution is divided into several portions and each of them is kept in contact with different solid amounts. The analysis of the solution before and after the contact allows to know the difference of concentration of the considered compound in solution due to the adsorption onto the material.

Column experiments provide a column packed by the adsorbent material, recreating a packed adsorption bed, and the contaminant solution is sent into the column up to the exhaustion concentration, that is defined as the 0,95 of the inlet concentration. The experiment is repeated changing every time the contaminant inlet concentration. Every exhaustion point represents an isotherm point. Indeed, from column experiments is possible to carry out a breakthrough curve and by it calculating the amount of contaminant adsorbed onto the packed bed, normalizing it for the amount of material composing the bed. In these experiments another important parameter is the breakthrough point that is the point of time and concentration at which the last portion of the bed start to be saturated by contaminants adsorption. Generally the breakthrough point can vary from 0,05 to 0,5 of the inlet concentration depending on the required performances of the packed bed.

All the described experimental methods allow to draw an experimental curve, called adsorption isotherm, in which the residual contaminant concentration (considered as the equilibrium one) is related to the adsorbed contaminant amount. The most ancient classification of adsorption isotherms was proposed by Giles and Smith (Giles and Smith, 1974). Therefore, isotherms are divided into four groups considering the shape

of the experimental point arrangements (Limousin et al., 2007)). The first group is called “C” isotherms and their shape is a line of zero origin (linear isotherm), in a way that the main characteristic is the linearity correlation between equilibrium concentration in solution and the adsorbed amount of contaminant. This linearity indicates that the ratio between the equilibrium concentration in solution and the adsorbed amount on the solid is the same at any concentration. Generally, this ratio is named ‘‘distribution coefficient’’ or ‘‘partition coefficient’’: K_d or K_p ($L \cdot kg^{-1}$). Formally this isotherm is similar to Henry’s law, concerning the solubility of a gas in water medium. This similarity can be explained by the adsorption of organic substances onto natural soils. The organic part of soil acts as a selective adsorbent for organic pollutant with a mechanism of adsorption in which the organic compounds dissolve into the organic fraction of soils at the same way in which a gas dissolves into water. Besides the ‘‘C’’ isotherm usually refers to situations in which the concentration of contaminants are very low, such as for trace level of pollutants. Indeed this isotherm can be seen as a part of a more general isotherm, representing the first part of it.

The second class of isotherms is called ‘‘L’’ isotherm. Under this class are grouped all the isotherms that show an initial increase of the adsorbed compound followed by a plateau in which the adsorbed amount does not change increasing the concentration of the solution. Generally, the experimental points are arranged to represent a concave curve.

The third group of isotherm is named “H” and it can be seen as a sub-group of the previous one. Its peculiarity is due to the high affinity between solid surface and contaminant which leads to a very strict initial slope. The last group is called “S” and includes all the curves that show a typical S shape. The presence of an inflection point divides the curve into two different parts: the first at low concentration and the second

at higher concentration. The change of the curve concavity is symptomatic of the transaction from an adsorption mechanism to another. The adsorption of non-polar organic compounds onto clay minerals shows an S type isotherm. Indeed the affinity of these compounds for the clay surface is very low (first part of the S, low concentration low adsorption) but as soon as a critical solution concentration is overcome the adsorbed amount starts to increase. This critical concentration corresponds to the inflection point and indicates the covering of the clay surface by the molecules of the considered compound. The presence of this monolayer favors the adsorption of other molecules up to fill the clay pores at high concentration. This phenomenon is called ‘‘cooperative adsorption’’ (Hinz, 2001).

2.2 Relevant adsorption model

The most famous isotherm model is doubtless the Langmuir adsorption model. It was at first derived for gas adsorption onto inorganic solid adsorbent and then adapted for adsorption of chemicals from liquid phase (Langmuir, 1916). Langmuir model considers the adsorption as a chemical reaction between the solid surface and the adsorbing compounds. It assumes that all the adsorption sites are identical, each site retains one molecule of the given compound, all sites are energetically and sterically independent of the adsorbed quantity and the adsorption proceeds up to the formation of a monolayer. The model equation can be written as:

$$q_e = q_{max} \cdot \frac{K_{ads} \cdot C_e}{1 + K_{ads} \cdot C_e}$$

Where q_e (mg/g) is the equilibrium solid concentration of the considered compound, C_e (mg/L) is the equilibrium liquid concentration, q_{max} (mg/g) is the maximum adsorbable amount and K_{ads} (L/g) is the affinity constant.

This isotherm has a typical shape by which it is possible to recognize three different domains. The domain at low concentration can be approximate to a straight line, thence the equilibrium concentration is proportional to the adsorbed amount and the affinity constant (K_{ads}) takes on a specific value resulting from the solid-liquid concentration ratio of the considered compound. Thus it is possible to define the affinity constant as a parameter that expresses the pollutant tendency to switch from the liquid bulk to the solid surface. The second domain is a transaction zone in which the affinity constant value is not more independent from the solid and the liquid concentration and its value is represented by the derivative of the isotherm in each point included in this part of the curve. Finally the third domain, at high concentration, in which the adsorbed amount is independent from the liquid concentration and the affinity constant assumes the zero value. This part of the isotherm is identified by a plateau and it is the asymptote of the curve that represents the second typical parameter of the isotherm, namely the maximum adsorbable amount of the compound (q_{max}). The q_{max} value is allows to know about the adsorption performances of the examined material. In the Langmuir model it also expresses the solid compound concentration corresponding to the monolayer (in this sense q_{max} assumes the meaning of the maximum covering degree of the material surface).

Freundlich isotherm model is the second most used isotherm model in the adsorption studies (Freundlich, 1906). This model, conversely to Langmuir model, predicts the adsorption behavior on the basis of a non-ideal and reversible adsorption and is not restricted to the formation of a monolayer. Its main characteristic is the capacity to describe the adsorption onto heterogeneous surface.

The model equation can be written as:

$$q_e = K_{ads} C_e^{\frac{1}{n}}$$

Where q_e (mg/g) is the equilibrium solid concentration of the considered compound, C_e (mg/L) is the equilibrium liquid concentration, K_{ads} (L/g) is the affinity constant and 1/n is a dimensionless parameter.

This model is often applied to materials that show a multilayer adsorption, with a non-uniform distribution of the adsorption heats and affinities over their heterogeneous surface (Damson and Gast, 1997). In this sense, the amount adsorbed can be considered as sum of the adsorption on all sites (each having a bond energy), where the stronger binding sites are occupied first, until the adsorption energy are exponentially decreased upon the completion of the adsorption process (Zeldowitsch, 1934). The *1/n* value can change between 0 and 1 and it indicates a measure of the adsorption intensity or surface heterogeneity, becoming more heterogeneous as its value gets closer to zero. Whereas, a value below 1 implies a chemisorption process when *1/n* is greater than one it is indicative of cooperative adsorption mechanism (Haghseresht and Lu, 1998). Recently, Freundlich isotherm has been criticized for its limitation due to a lack of a fundamental thermodynamic basis, not approaching the Henry's law at very low concentrations (Alhakawati et al., 2003).

The most important difference between Langmuir and Freundlich models consists of the energy of adsorption: the former implies an independent and definite value of it, while the latter considers a function of energies as resulting of site heterogeneity.

In this sense it is possible to consider Freundlich isotherm as a "sum of more single isotherms describing the adsorption of compounds onto each material surface sites. The global resulting isotherm, in this case the Freunlich one, is simply the sum of each contribution and considering these contributions as Langmuir types, the Freundlich isotherm is a sum of each Langmuir type contribution.

Most others isotherm models have been developed during this last century and most of them were derived from a combination of Freundlich and Langmuir isotherm or from their modifications. However it is possible to generalize the above exposed concept of isotherm. On the basis of the Langmuir model, a generalized model was constructed (Sips, 1948; Sposito, 1984; Nederlof et al., 1990). This model considers any isotherm as integral of Langmuir's isotherms (Limousin et al., 2007):

$$q = \int_{-\infty}^{+\infty} g(L) \frac{LC}{1 + LC} dK \qquad (1)$$

This integral is composed of a density function g(L) which corresponds to the statistical distribution of the local affinity constant L. Conceptually, each adsorption site provides an elementary isotherm having its own affinity L. The complete isotherm is seen as the sum of all the elementary isotherms and K represents the overall affinity constant . The function g has been named a ''weighting function'' (Sposito, 1980), a ''site affinity distribution function'' (Kinniburgh et al., 1983), or a ''frequency distribution of the

local affinity coefficient L'' (Perdue and Lytle, 1983). By varying the density function g, any type of isotherm can be described by Eq. (1) (Sposito, 1984, p. 120; Hinz et al., 1994). For example the resolution of the equation (1), considering the sum of the isotherms for those sites which show the same affinity constant L_m, gives the Langmuir isotherm. In the case of the Freundlich isotherm, g must be a log-normal distribution function, according to the concept that adsorption energy has to decrease logarithmically as the fraction of occupied sites increases (as predicted by Freunlich model). In this sense the Freundlich isotherm becomes the sum of individual Langmuir isotherms with a log-normal distribution of their affinity constants (Sposito, 1984, p. 121; Kinniburgh et al., 1983; Hinz et al., 1994).

Another general approach was introduced by Hinz (Hinz, 2001), who proposed an equation that could describe any type of isotherm introducing some simple principles:

$$q = q_{max} \sum_{i=1}^{w} f_i \prod_{j=1}^{\tau_i} \left(\frac{A_{ij} C^{P_{ij}}}{1 + B_{ij} C^{P_{ij}}} \right)^{r_{ij}}$$

where q_{max} denotes the asymptotic amount of adsorption at high concentrations, f_i is the fraction of sites of type i (whereas the total number of different types of site is ω), and τ_i gives the number of interaction terms among the different types of sites. $A_{i,j}$ and $B_{i,j}$ are empirical affinity constants and $p_{i,j}$, $q_{i,j}$ and $r_{i,j}$ are dimensionless empirical parameters. Although this equation is totally empirical and includes many fitting parameters, it has the advantage of decomposing any isotherm into different types of sites.

2.3 Kinetic point of view

The thermodynamic point of view allows to know the equilibrium characteristic of an adsorption system and the laws and equations that regulate it. To understand how the system reaches up the equilibrium condition , the kinetic point of view needs to be considered. In this sense, studying the kinetic process means to focus the attention to the variation of a property of the matter that changes in time; this property is the amount of matter. Indeed, the amount of matter is usually substituted by concentration (amount of matter per unit of volume). For the specific case of heterogeneous system such, as the adsorption one, the global kinetic is a sum of different contribution due to the system heterogeneity. The first contribution is the transport of the compound from the liquid bulk toward the interface zone of the liquid and solid material. This contribution is controlled by the concentration difference that occurs between the bulk and interface and by a parameter (transport coefficient) that includes the diffusivity of the compound in the considered medium, the fluid-dynamic conditions, medium viscosity and temperature. The influence of bulk diffusivity and transport can be nullified by stirring the solution in a proper way. The second contribution is due to the transfer of chemical species from liquid to solid phase and, also in this case, the kinetic process is ruled by the gradient concentration and transfer properties of the interface (global coefficient of mass transfer, specific area of transferring, interface thickness). This contribution is more difficult to control, being the global coefficient mass transfer strictly dependent from the thermodynamic properties of the system. However, it is possible to minimize this contribution decreasing the average dimension of solid particles without overcoming certain limit to avoid an excessive pressure drop.

Finally, the third and most important contribution is linked to the adsorption process whose rate is dependent from the mechanism of adsorption. When the mass transport in the liquid bulk phase and the mass transfer at the liquid-solid interface can be neglected,

the global rate of adsorption becomes merely a function of the adsorption rate. The adsorption kinetic can be seen like a chemical reaction between the adsorbing chemical species and active adsorptive sites present at the solid surface. From this point of view it is possible to study the system through kinetic experiments to know the order of reaction and the mechanism that rules it. Kinetic experiments consist of monitoring the variation of the species concentration (its decreasing) in time. After having collected the kinetic data, it is necessary make some hypothesis about the order and typology of reaction and verify if these hypothesis are consistent with reality. Thence ,as for the adsorption isotherms, also kinetic experiments bring to the formulation of models which have to be verified by experimental data. First of all a kinetic model is formulated on the basis of the stoichiometry of the hypothesized adsorption reaction, on the mass balance equations of the involved chemical species. Often to simplify calculations some approximations are introduced: for example it is very common to consider the active site concentration independent from the proceeding of adsorption, so it can be assumed constant and annexed to the rate constant. This approximation becomes reasonable if the system is far from the saturation state of solid surface and the active site concentration is much higher than the adsorbing compounds. In this sense, the adsorption kinetic is dependent only from the adsorbing species concentration. Commonly this kind of reaction are known as pseudo-first or pseudo-second order where the pseudo prefix needs to take into account the eventual approximations and also the parallelism with the first and second order chemical reaction. Kinetic experiments are very valuable for understanding the required time for attaining the equilibrium state. If this time is very short and compatible to industrial and real processes, it means that thermodynamic and kinetic are in agreement and it is possible to exploit all the adsorptive capacity of the material. When the equilibrium state is reached up in long time it is preferable to stop

the process before the equilibrium state, sacrificing the maximum adsorption capacity but ensuring a liquid-solid contact time useful for industrial purposes. By this point of view, the adsorption kinetic allows to know the operational adsorption capacity of materials, more useful for remediation goals than the thermodynamic ones.

As for isotherms models, it is possible to find a lot of kinetic models in literature, but each of them can be classified like a pseudo-first or pseudo-second order. The difference among these models is due to the different basic concept used for deriving them. For example, Blanchard et al. (Blanchard et al., 1984) developed an adsorption kinetic model or pseudo first order to describe the adsorption of ions onto organic zeolite, while Liu et al. (Liu et al., 2008) supposed a pseudo-first order and reversible reaction between active sites on material surface and soluble adsorbate in solution.

2.5 References

Adamson A.W. , A.P. Gast, Physical Chemistry of Surfaces, sixth ed., Wiley-Interscience, New York, 1997.

Alhakawati M.S. , C.J. Banks, S. Smallman,Water Sci. Technol. 27 (2003) 143.

Blanchard G. , M. Maunaye, G. Martin, Water Res. 18 (1984) 1501.

Fenglian Fua, Qi Wangb Removal of heavy metal ions from wastewaters: A review Journal of Environmental Management Volume 92, Issue 3, March 2011, Pages 407–418

Freundlich HMF. Über die Adsorption in Lösungen. Phys Chem. 1906; 57 (A): 385–470

Giles Charles H , David Smith A general treatment and classification of the solute adsorption isotherm. I. Theoretical Journal of Colloid and Interface Science Volume 47, Issue 3, June 1974, Pages 755–765

Haghseresht F., G. Lu, Adsorption characteristics of phenolic compounds ontocoal-reject-derived adsorbents, Energy Fuels 12 (1998) 1100–1107.

Hinz Christoph, Description of sorption data with isotherm equations Geoderma Volume 99, Issues 3–4, February 2001, Pages 225–243

Langmuir Irving The constitution and fundamental properties of solids and liquids. Part I solids. J. Am. Chem. Soc., 1916, 38 (11), pp 2221–2295

Limousin G., J. P. Gaudet, L. Charlet, S. Szenknect, V. Barthe`s, M. Krimissa. Sorption isotherms: A review on physical bases, modeling and measurement Applied Geochemistry 22 (2007) 249–275

Liu Yu, Ya-Juan Liu. Biosorption isotherms, kinetics and thermodynamics Separation and Purification Technology 61 (2008) 229–242

Nederlof B., B. Mathieu, G. Seyffart Development of Membranes for Dialysis Biomedical Engineering Volume 29, Issue 6 (Jan 1984)

Oura, K.; V. G. Lifshits; A. A. Saranin; A. V. Zotov; M. Katayama (2003). Surface Science, An Introduction. Berlin: Springer. ISBN 3-540-00545-5.

Sips Robert On the Structure of a Catalyst Surface J. Chem. Phys. 16, 490 (1948)

Sposito Garrison and Philip Fletcher Sodium-Calcium-Magnesium Exchange Reactions on a Montmorillonitic Soil: III. Calcium-Magnesium Exchange Selectivity1 Soil Science Society of America Vol. 49 No. 5, p. 1160-1163

Sudam K. Parida, Sukalyan Dash, Sabita Patel, B.K. Mishra, Adsorption of organic molecules on silica surface Advances in Colloid and Interface Science Volume 121, Issues 1–3, 13 September 2006, Pages 77–110

Thanh H. Nguyen, Hyun-Hee Cho,Dianne L. Poster and William P. Ball Evidence for a Pore-Filling Mechanism in the Adsorption of Aromatic Hydrocarbons to a Natural Wood Char Environ. Sci. Technol., 2007, 41 (4), pp 1212–1217

Zeldowitsch J. , Adsorption site energy distribution, Acta Phys. Chim. URSS 1(1934) 961–973.

CHAPTER 3

ZEOLITE AND RELATED MATERIALS

The porous solid medium of a given adsorption process is a critical variable. The success or failure of the process depends on how the solid performs in both equilibrium and kinetics. A solid with good capacity but slow kinetics is not a good choice as the adsorbate molecules take too long time to reach the particle interior. This means long molecular residence time and then a low throughput. On the other hand, a solid with fast kinetics but low capacity requires a large amount of solid for a given throughput. Thus, the right solid is the one that provides good adsorptive capacity as well as good kinetics. To satisfy these two requirements, the following aspects must be considered: (a) the solid must have reasonably high surface area or micropore volume, (b) the solid must have relatively large pore network for the transport of molecules to the interior. To satisfy the first requirement, the porous solid must have small pore sizes with a reasonable porosity. This suggests that a good solid is composed of a combination of two pore ranges: the micropore range and the macropore range. The classification of pore sizes as recommended by IUPAC (Sing et al., 1985) is often used to delineate these ranges:

Micropores: d < 2 nm

Mesopores: 2 < d < 50 nm

Macropores: d > 50 nm

This classification is arbitrary and is based on the adsorption of nitrogen at its normal boiling point on a wide range of porous solids. The practical solids commonly used in industries do satisfy these two criteria, with solids such as activated carbon, zeolite, alumina and silica gel. The industries using these solids are chemical, petrochemical, biochemical, biological, and biomedical industries. In this chapter a brief description and characterization of some important adsorbents commonly used in various industries can be found.

3.1 Activated carbon

Among the solids used in industries, activated carbon is one of the most complex solids but it is the most versatile because of its extremely high surface area and micropore volumes. Moreover, its bimodal (sometimes trimodal) pore size distribution provides good access of sorbate molecules to the interior. The structure of activated carbon is complex and it is basically composed of an amorphous structure and a graphite-like microcrystalline structure. The graphitic structure is important for the capacity as it provides "space" in the form of slit-shaped channel in which the molecules can accommodate. Because of the slit shape, the micropore size for activated carbon is reported as the micropore half-width rather than radius (as in the case of alumina or silica gel). The arrangement of carbon atoms in the graphitic structure is similar to that of pure

graphite. The layers are composed of condensed regular hexagonal rings and two adjacent layers are separated with a spacing of 0.335 nm. The distance between two adjacent carbon atoms on a layer is 0.142 nm. Although the basic configuration of the graphitic layer in activated carbon is similar to pure graphite, there are some deviations, such as the interlayer spacing ranges from 0.34 nm to 0.35 nm. Furthermore, there are crystal lattice defect and the presence of built-in heteroatoms. The graphitic unit in activated carbon usually is composed of about 6-7 layers and the average diameter of each unit is about l0 nm. The size of the unit can increase under the action of graphitization and this is usually done at very high temperature (>1000°C) and under inert atmosphere. The linkage between graphite units is possible with strong cross linking. The interspace between those graphite units will form a pore network and its size is usually in the range of mesopore and macropore.

Typical characteristics of activated carbon are listed below. Macropore having a size range greater than 100 nm is normally not filled with adsorbate by capillary condensation (except when the reduced pressure is approaching unity). The volume of macropore is usually of 0.2-0.5 cc/g and the area contributed by the macropore is usually very small, of the order of 0.5 m^2/g, which is negligible compared to the area contributed by the micropore. Macropores, therefore, have no significance in terms of adsorption capacity but they act as transport pores, allowing adsorbate molecules to diffuse from the bulk into the particle interior.

Mesopore has a size range from 2 nm to 100 nm, and it is readily filled during the region of capillary condensation (P/Po > 0.3). The volume of mesopore is usually in the range of 0.1 to 0.4 cc/g and the surface area is in the range of 10-100 m^2/g. Mesopore contributes marginally to the capacity at low pressure and significantly in the region of capillary condensation. Like macropores, mesopores act as transport pores when capillary

condensation is absent and they act as conduit for condensate flow in the capillary condensation region. Micropores are pores having size less than 2 nm. These pores are slit-shaped and, because of their high dispersive force acting on adsorbate molecule, provide space for storing most of adsorbed molecules; the mechanism of adsorption is via the process of volume filling. Chemical nature of the surface of activated carbon is more complex than the pore network. This property depends on many factors, for example the source of carbon as well as the way how the carbon is activated. Activated carbon is made of raw materials which are usually rich in oxygen and therefore many functional groups on activated carbon have oxygen atom. Moreover, oxygen also is introduced during the preparation, such as coal activation by air or gasified by water vapor. Oxygen carrying functional groups can be classified in two main types: acidic group and basic group. The functional groups of an activated carbon can be increased by treating it with some oxidizing agents or decreased by exposing it to a vacuum environment at very high temperature. Commercial activated carbon has a very wide range of properties depending on the application. For liquid-phase applications, however, due to the large molecular size of adsorbate, activated carbon will possess larger mesopore volume and larger average pore radius for the ease of molecule diffusion to the interior. Activated carbon has been largely used and still represents a good solution for many industrial applications. The most important use is for environmental purposes such as: spill cleanup, groundwater remediation, drinking water filtration, air purification, volatile organic compounds capture from painting, dry cleaning, gasoline dispensing operations and other processes. Filters with activated carbon are usually used to purified air or gaseous steam exiting from production process or waste incineration to remove oil vapors, hydrocarbons and other organic pollutants from the air. The same is applied for water purification especially in those case in which organic pollutants are predominant.

Indeed, heavy metals removal by activated carbon is more difficult because these material has weak retention capacity for inorganic anionic and cationic contaminants .

Recent studies (De La Casa-Lillo et al, 2002; Dicks, 2006) describe the use of active carbon as fuel storage, especially gaseous fuel such as light hydrocarbons and hydrogen. The particular structure of active carbon is suitable to accommodate gaseous molecules. Under the required temperature and pressure condition, activated carbon acts like a sponge that absorb gas and stored it inside the pores. Gas can be recovered by thermal desorption and burned to produce work or, as in the case of hydrogen, used in a fuel cell.

AC is not used exclusively as adsorbent, catalytic application are also documented especially as catalyst support. In this case the catalytic particles, mostly transition metal and their oxides, are dispersed in a carbon matrix that guarantee an high surface and a good dispersion of metal particles.

3.2 Alumina

Alumina is normally used as adsorbent in those industrial process requiring the water removal water from gas stream. It can be used as dryer thanks to the high functional group density on the surface, which provide active sites for the adsorption of polar molecules (e.g. water). There are several available alumina adsorbents, but the common solid used in drying is γ-alumina. The characteristics of a typical γ-alumina are given below (Biswas et al., 1987) (Table 3.1).

True density	2.9 - 3.3 g/cc
Micropore porosity	0.4 - 0.5
Macropore volume	0.4 - 0.55 cc/g
Micropore volume	0.5 - 0.6 cc/g
Specific surface area	200 - 300 m^2/g
Mean macropore radius	100 - 300 nm
Mean micropore radius	1.8 - 3 nm
Particle density	0.65 - 1.0 g/cc
Macropore porosity	0.15 - 0.35
Total porosity	0.7 - 0.77

Table 3.1. Typical characteristics of γ-alumina

As seen in the previous table, y-alumina has a good surface area and a good macropore volume for adsorption, while the mean pore size is suitable for fast transport of molecules from the surrounding to the interior.

3.3 Silica gel

Silica gel is formed from the coagulation of a colloidal solution of silicic acid. The term gel simply reflects the conditions of the material during the preparation step, not the nature of the final product. Silica gel is a hard glassy substance and milky white in color. This adsorbent is used in most of the industries for water removal, due to its strong hydrophilicity of the surface towards water. Some of the applications of silica gel are:

(a) water removal from air

(b) drying of non-reactive gases

(c) drying of reactive gases

(d) adsorption of hydrogen sulfide

(e) oil vapour adsorption

(f) adsorption of alcohols

The following table 3.2 shows the typical characteristics of silica gel.

Particle density	0.7 - 1.0 g/cc
Total porosity	0.5 - 0.65
Pore volume	0.45 - 1.0 cc/g
Specific surface area	250 - 900 m^2/g
Range of pore radii	1 to 12 nm

Table 3.2. Typical characteristics of silica gel

Depending on the conditions of preparation, silica gel can assume a range of surface area ranging from about 200 m^2/g to 900 m^2/g. The high end of surface area is achievable but the pore size is very small. For example, the silica gel used by Cerro and Smith (1970) is

a high surface area, having a specific surface area of 832 m^2/g and a mean pore radius of 11 Angstrom.

3.4 Polymeric resin

Polymeric resins are synthetic material used in adsorption technologies to recovery heavy metals or inorganic ions from liquid phase. All the resins are characterized by a polymeric matrix usually composed of monomeric units of styrene and divinylbenzene (copolymer) with a regular repetition of functional groups along the polymer chain. Based on the nature of the functional groups, polymeric resins can be divided into anionic and cationic exchange resins. Considering the strength of the functional groups, anionic and cationic resins can be distinguished into two subcategories: weak acid and strong acid exchange resin (cationic resin) and weak basic and strong basic exchange resin (anion resin). Ion exchange is not the only adsorption mechanism possible with polymeric resin. Indeed, when poly-functional non ionic group are presented, the chelating mechanism is responsible for the ionic uptake. Resuming, five kind of resin are just describe:

- *Strong cationic resin*: their functional groups derive from strong acid and they are hardly hydrolyzed both in acid and salted form in a large pH range. They are usually used with H^+ or Na^+ as counter-ion; usually, the sodium form is indicated for water softening. The regeneration takes place through a solution of H_2SO_4 o HCl with efficiency that can vary from 30% to 50%.

- *Weak cationic resin*: their functional groups derive from weak acids as carboxylic acid (—COOH) or phenol (—Ph). These resins has a low dissociation degree and they cannot react with neutral salts but they can remove carbonate and bicarbonate from water, giving carbonic acid. The dissociation degree of a weak acid resin is strongly influenced by the pH value and its removal capacity is flattened at pH value lower than 6. They have a great affinity for H^+ respect to strong cationic ones that allows to regenerate them with a lower amount of acid with an efficiency near to 100%.

- *Strong anionic resin*: Their functional group derive from strong base such ammonium quaternary salt with idroxyl ion as counter-ion (—R_4N^+OH). They can be used in all the pH range and, when the hydroxyl ion is present is ,they are used for deionizing water. The usual reaction with acid species can be outlined as follow:

$$RNH_3OH + HCl \rightarrow RNH_3Cl + HOH$$

The regeneration is made by NaOH concentrated solution with an efficiency from 30% to 50%;

- Weak anionic resin: they have weak basic group such primary, secondary and tertiary amine and their ionization degree depends on the pH value. they cannot exchange when the pH overcomes the value of 7. They do not react with neutral salts but they can remove acid molecules by adsorption:

$$RNH_2 + HCl \rightarrow RNH_2HCl$$

Regeneration is possible with non-concentrated acid solution with an efficiency of 100%.

- *Chelating resin:* they are very specific for heavy metal removal. The functional group is often EDTA group in the form of R – EDTA – Na. Other functional groups able to form strong complex with heavy metals are: iminodiacetic acid, amine, amide, ammidoxime (Warshawsky, 1986; Vernon et al., 1983). Resin such as Chelamine (Fluka), Bio-Rex-70 e Chelex 100 (Bio-Rad Laboratoires) are some examples of chelating commercial resins. The high selectivity that chelating resins shows allow to recover heavy metal both from dilute solution and high saline water, as in the case of Uranium recovery from marine water.

3.4.1 Purolite® S910 resin

Purolite S910 resin is a chelating macroporous resin specific for heavy metals removal (also at trace levels) from water. It can form a lot of complexes with different metal ions at different stability:

- Extremely stable: Cu^{2+}, Au^{3+}, $V^{2+,3+,4+,5+}$, U^{4+}, $Fe^{2+,3+}$, Rh^{3+}, $Pd^{2+,4+}$, $Pt^{2+,4+}$
- Very stable: $Ru^{3+,4+}$, $Ir^{3+,4+}$, $Os^{3+,4+}$, Cd^{2+}
- stable: Zn^{2+}, $Pb^{2+,4+}$, Cr^{3+}, Th^{4+}, $Co^{2+,3+}$, $Ni^{2+,3+}$
- moderately stable: Ag^{1+}, Sb^{3+}, $Sn^{2+,4+}$, $Mn^{2+,3+}$, Hg^{2+}, Bi^{3+}

In Table 3.3 the main physical and chemical characteristic of Purolite S910 are reported:

POLYMERIC STRUCTURE	Polyacrilic
ASPECT	Spheric particle
FUNCTIONAL GROUP	-C(NH2)NOH
IONIC FORM	FB
TOTAL EXCHANGE CAPACITY	FB 1.9 eq/l min
WATER ABSORPTION	FB 52 - 60 %
SIZE DIMENSION RANGE OF PARTICLE	0.300 - 1.200 mm con 1 % max < 0.300 mm 5 % max > 1.200 mm
SPECIFIC WEIGHT	1.15 - 1.19 g/L
MAXIMUM OPERATIVE TEMPERATURE	35 °C
PH RANGE	0 - 14

Table 3.3 Physical-chemical characteristics of resin Purolite S910 (www.purolite.com)

Polymeric material with amodixime groups similar to Purolite S910 are becoming very popular in these last decay, especially for uranium recovery from marine water (Saito et al., 1986; Omichi et al., 1986). Since the 70's the high affinity between uranium (as uranile ion) and polyamidoxime was studied. Uranium is present in marine water just for 3 µg/L (American Nuclear Society) and the total amount of uranium considering all the world marine water is approximately 4 billions of tons in a way that it a huge reservoir

for future needs. Unfortunately, because of the low concentration of this radionuclide in seawater, its extraction results very difficult. At first ferrous hydrate was used as adsorbent material with poor results; successively, the efficacy of chelating resin (amidoxime resin) to capture uranium was discovered. Whereupon the same chelating resins were employed for other heavy metals, Colella *et al*. (1980) have then demonstrated that amidoxime group are able to adsorb metals from aqueous solution.

This functional group is a bidentate group composed of a central carbon bond to an ammine group and an oxime group. It exists prevalently in sin conformation and it is stabilized by an intramolecular hydrogen bond. It can coordinate ions without undergoing any dissociation, however it loses the hydrogen of the oxime hydroxyl group in presence of heavy metals ion (Bernabè *et al*., 1999).

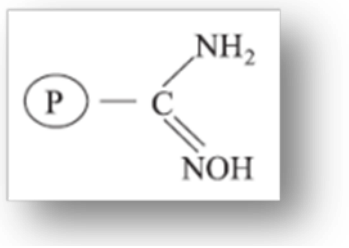

Figure 3 .1. Schematic representation of amidoxime group.

The amodoxime group is pH sensible and its structure changes passing from acid to basic solution ; in figure 3.2 is shown its equilibrium reaction.

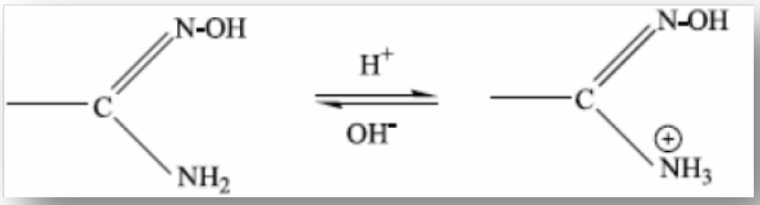

Figure 3.2. Equilibrium reaction of amidoxime group in water solution

This is a very important detail, because depending on the structure a different adsorption capacity occurs. At low pH value the protonated form of the group prevents the adsorption of metal cations, instead at higher pH the neutral form is able to coordinate cations. Indeed, Purolite S910 does not work in acid conditions.

Two different bonding mechanisms are found in literature:

Lutfor *et al*. (1999) proposed a cooperation mechanism in which two adjacent amidoxime group bond the same metal ion:

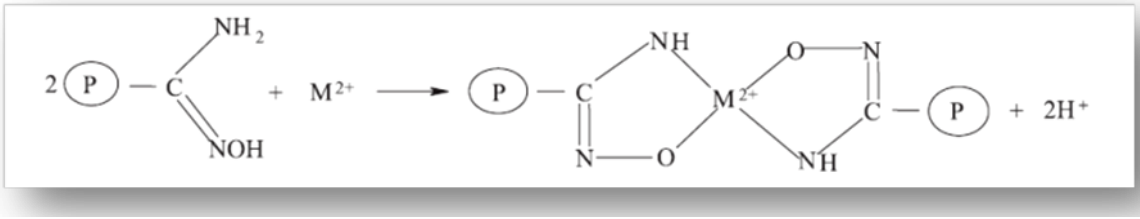

Figure 3.3. Possible chelating mechanism of amidoxime group by Lutfor et al. (1999).

Baojiao Gao *et al.* (2010) affirmed that amidoxime group can form a four-membered ring in which the metal ion is on the center or a single amidoxime group bond a cation that coordinates two water molecules as shown in fig 3.4.

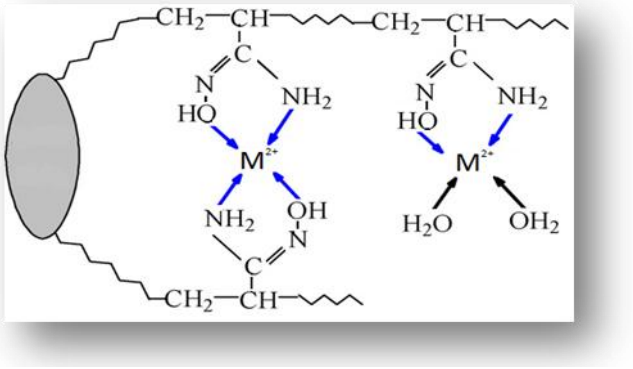

Figure 3.4. Possible chelating mechanism of amidoxime group by Baojiao Gao et al. (2010)

3.5 Zeolite

The name zeolite (from the Greek words zeo "to boil" and lithos "stone") was introduced by A. F. Cronstedt (a Swedish mineralogist) in 1756. He heated the stilbite (a kind of zeolite) and observed the bubbling of this material due to the evaporation of interstitial water.

Zeolites are a class of microporous minerals, largely used for ion exchange, adsorption and catalysis. More than forty different forms of zeolite were counted in nature, but their number is bigger considering all the zeolites produced by synthetic via. Their properties are strictly linked to their microporous crystal structure.

3.5.1 Structure and composition

The first meaning of zeolite proposed by Smith thirty years ago (1963) was alluminosilicate with opened tridimensional tetrahedral framework (called only framework) composed of a lot of cavities in which water molecules and extra-framework cations can be hosted. The high mobility of these cations and water are responsible for the cationic exchange property and the reversible dehydration of zeolite. The zeolite crystalline structure is made of tetrahedral TO_4 (T = tetrahedral species, Si, Al, etc.), where the oxygen atoms are shared by all the adjacent silicon atoms. The general chemical formula of zeolite can be written as follow:

$$\mathbf{M_{2/n}:Al_2O_3:xSiO_2:yH_2O}$$

Where M is the counter-ion (or extra-framework ion), n is the ion valence, x is usually a value bigger than 2 while y represents the water molecules inside the cavities (McCusker et al., 2001).

The tetrahedral shape is very regular while the value of T-O-T angles can change from 125° to 180°. Indeed, the tetrahedral units can join by different shapes very common in nature, such as 4, 5 and 6 membered rings of tetrahedra. The structure of a lot of zeolite is based on 24 tetrahedra of Si and Al joined together, the so-called sodalite unit (β cage) reported in 3.5.

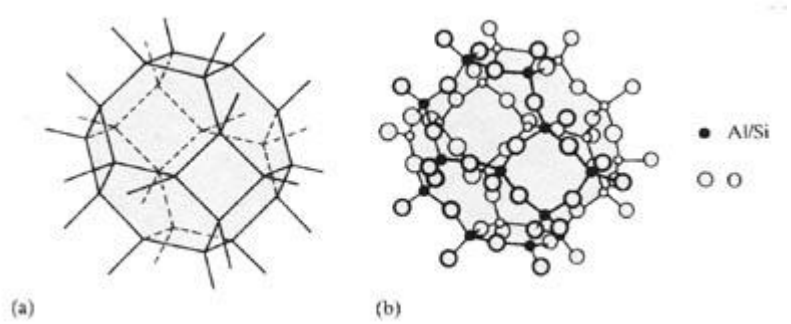

Figure 3.5. Sodalitic unit of zeolites

The SiO_4 tetrahedra are electrically neutral and they bind one another to form a tridimensional frame work as quartz. The isomorphic substitution of Si(IV) with Al(III) in the structure creates a charge unbalancing- Thus, to preserve the electroneutrality, each AlO_4 tetrahedra is associated with a counter positive ion (the extra-framework cation). The alteration of Si/Al ratio brings to a modification of the number of extra-framework cations; few Al atoms in the framework (high Si/Al ratio) involve few exchangeable cations, lots of Al atoms (low Si/Al ratio) imply a great number of these ions. For this reason zeolite characterized by high silicon content are considered more hydrophobic with a great affinity for organic compounds.

The most important feature of zeolite is the presence of internal pores and cavities linked each other by channels to form a porous network. These pores have diameters similar to molecular size and they can accommodate chemical substances of this dimension. Indeed, the possibility to host a molecule inside the pore is regulated by the dimension of the pore opening. The size of this opening depends on the tetrahedra number of the first of the several rings that composed the pore and they can vary from 300 pm to 1000 pm (Figure 3.6). As a consequence, zeolite has a high surface area suitable to adsorb huge

amount of chemical species. Typical value of surface area are about 300-700 m^2 g^{-1} , with crystallite dimension of 0.1-5 mm; more than 98% of this surface area is internal.

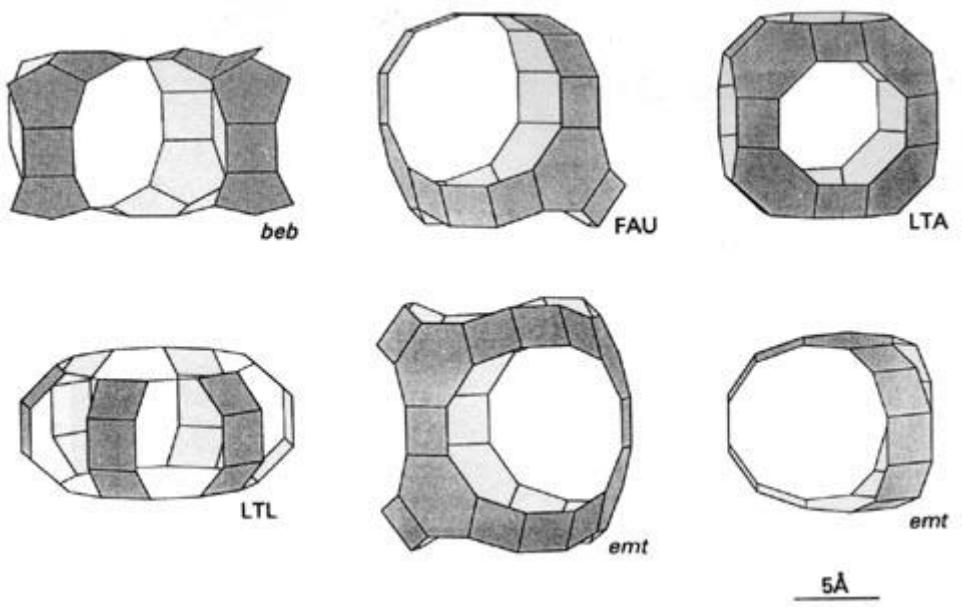

Figure 3.6. Some examples of zeolite's cavities

Zeolites can be classified into three categories based on the channel direction:

- ✓ Single direction (fibrous zeolite);
- ✓ Two directions on two parallel planes (lamellar zeolite);
- ✓ three directions (framework zeoliti).

However, many structures do not belong clearly to any of these categories.

From the structural point of view it is possible to distinguish two components: the tetrahedra framework and the extra-framework ions. On these two components is based

the general criterion of classification approved by the “Structure commission” of the “International Zeolite Association”.

Zeolite material and zeolite-like material are classified using a structural type system: materials that can have the different composition, symmetry, cell size, extra-framework content but the same frame work typology belong to one structural type.

However the most important classification was introduced by W.M. Meier & D.H. Olsen, (1996) in the "Atlas of Zeolite Structure Type" and is based on framework density. This parameter is strictly linked to porosity, providing a quantitative assessment of it.

Besides it is possible to operate a general distinction between natural and synthetic zeolite applications. In the first case we have massive use of zeolite linked to the cation exchange capacity, that made zeolite suitable to wastewater treatment (urban, nuclear or zootechnical wastewater).These processes do not required pure material, hence they do not involve high cost of operation and maintenance.

Generally, the applications of synthetic zeolites concern the catalytic operations such as cracking, reforming and isomerization of hydrocarbons. These last are not low cost applications because they require high pure materials for high catalytic activity.

In this context the use of a natural zeolite for heavy metal removal could be an excellent low-cost solution. Clinoptilolite is a natural zeolite, widely used for ammonia removal from water. It represents one of those material tested in this work to evaluate its likely usage for removing ionic metals from petrochemical wastewater.

3.5.2. Clinoptilolite

Clinoptilolite is the most abundant zeolite in nature and it can be mainly found in sedimentary rocks of volcanic origin (C. Colella, 2005).

This zeolite is extracted from its deposits through very simple techniques and it presents high purity in terms of crystalline phase and chemical composition. For these reasons the market demand of clinoptilolite is constantly increasing in these last decades. Its annual world consumption is about 3 million of tons, with costs that vary from 50 to 300 $ per ton. Clinoptilolite is a microporous crystalline material having the following chemical formula (Galli *et al.*,1983):

$$\mathbf{Na_{0.1}K_{8.57}Ba_{0.04}\ (Al_{9.31}Si_{26.83}O_{72})^{*}\ 19.56H_2O}$$

With percentage of feldspate, quartz glass and clay that vary from 10% to 40%.

The bulk structure is lamellar and it is reported in Figure 3.7:

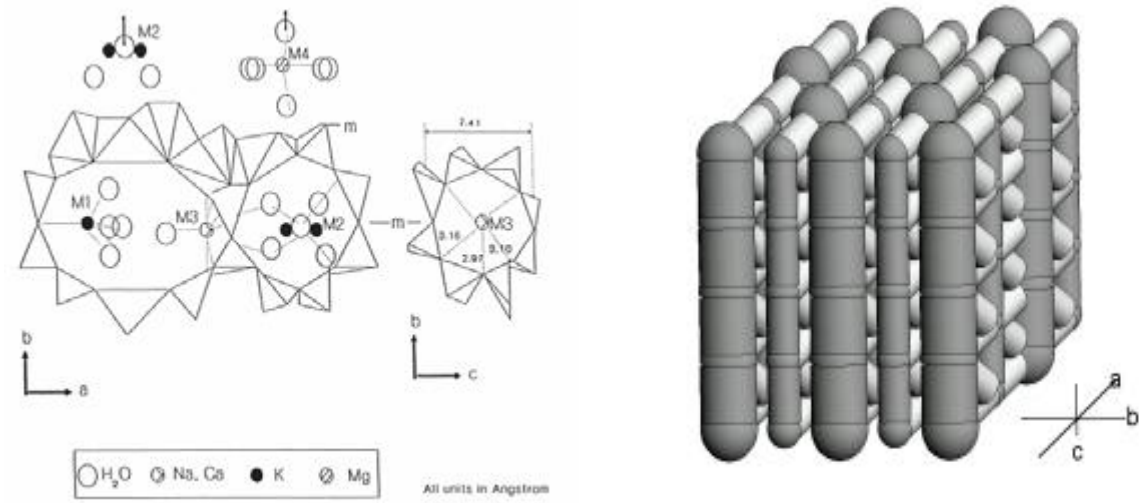

Figure 3.7. Cristalline structure of clinoptilolite

The crystal lattice involves channels of two different sizes: elliptical cage of 7,9 Å per 3,5 Å and cage of 4,4 Å per 3 Å (Barrer *et al*., 1967). Thanks to this different dimension of cages, clinoptilolite shows different selectivity for the different considered cations. The main physical properties of clinoptilolite are reported in Table 3.5.

Colour	Ivory white	**Abrasion**	87(mg/100g)
Porosity	45÷50%	**Water absorption**	42÷50%
Durezza	2÷3 Mohs	**Oil absorption**	57 (ml/100g)
Solubility	None	**Microporous area**	11 m^2/g
pH	7÷8	**Mesoporous area**	29 m^2/g
Bulk Density	0,6÷0,8 g/cm^3	**Softening point**	1150˚C
Real density	2,2÷2,4 g/cm^3	**Melting point**	1300˚C

Table 3.5. Physical properties of clinonoptilolite (www.rotamadencilik.com.tr)

The main applications of clinoptilolite are:

- ammonium (NH_4^+) removal from urban, industrial and zootechnical wastewaters due to the high selectivity of clinoptilolite for this cation (Ames,1961). The presence of ammonium ion in water is due to the composition of organic substances (proteins and nucleic acid) by microorganisms or to the direct use of ammonia and its salts in agriculture (fertilizers) and industry. Ammonium salts represents a serious danger for environment especially water body; ammonium has toxic effects on micro and

macrorganism (fishes, clams…), while nitrogen compounds (as phosphorous compounds as well) lead to eutrophication (the huge growth of algae) of lakes.

Chemical-physical methods for ammonium removal include (Cassel *et al.*, 1972): air-stripping, chlorination, biological nitrification/denitrification, selective ion exchange. The last one seems to be the most efficient and convenient approach. The use of the traditional exchange resins did not give the required performances due to the low affinity for ammonium ion and to its challenging regeneration after adsorption. Bench scale and pilot plant results (Mercer *et al.*, 1970) showed that the use of clinoptilolite for ammonium removal is the most recommended (Breck, 1974).

- Radionuclide removal from nuclear central wastewaters. Their composition changes depending on the typology of nuclear reactor, the fissile material and their usage (washing water, cooling water); however they always contain some typical radionuclide. (Sitting, 1973). The main ones (present as cations) are: ^{137}Cs,^{90}Sr,^{90}Y,^{226}Ra,^{60}Co, and others in lower quantities (Bianucci, 1977). Among these, ^{137}Cs,^{90}Sr are generally present at high concentration how seen during the Chernobyl nuclear disaster and they have half-lives at about 30 years (Chelishchev, 1995).

Radioactive effluents treatment are based on the containment of radionuclide in less dispersive phase (such as solid phase) than their origin phase. After the removal from effluents, radionuclide and containment material are stocked in special landfills, able to guarantee high impermeability for long time.

For this reason zeolites represent a good mean to sequestrate radionuclide from water by adsorption essentially due to (Pansini, 1996):

- High selective for some radionuclide such as Cs, even if at trace levels.
- Good resistance to radiation and heat;
- Possibility to incorporate in cement matrix or vetrify it after adsorption or
- Low costs

3.6 Mesoporous material

Mesoporous materials are crystalline or amorphous materials containing pores with diameter between 2 nm and 50 nm. Porous materials are classified according to their size. According to IUPAC notation, microporous materials have pore diameters of less than 2 nm and macroporous materials have pore diameters of greater than 50 nm; the mesoporous category thus lies in the middle. Typical mesoporous materials include some kinds of silica and alumina that have similarly-sized fine mesopores, mesoporous oxides of niobium, tantalum, titanium, zirconium, cerium and tin. According to IUPAC, a mesoporous material can be disordered or ordered in a mesostructure. A procedure for producing mesoporous materials (silica) was patented around 1970 (Davies, 2002; Corina, 1997; Tanev et al., 1995). It went almost unnoticed (Bagshaw et al., 1995) and was reproduced in 1997 (Attard et al., 1995). Mesoporous silica nanoparticles (MSNs) were independently synthesized in 1990 by researchers in Japan (Templin et al., 1997) They were later produced also at Mobil Corporation laboratories (Kresge et al., 1999) and named Mobil Crystalline Materials (Beck et al., 1992). These materials are part of a family of silica mesoporous materials called M41S and the most common representants are MCM-41, MCM-48 and MCM-50. MCM-41 is an amorphous silica with hexagonal

porearrangement, MCM-48 presents a cubic arrangement while MCM-50 has a lamellar structure. Since then, research in this field has steadily grown. It was discovered that varying the synthesis method it is possible to originate several different families of mesoporous materials. The most important are:

- Hexagonal Mesoporous Silica (HMS);
- Michigan State University (MSU);
- Korea Advanced Institute of Science and Technology (KIT);
- Santa Barbara Amorfous (SBA);
- Porous Clay Heterostructure (FSM).

These classes are characterized by high internal surface area (more than 1000 m^2/g), pore volume grater than a 0.8 (ml/g) with uniform and adjustable size and high thermal stability (Wang et al., 2005). For their characteristics mesoporous materials are largely employed; notable examples of applications are catalysis, sorption, gas sensing, ion exchange, optics and photovoltaics.

For these applications thermal stability and mechanical resistance are very important. For example the members of the M41S family show little resistance to compression and they undergo hydrolysis in boiling water due to the thin walls of mesopores and absence of a real crystalline structure (Gusev et al., 1996). To overcome these limits, variations of the synthetic via or post-synthetic modifications were introduced. The addition of inorganic salts during the synthesis improves the mechanical stability of the pore walls. The

hydrothermal resistance was increased by post-synthetic via. The most important is the silanization of pore walls by silylation agents such as trialkylsilanes. These methods were effective to increase the wall thickness of pores that is the most important factor for mechanical stability of siliceous materials (Mokaya, 1999). In this section some examples of mesoporous materials are presented in particular the ones that were tested during the present thesis work

3.6.1 MCM-41

Synthesis

MCM-41 is one of the member of the M41S family. Its synthesis was optimized by several studies and researchers of Mobil oil proposed two different synthetic mechanisms (Beck et al., 1992). Both the mechanisms provide a surfactant, a solvent, a source of silicon and a basic catalyst. The difference among the mechanisms is the order of ingredient addition. In the first, the surfactant (with structuring task) is added before silicon precursor, which is the responsible for micelle formation. The second mechanism provides the presence of silicon before the addition of surfactant. In the specific case of MCM-41, the synthesis was realized using alkyltrimethylammonium chloride as surfactant, precipitated silica as silicon source and sodium hydroxide and tethramethylammonium hydroxide as basic agents. The kinetic of synthesis is strictly influenced by the length of surfactant alkyl chains because they regulate the silica condensation rate. MCM-41 is synthesized at lower time when alkyl chain are long. After synthesis the surfactant has to be removed. The simplest method consists of calcination of the material but this operation brings to a structural changes of the internal surface area, the size and volume of pores. Further methods have been developed and they provide the

use of solvents for extraction (both normal solvent or supercritical fluids). The extraction process with organic solvents require large amounts of solvent and it is always followed by calcination. The use of supercritic fluid is more convenient because it allows the complete recovery of the surfactant (which can be re-used) and the resulting material presents better physical properties (Beck et al., 1992).

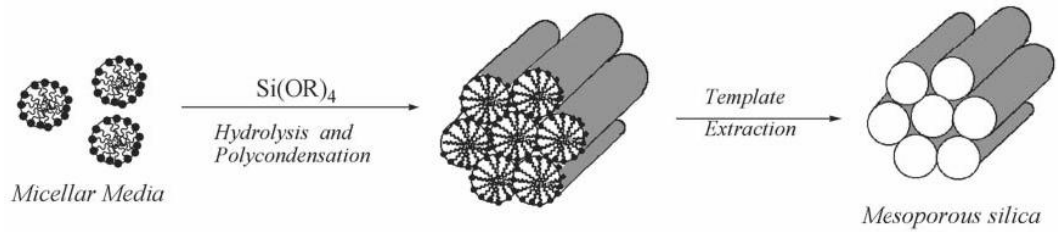

Fig 3.8 Schematic procedure of MCM-41 synthesis

Structure and properties

The MCM-41 has an high surface area, characterized by mesopores ordered in hexagonal arrangement. Connections among adjacent mesopores are absent and their opening diameter varies from 2 to 8 nm. (fig. 3.9). The internal surface presents free hydroxyl groups able to interact with polar protic molecules to form hydrogen bonds. They are also used to functionalized MCM-41 (Corma et al., 2002).

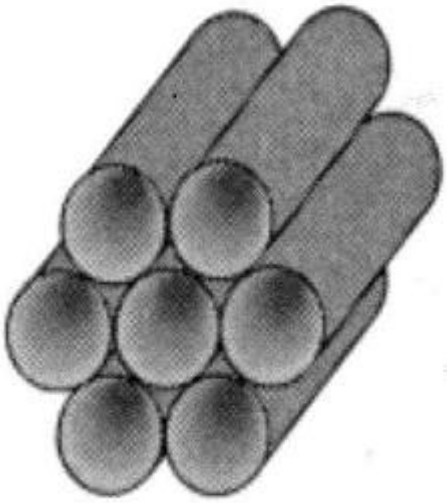

Fig. 3.9 hexagonal arrangements of mesopores in MCM-41

Functionalization

Functionalization of MCM-41 can be realized to satisfy particular requirements. Functionalizing agents react with hydroxyl groups present at surface, changing the superficial properties of MCM-41. A process of silanization is used to increase superficial hydrophobicity; the most used silanizing agents are the alkylsilanes that react with the hydroxyl groups, eliminating an acid chloride molecule. This modification is necessary to increase the affinity of the MCM-41 surface for hydrophobic molecules such as organic compounds or hydrocarbons (Matsumoto et al., 2002). The proper functionalization is operated when the alkylsilane brings a particular functional group, placed at end of one or all of its alkyl chains. The most widespread functional groups are $–NH_2$, -SH, -S-, which satisfactorily interact with metal ions such Cu^{2+}, Cd^{2+}, Hg^{2+}, Ni^{2+} (Diaz et al., 1997; Zhu et al., 2012). Functionalization leads to a decrease of pore volumes and modified both the

surface reactivity and the chemical-physical properties such as acidity, thermal stability, resistance and polarity (Zhao et al., 1998).

3.6.2. MSA

Synthesis

The MSA is an amorphous mesoporous silica. It is synthesized by sol-gel procedure using thetrapropilammonium hydroxide (TPA-OH) as structuring agent (Carati et al., 2003).

Structure and properties

MSA is characterized by an high surface area with narrow pore size distribution centered at about 40 Å. When aluminum is added to the synthesis the MSA presents a lot of Lewis acid sites very useful for acid catalysis. It is thermally stable with good mechanic resistance (Carati et al., 2003).

Applications

The MSA has not industrial applications. This material is still under studying and development and at the beginning it was synthesized for catalytic applications. In industrial field the research of appropriate catalysts is always very active. Catalysts for acid catalyzed reactions such as alkylation of aromatic hydrocarbons, oligomeration and acylation have been widely developed (Flego et al., 2003; Perego et al., 2006). At the beginning this kind of reaction was catalyzed by mineral acid (HF, H_2SO_4, $AlCl_3$), with consequent problems for safety, corrosion of devices, waste treatment and catalyst recovery. To overcome these problems a supported catalysts (such as supported phosphoric acid) was introduced. However its use was not convenient, leaving unsolved

all the problems linked to corrosion and regeneration. After, the attention was focused on solid catalysts with intrinsic acidity. Amorphous gel of silica and alumina were employed for gaseous alkylation of benzene with ethylene and propylene. Successively, amorphous gel was substituted by zeolite catalyst more efficient and cheaper. From zeolites the step to mesoporous material was short. Mesoporous catalyst can virtually catalyze major amount of reagents due to their bigger pores; besides it is possible to control their intrinsic acidity and porosity. An example of this are MCM-41, MSA, HMS successfully employed in some typical industrial reaction of hydrocarbon transformation.

In particular the MSA has shown major selectivity and activity than some zeolites Y in cumene production from alkylation of benzene with propylene. Besides it had very good performances for the synthesis of ethylbenzene (EB). For transalkylation and isomerization reactions the MSA showed the same activity of supported phosphorous acid but lower than beta zeolite (Perego et al., 1999)

The use of the MSA for environmental purposes is recently arising. The main goal is to test the applicability of the MSA as solid adsorbent for hydrocarbons removal from water. The basic idea is to recover water polluted by emulsioned and dispersed oil through a mesoporous material. The pores of the MSA (and the other mesoporous materiasl) are larger than those of common zeolite and are more suitable to accomodate hydrocarbons molecules but especially oil drops. From this point of view few studies are present about the application of mesoporous materials in water treatment leaving considerable leeway to future studies and researches.

3.6.3 Zeolite Y

Synthesis

The synthesis of Zeolite Y is achieved through a gelling process. In alkaline aqueous solution, sources of alumina (sodium aluminate) and silica (sodium silicate) are mixed together to give a gel. The gel is usually heated to 300ºC to generate the crystalline structure of zeolite. Generally, after synthesis the zeolite is present in Na^+ form (sodium ion occupies the exchange sites) and must be converted to acidic form, the most useful for catalytic purposes (US Patent 3920798) . It is not possible to convert the zeolite Y to acidic form for direct contact with concentrated acid solution because of the low resistance of zeolite to acids. To prevent disintegration of the structure from acid attack, it is at first converted to the NH_4^+ form. In particular application a deposit of metal inside the zeolite framework is needed, generally metal with strong catalytic properties. For example, in the hydrogenation of unsaturated hydrocarbons platinum atoms are deposited on the Zeolite Y surface via impregnation or ion exchange (Malyala et al., 2000). In this case the zeolite is no more the catalyst but the support for platinum that is the real catalyst.

Structure and properties

Zeolite Y is the synthetic counter-part of Faujasite, a natural zeolite. It has the same framework structure based on the sodalitic cage but different molar ratio of silicon and aluminum: faujasite has Si/Al ratio between 2,14 and 2,70 while zeolite Y between 1,5 and 3. Zeolite Y has a 3-dimensional pore structure with pores running perpendicular to each others in the x, y, and z planes, and is made of secondary building units 4, 6, and 6-6. The pore diameter is large at 7.4Å since the aperture is defined by a 12 member oxygen ring and leads into a larger cavity of diameter 12Å. The cavity is surrounded by

ten sodalite cages (truncated octahedra) connected on their hexagonal faces. The unit cell is cubic (a = 24.7Å) with Fd-3m symmetry. Zeolite Y has a void volume fraction of 0.48. It thermally decomposes at 793ºC.

Applications

The most important use of zeolite Y is as cracking catalyst. It is used in acidic form in petroleum refinery catalytic cracking units to increase the yield of gasoline and diesel fuel from crude oil feedstock by cracking heavy paraffins into gasoline grade napthas. Zeolite Y has superseded zeolite X in this use because it is both more active and more stable at high temperatures, due to the higher Si/Al ratio. It is also used in the hydrocracking units as a platinum/palladium support to increase aromatic content of reformulated refinery products (Malyala et al., 2000)

3.6.4 SBA-15

The mesoporous SBA-15 (Santa Barbara amorphous) is an amorphous mesoporous material characterized by the simultaneous presence of micropores and mesopores in its structure.

Synthesis

Typical synthesis of SBA-15 requires triblock copolymer, typically non-ionic triblock copolymer (Zhao et al., 1998b), as structure directing agent and Tetramethyl Orthosilicate (TMOS) (Zhao et al., 2000), Tetraethyl Orthosilicate (TEOS) (Zhao et al., 1998a) or Tetrapropyl Orthosilicate (TPOS) (Zhao et al., 1998b) as silica source. This synthesis is very different from synthesis of other mesoporous materials, not involving a template but a triblock copolymer to generate micro and mesopores. According to Zhao et al. (2000)

the formation of ordered hexagonal SBA-15 with uniform pores up to 30 nm was synthesized using amphiphilic triblock copolymer in strong acidic media i.e., pH ~1. Indeed, low pH value is necessary to guarantee the precipitation and formation of silica gel. Copolymer removal is one of the critical aspects of mesoporous silica synthesis because this procedure could modify the final properties of the material. The usual method of removing template is calcination. Indeed, holding silica at high temperature can modify the structure and surface and so the properties of the silica.

Structure and properties

As already mentioned, SBA-15 is an amorphous mesoporous silica. The main characteristic of this material is the simultaneous presence of mesopores and micropores in the structure. Hence SBA-15 does not have a crystalline structure but the mesopores are highly ordered following an hexagonal geometry such as in MCM-41. Micropores instead are not ordered but they represent a parallel and disordered pores system that acts as interconnection channel system for mesopores. In this sense SBA-15 is part of a family of material called hierarchic material, in which it is possible to visualize different level of organization: disordered framework (amorphous material), disordered micropores and ordered mesopores. As other mesoporous material SBA-15 has great internal surface and high pore volume and it also is very thermally stable. It has not a great mechanical and chemical resistance.

Applications

Full scale and industrial applications of SBA-15 are not reported in literature, being SBA-15 recently developed. A lot of experimentations are instead present (Wang et al., 2005; Martinez et al., 2003), especially as catalyst for many reactions of industrial interest. SBA-15 is not suitable only for catalyst; it can have different uses as gas storage in

energy field or as pollutants adsorbent for environmental protection. Rahamat et al. (2010) described the use of SBA-15 as catalyst for biorefinery application or waste transformation, in particular for production of fine chemicals and hydrogen from typical compounds of biological process such ethanol, fatty acids and sugars. As synthesized and modified SBA-15 was tested as adsorbent material for recovery of pollutants or chemicals from water. Lombardo et al (2012) described the use of SBA-15 with functionalized surface for Cu (II) removal. The functionalizing agents, an aminopropyl chain, showed high efficiency for Cu (II) uptake transforming SBA-15 into an ion exchanger. Without any post-synthetic modifications SBA-15 could potentially be a good non-polar hydrocarbon adsorbent especially if dehydroxylated.

3.7 References

Ames L.L. Jr.. Cation sieve properties of the open zeolites chabazite, mordenite, erionite and clinoptilolite. Am. Mineral., (1961) 46, p.7120

Andrew L. Dicks. The role of carbon in fuel cells. Journal of Power Sources Vol. 156, Issue 2, 1 June 2006, Pages 128–141

Attard G. S., J.C.Glyde, C. G. Goltner, Nature, 378 (1995)366.

Bagshaw S. A. , E. Prouzet, T. .I. Pinnavaia, Science, 269 (1995) 1242.

Baojiao Gao, Yuechao Gao, Yanbin Li (2010). Preparation and chelation adsorption property of composite chelating material poly(amidoxime)/SiO2 towards heavy metal ions. Chemical engineering journal, 158, pp. 542-549

Barrer R.M., Papadopoulos R., Rees L.V.C., (1967). Exchange of sodium in clinoptilolite by organic cations. Inorg. Nucl. Chem. 29, p. 2047

Beck J.S., J.C.Vartu1, W.J.Roth, M.E.Leon0wicz, C.T.Kresge, K.D.C Schmitt, T.W.Chu, .D.H.Olson, E.W.Sheppard, S.B.McCullen, J.B Higgins, J.L. Schlenker, J. Am. Chem. Soc., 114(1992) 10834.

Bernabè L. Rivas, Hernan A. Maturana, Villegas S., (1999). Adsorption behavior of metal ions by amidoxime chelating resins. Journal of Applied Polymer Science, 77, pp. 1994-1999

Bianucci G. e Ribaldone Bianucci E. (1977). Il trattamento delle acque residue industriali e agricole. Hoepli, Milano, p. 381

"Biswas J. , D.D. Do, P.F. Greenfield, J.M. Smith. Evaluation of bidisperse transport properties of a reforming catalyst using a diffusion cell I. Theoretical development. Applied Catalysis, Volume 32, 1987, Pages 217–234

Breck, D. W. (1974). Zeolite molecular sieves. Wiley, New York

Carati et al. Preparation and characterisation of mesoporous silica–alumina and silica–titania with a narrow pore size distribution. Catalysis Today 77 (2003) 15–323.

Cassel A.F., Pressley T.A., Schuk W.W., Bishop D.F. (1972). Physicalchemical nitrogen rimoval from municipal wastewater. AIChE, Symp. Ser. 68 (124), p. 56

Chelishchev N.F. (1995.) Use of natural zeolites at Chernobyl: Natural Zeolites '93. Occurence, Properties, Use. D.W. Ming e F.A. Mumpton (eds.), International Committee on Natural Zeolites, Brockport, New York 14420, p. 525

Colella M.G., Siggia S., Barnes R.M. (1980). Anal Chem, 52, p. 967

Colella C. (2005). Natural zeolites. Studies in Surface Science and Catalysis, 157, pp.13 - 40

Corina A. , Chem. Rev., 97 (1997) 2373.

Corma Avelino , Hermenegildo García, Ahmed Moussaif, María J. Sabater,Rachid Zniber and Achour Redouane. Chiral copper(II) bisoxazoline covalently anchored to silica and mesoporous MCM-41 as a heterogeneous catalyst for the enantioselective Friedel–Crafts hydroxyalkylation. Chem. Commun., 2002, 1058-1059

Davis M. E. , Nature, 417 (2002) 813.

De la Casa-Lillo M. A. , F. Lamari-Darkrim, D. Cazorla-Amorós and A. Linares-Solano. Hydrogen Storage in Activated Carbons and Activated Carbon Fibers J. Phys. Chem. B, 2002, 106 (42), pp 10930–10934

Díaz J. Felipe, Kenneth J. Balkus Jr., Fethi Bedioui, Vadim Kurshev and Larry Kevan. Synthesis and Characterization of Cobalt−Complex Functionalized MCM-41. Chem. Mater., 1997, 9 (1), pp 61–67

Flego et al. Reaction and deactivation study of mesoporous silica–alumina (MSA) in propene oligomerisation. Journal of Molecular Catalysis A: Chemical 204–205 pp. 581–589. 2003.

Galli E., G. Gottardi, H.Mayer, A. Preisinger, E. Passaglia (1983). Acta Crystallogr. Sect. B 39, p. 189.

Gusev V.Y. , X.Feng, Z. Bu, G.L. Haller, J.A. O'Brien, Journal Physical Chemistry B. 1996.

Kresge C.T., M.E. Leonowicz, W.J. Roth, J.C. Vartuli, J.S. Beck, Nature, 359 (1992) 710.

Lutfor M.R., Sidik Silong, Wan Md Zin, M.Z. Ab Rahman, Mansor Ahmad, Jelas Haron (1999). Preparation and characterization of poly(amidoxime) chelating resin from polyacrylonitrile grafted sago starch. European polymer journal, 36, pp. 2105-2113

M.V. Lombardo, M. Videla, A. Calvo, F.G. Requejo, G.J.A.A. Soler-Illia. Aminopropyl-modified mesoporous silica SBA-15 as recovery agents of Cu(II)-sulfate solutions: Adsorption efficiency, functional stability and reusability aspects. Journal of Hazardous Materials, Volumes 223–224, 15 July 2012, Pages 53–62

Martínez Agustín, Carlos López, Francisco Márquez, Isabel Díaz. Fischer–Tropsch synthesis of hydrocarbons over mesoporous Co/SBA-15 catalysts: the influence of metal loading, cobalt precursor, and promoters. Journal of Catalysis, Volume 220, Issue 2, 10 December 2003, Pages 486–499

Matsumoto Akihiko, Kazuo Tsutsumi Kai Schumacher and Klaus K. Unger Surface Functionalization and Stabilization of Mesoporous Silica Spheres by Silanization and Their Adsorption Characteristics. Langmuir, 2002, 18 (10), pp 4014–4019

McCusker L.B., Baerlocher C., (2001). Zeolite structures. In: Introduction to zeolite science and practice, Van Bekkum, H., Flanigen, E.M., Jacobs, P.A., Jansen, J.C., Studies in Surface Sci. and Catalysis 137, p.37

Meier W.M. & D.H. Olson, 1996. Atlas of zeolite structure type. International zeolite association, structure commission, pp. 99

Mercer B.W., Ames L.L., Touhill C.J., Van Slike W.J., Dean R.B. (1970). Ammonia removal from secondary effluents by selective ion exchange. J. Water Pollut. Control Fed. 42 (2), R95

Mokaya R., Journal Physical Chemistry B. 1999.

Omichi H., Katai A., Sugo T., Okamoto J., 1986. A new type of amidoxime-group containg adsorbent for recovery of uranium from seawater II. Effect of grafting of hydrophilic monomers. Science Technologies, 21 (3), pp. 299-313

Pansini M. (1996) Natural zeolites as cation exchange for environmental protection. Mineralium Deposita, 31, p. 563

Perego et al. Amorfous aluminosilicate catalysts for hydroxyalkylation of aniline and phenol. Applied Catalysis A: General 307 (2006) 128-136

Perego, S Amarilli, A Carati, C Flego, G Pazzuconi, C Rizzo, G Bellussi. Mesoporous silica-aluminas as catalysts for the alkylation of aromatic hydrocarbons with olefins Microporous and Mesoporous Materials Volume 27, Issues 2–3, February 1999, Pages 345–354

R.V. Malyala, C.V. Rode, M. Arai, S.G. Hegde, R.V. Chaudhari. Activity, selectivity and stability of Ni and bimetallic Ni–Pt supported on zeolite Y catalysts for hydrogenation of acetophenone and its substituted derivatives. Applied Catalysis A: General Volume 193, Issues 1–2, 28 February 2000, Pages 71–86

Rahmat Norhasyimi, Ahmad Z. Abdullah and Abdullah R. Mohamed. A Review: Mesoporous Santa Barbara Amorphous-15, Types, Synthesis and Its Applications towards Biorefinery Production. American Journal of Applied Sciences, Volume 7, Issue 12 Pages 1579-1586

Ramon L. Cerro and J. M. Smith. Chromatography of nonadsorbable gases. AIChE Journal Vol. 16, Issue 6, pages 1034–1038, November 1970

Saito K., Hori T., Furasaki S., Sugo T., Okamoto J., 1986. In 3rd World congress of Chemical Engineering, Tokyo, pp. 683-686

Sing K. S. W. , D. H. Everett, R. A. W. Haul, L. Moscou, R. A. Pierotti, J. Rouquerol, T. Siemieniewska Reporting physisorption data for gas/solid systems with special reference to the determination of surface area and porosity. Pure & Applied Chemestry Vol. 57, No. 4, pp. 603—619, 1985.

Sitting M. Pollutant Removal Handbook. Noyes Data Corporation, Park Ridge, New Jersey, (1973) p. 478;

Tanev P. T. ,T. J. Pinnavaia, Science, 267(1995) 865.

Templin M. , A. Franck, A. DuChesne, H. Leist, Y. M. Zhang, R. Ulrich, V. Schadler and U. Wiesner, Science, 278(l997) 1795.

US Patent 3920798

Vernon F., Shash T.. Synthesis of carboxyl group containing hydrazine-modified polyacrylonitrile fibres and application for the removal of heavy metals. React. Polim, (1983) 1, p 301

Wang Geun Shim, Jae Wook Lee, Hee Moon. Adsorption equilibrium and column dynamics of VOCs on MCM-48 depending on pelletizing pressure. Microporous and Mesoporous materials. 2005

Wang Xueguang, Kyle S. K. Lin , Jerry C. C. Chan , and Soofin Cheng. Direct Synthesis and Catalytic Applications of Ordered Large Pore Aminopropyl-Functionalized SBA-15 Mesoporous Materials. J. Phys. Chem. B, 2005, 109 (5), pp 1763–1769

Warshasky A. (1986). Ion Exchange: Science and Thecnology

Zhao X. S. and G. Q. Lu. Modification of MCM-41 by Surface Silylation with Trimethylchlorosilane and Adsorption Study. J. Phys. Chem. B 1998, 102, 1556-1561

Zhao, D., J. Feng, Q. Huo, N. Melosh and G.H. Fredrickson. Triblock copolymer syntheses of mesoporous silica with periodic 50 to 300 angstrom pores. Science, 1998a, 279: 548

Zhao, D., J. Sun, Q. Li and G.D. Stucky. Morphological control of highly ordered mesoporous silica SBA-15. Chem. Mat., 12, 2000, 275-279.

Zhao, D., Q. Huo, J. Feng, B.F. Chmelka and G.D. Stucky. Nonionic triblock and star diblock copolymer and oligomeric surfactant syntheses of highly ordered, hydrothermally stable, mesoporous silica structures. J. Am. Chem. Soc., 1998b, 120, 6024-6036.

Zhu Zhen, Xinxin Yang, Liang-Nian He and Wei Li. Adsorption of Hg2+ from aqueous solution on functionalized MCM-41. RSC Advances, 2012, 2, 1088–1095

CHAPTER 4

NEW MATERIAL FOR HEAVY METALS REMOVAL: BATCH TESTS

Production water from petrochemical activities are contaminated by hydrocarbons (dissolved and dispersed) and also by heavy metals at trace levels. Environmental and toxicological effects of heavy metals are more relevant and dangerous than the hydrocarbon's and it is necessary to remove them from water in association to organic compounds removal. In this chapter we analyzed the use of some known adsorptive materials for the heavy metals uptake exploring different environmental conditions and then we compared their performances with ones of a new material whose performances towards heavy metal removal are unknown. Clinoptilolite (natural zeolite) and Purolite S910 resin (commercial material) are chosen as reference materials while a mesoporous silica alumina (MSA) is the new material to test.

4.1 Materials

The clinoptilolite zeolite used in this work came from a cave in Turkey in the locality of Rota, and the synthetic Purolite® S910 Resin was bought from Purolite. The mesoporous silica material (MSA) was synthesized according to the procedures found in the literature (Carati et al., 2003). After synthesis, the MSA particles were extruded in a cylindrical shape, using Al_2O_3 as a binder. This extrusion was considered for future full-scale applications of the MSA. A textural characterization of this material yielded a BET

surface of 487 m^2/g, pore volume of 1,04 cm^3/g (Gurvitsch method) and an average pore diameter of 50 nm (NDLFT method).

4.2 Methods

Before use, the clinoptilolite was sieved to a size range of 500-1000 µm, washed with deionized water twice for 24 hours and then put in contact with a sodium chloride 2 M solution for a further 24 hours. This last step ensured the presence of Na^+ as an exchangeable ion in almost all of the active sites, introducing homogeneity to the exchange process. The pretreatment on chelating Purolite® S910 Resin included a rinsed step with deionized water and a secondary activation step by keeping the material in contact with a sodium chloride solution for 24 hours. This latter step was necessary to remove all the H^+ ions present after the synthesis and substitute them with Na^+. No preliminary steps were required for the mesoporous material; it was stored overnight in an oven at 550 °C to remove adsorbed water and synthetic residuals, and then stored in a desiccator.

A kinetic study was carried out in a batch configuration to compare the material behavior under different conditions and evaluate the time needed to attainment equilibrium (to be used in the isotherm experiments). Monocomponent solutions of the targeted heavy metals, Ni^{2+}, Pb^{2+} and Cd^{2+}, and of two organic pollutants, benzene and toluene, were used to perform adsorption kinetic experiments on each adsorbent, the clinoptilolite, Purolite® S910 Resin and MSA. The initial heavy metal concentration was approximately 1 mg/L and those of toluene and benzene were 400 mg/L and 600 mg/L, respectively. These concentrations were always under the solubility limit in water of toluene and benzene (respectively 550 mg/L and 1779 mg/L). The samples were collected

at a fixed time and analyzed using an ICP-OES (Vista MPX, Varian®) for the heavy metals and a TOC-CSV analyzer (Shimadzu®) for the organic compounds.

A second experimental set was performed to obtain adsorption isotherms. 0.05 g of each adsorbent material was put in contact with 50 ml of a monocomponent solution at increasing initial concentrations, maintaining a constant solid vs. liquid ratio of approximately 1 g/L under continuous rotative stirring. Based on the previous kinetic study, 24 hours of contact time was considered adequate to establish equilibrium conditions. Additional tests were also performed as blanks without the presence of sorbent materials. Reactive and blank samples were collected and analyzed at a set time. The influence of increasing ionic strength and possible adsorption interference due to the presence of organic contaminants was investigated during the heavy metal tests. 10^{-3} M and 10^{-1} M $NaNO_3$ solutions were used to simulate two different ionic strength conditions related to groundwater and seawater, respectively.

The effect of the presence of organic contaminants on the performance of clinoptilolite and synthetic Purolite® S910 Resin were also explored. Isotherm batch experiments were carried out by adding benzene as an organic co-contaminant, which was chosen because it can be considered a good representative of oil co-contamination, being part of the BTEX group (benzene, toluene, ethylbenzene and xylene).

4.3 Data evaluation

4.3.1 Kinetic and thermodynamic models

The kinetic data in the single experiments were interpreted using a pseudo-first order kinetic model in which the constant rate includes the contribution of several mechanisms

typical of a heterogeneous reaction. The adsorption process is a chemical-physical process taking place until the exhaustion of the driving force (which is the distance from the corresponding equilibrium condition). Thus, the kinetic experiments were interpreted based on the following equation:

$$\frac{dC}{dt} = k_{obs} \cdot (C - C_e) \quad (1)$$

where C is the contaminant concentration in mg/L (hydrocarbons) or µg/L (heavy metals) at time t, C_e is the equilibrium concentration in mg/L (hydrocarbons) or µg/L (heavy metals) of the contaminant at the end of the experiment (as calculated during the regression procedure), kobs is the adsorption rate constant in min^{-1} and t is the time in minutes. Integrating eq. 1 from time 0 to the generic time t, corresponding to the integration between C_0 (initial concentration) and C, we obtained:

$$C = C_0 + C_e \cdot (1 - e^{k_{obs} \cdot t}) \quad (2)$$

This kinetic expression is valid under the hypothesis of linear adsorption isotherm. In this case, as will be seen later, the adsorption of heavy metals onto clinoptilolite and resin Purolite® is not described by a simple linear isotherm. However the kinetic study was performed using a starting metal concentration of about 1 mg/L that is largely inside the linear range of their adsorption isotherm. Under this assumption the application of this kinetic model could be justified despite the global isotherm is not linear. All of the kinetic data were fitted using this model, and the optimized parameters were obtained by nonlinear regression using commercial software.

The equilibrium ion exchange and heavy metal chelating process were described by a specifically designed adsorption isotherm, whereas the benzene and toluene adsorption onto MSA was described using the model created by (Lee et al, 2003).

The ion exchange and chelating model was developed assuming a 1 - 2 stoichiometry (two Na^+ ions that exchange with a Me^{2+} ion) for the exchange/chelating process, as expressed by the following reaction:

$$2Na^+S^- + Me^{2+} \leftrightarrow Me^{2+}S_2^{2-} + 2Na^+ \quad (3)$$

where S indicates the generic active site and Me^{2+} the generic heavy metal cation. Next, the mass balance of the total generic active sites S (equation 4) and the equilibrium law for the exchange/chelating process (equation 5) could be formulated as

$$S_T = \{Na^+S^-\} + 2 \cdot \{Me^{2+}S_2^{2-}\} \quad (4)$$

$$K = \frac{\{Me^{2+}S_2^{2-}\}[Na^+]^2}{\{Na^+S^-\}[Me^{2+}]} \quad (5)$$

where S_T indicates the total number of active sites, $\{Na^+S^-\}$ the number of active sites occupied by Na ions, $\{Me^{2+}S_2\}$ the number of active sites occupied by heavy metal cations and K the equilibrium constant. Assuming that the variation in Na^+ concentration was negligible due to the exchange phenomena, we incorporated $(Na^+)^2$ in the K value, transforming it into the conditional equilibrium constant K_{Na+}. $\{Na^+S^-\}$ was then explicated from eq. (4) and substituted into eq. (5). Rearranging eq. (5) to express the

metal sorbed ($\{Me^{2+}S_2\}$ as q_e) as a function of equilibrium concentration ((Me^{2+}) as C_e) and indicating S_T by q_{max}, the adsorption model was expressed as

$$q_e = \frac{1}{2} \cdot \left(\left[\frac{2K_{Na+} \cdot q_{max} \cdot C_e + 1}{K_{Na+} \cdot C_e} \right] - \sqrt{\frac{4K_{Na+} \cdot q_{max} \cdot C_e + 1}{(K_{Na+} \cdot C_e)^2}} \right) \quad (6)$$

where q_e is the equilibrium metal concentration in the solid in µg/g, q_{max} is the maximum metal concentration in the solid in µg/g, C_e is the metal equilibrium concentration in the liquid phase in µg/L and K_{Na+} is the conditional equilibrium constant of the adsorption process in L/µg.

The heavy metal isotherm data were fitted using this model, testing its adaptability to the different experimental conditions applied to the adsorption system.

4.4 Results and discussion

4.4.1 Adsorption kinetics: heavy metals

Figures 4.1, 4.2 and 4.3 show the adsorption kinetics of Pb^{2+}, Cd^{2+} and Ni^{2+} onto the clinoptilolite, Purolite® S910 Resin and MSA, respectively. High removal of each metal and fast adsorption kinetics were observed.

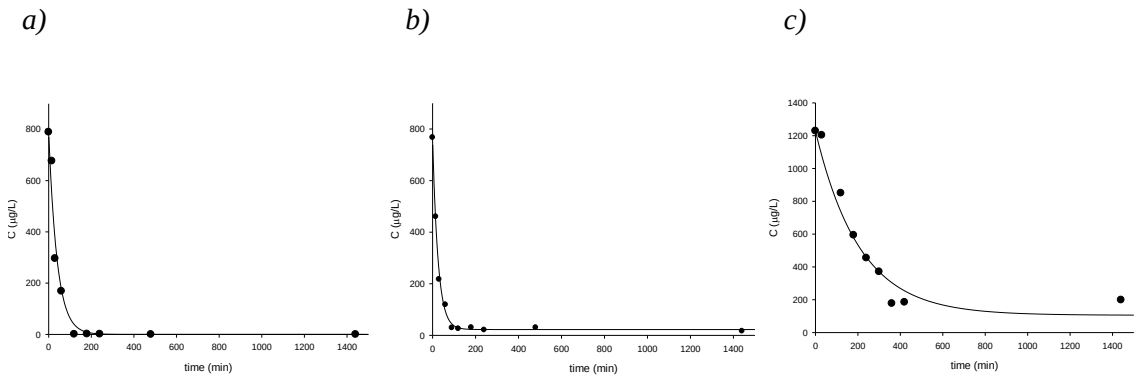

Fig 4.1 *Adsorption kinetics of Pb^{2+} onto a) Purolite S910 resin b) clinoptilolite c) MSA.*

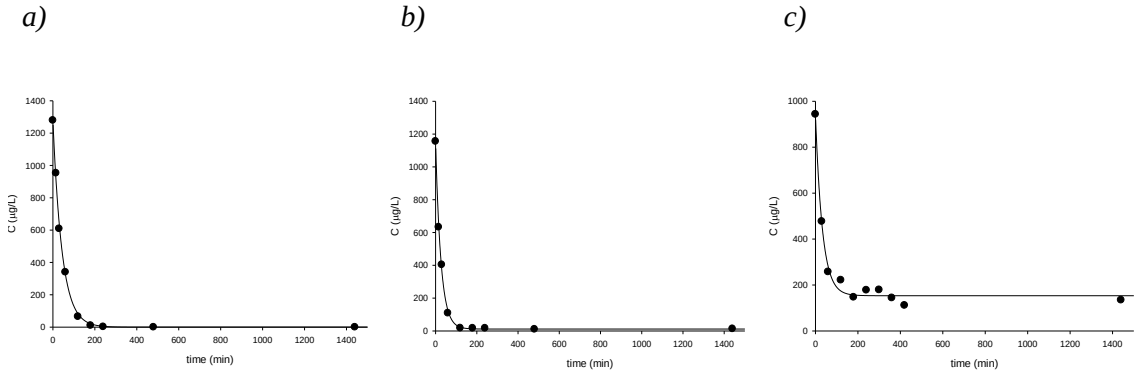

Fig 4.2. *Adsorption kinetics of Cd^{2+} onto a) Purolite S910 resin b) clinoptilolite c) MSA.*

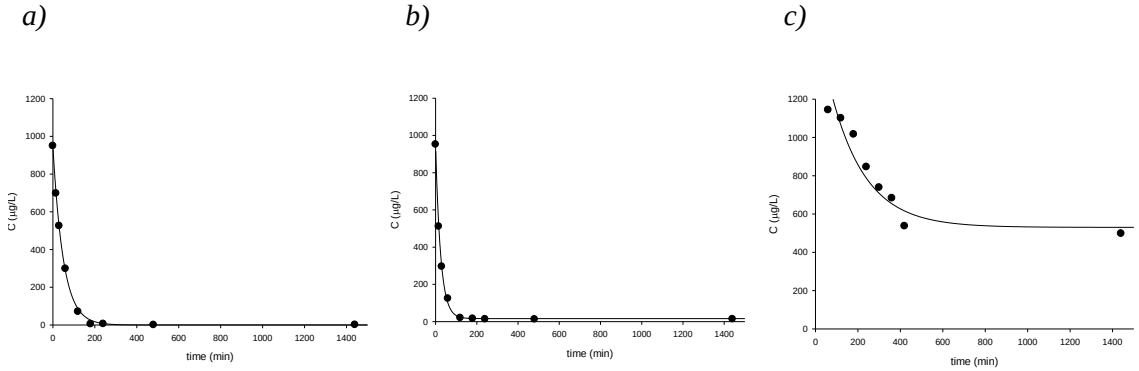

Fig 4.3. *Adsorption kinetics of Ni^{2+} onto a) Purolite S910 resin b) clinoptilolite c) MSA.*

The parameters obtained by the nonlinear regression according to the pseudo-first order model (eq. 1) are shown in Table 4.1, where each parameter is accompanied by the value of its own standard error. In this table and in the following tables the C_0 value has not to

be considered an optimized parameter obtained by the data fitting but a measured parameter.

		K_{obs} (min^{-1})	Ce (µg/L)	Co (µg/L)	R^2
Purolite Resin S910	Pb^{2+}	0.0251±0.033	(1.56±0.6)E-18	789±21	0.971
	Cd^{2+}	0.0229±0.0012	(3.45±0.38)E-17	1278±51	0.998
	Ni^{2+}	0.0200±0.0056	(2.91±0.35)E-18	950±12	0.999
Clinoptilolite	Pb^{2+}	0.0394±0.0069	22.6±32.8	767±27	0.995
	Cd^{2+}	0.0384±0.0025	11.74±16.90	1155±52	0.999
	Ni^{2+}	0.0403±0.0231	16.2±3.1	952±22	0.999
MSA	Pb^{2+}	0.0048±0.0005	105±28	1228±33	0.966
	Cd^{2+}	0.0305±0.0546	451.1±235.9	2775±55	0.989
	Ni^{2+}	0.0061±0.0012	530±312	1639±47	0.945

Table 4.1. *Kinetic parameters of Pb2+, Cd2+ and Ni2+ onto a) Purolite S910 resin b) Clinoptilolite and c) MSA*

.

The standard error for the adjustable parameters C_e and K_{obs} was calculated by the regression procedure, whereas the instrumental precision was referenced for the measured parameter C_0. The k_{obs} value was similar for all of the tested metals for both clinoptilolite and Purolite® S910 Resin, suggesting slight differences between each adsorption rate. The performance of the MSA in heavy metal removal was not as good as that of the Purolite® S910 Resin and clinoptilolite. The attainment of an equilibrium state occurred

within 100 minutes for the zeolite and Purolite® S910 Resin, whereas the equilibrium state was not reached before 200 minutes with the MSA. However, the model satisfactorily represented the kinetics of the selected heavy metal adsorption process, as also testified by the high Pearson coefficient (R^2) value.

4.4.2 Heavy metal adsorption isotherms: clinoptilolite and Purolite® S910 Resin

Figures 4.4, 4.5 and 4.6 show the adsorption isotherm of the target heavy metals onto the Purolite® S910 Resin and natural zeolite (clinoptilolite).

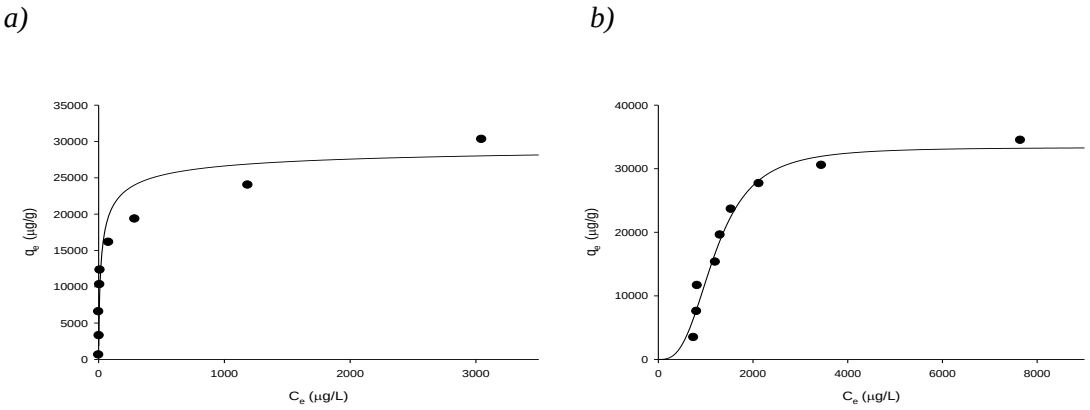

Fig 4.4*. Adsorption isotherm of Pb^{2+} onto a) Purolite S910 resin and b) clinoptilolite (comparison between experimental and calculated behavior according to equation (4), panel a, and (5), panel b).*

a) *b)*

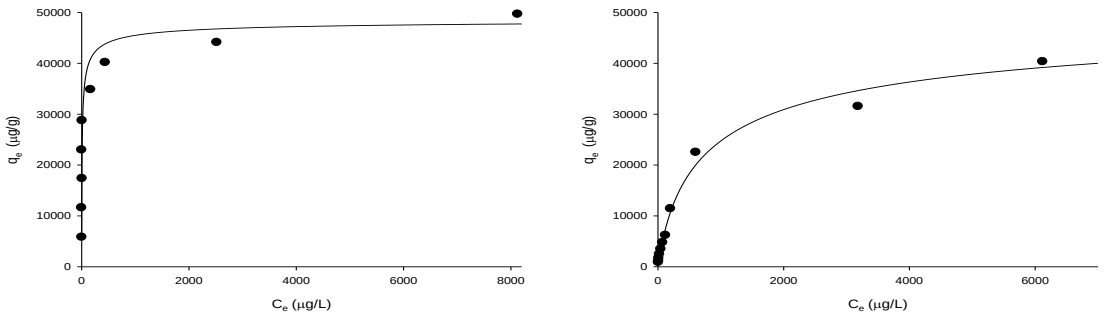

Fig 4.5. *Adsorption isotherm of Cd^{2+} onto a) Purolite S910 resin and b) clinoptilolite (comparison between experimental and calculated behavior according to equation (4)).*

a) *b)*

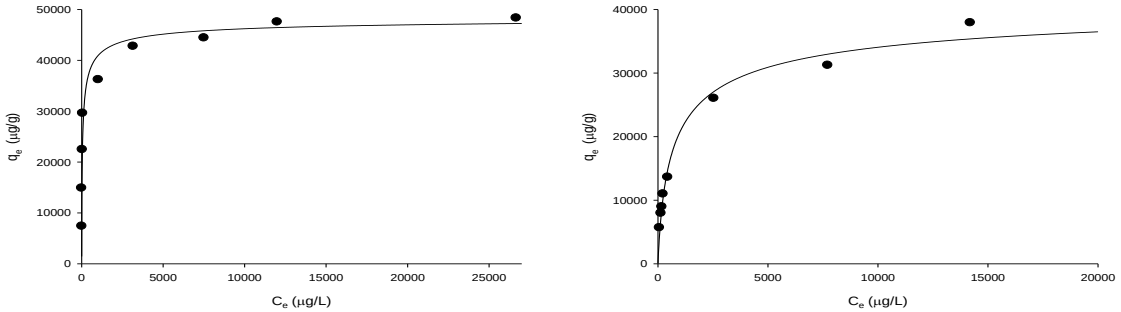

Fig 4.6. *Adsorption isotherm of Ni^{2+} onto a) Purolite S910 resin and b) clinoptilolite (comparison between experimental and calculated behavior according to equation (4)).*

It can be noted that the proposed model (equation 6) fitted the Purolite® S910 Resin and clinoptilolite adsorption data very well, except for Pb^{2+} adsorption onto clinoptilolite (which exhibited an inflection point in the lower concentration range). This different behavior was explained by the heterogeneity of the zeolite surface. As with other natural silica-alumina materials, it is well-known that the clinoptilolite surface is characterized by the presence of both ion exchange (a permanent negative charge due to the isomorphic substitution of Si^{4+} with Al^{3+}) and complexation sites (exposed hydroxyl functional

groups) (Akgul et al.,2008; Hu J. and Shipley J.H., 2013). This superficial -OH can thus offer an additional mechanism for metal adsorption (Pb^{2+}, Cd^{2+} and Ni^{2+}). In this regard, it has already been demonstrated that Pb^{2+} ion can create more stable hydroxo-complexes than Cd^{2+} or Ni^{2+} (Canepari et al., 1998), and this could have been the reason for the observed differences in the Pb adsorption behavior. Adsorption onto complexation sites will be active for all of the metals, but it will be significant, at lower ionic strength, only for the more affine Pb^{2+}. In this case, the developed model (6) was unable to adequately predict clinoptilolite Pb^{2+} adsorption because it considered only one adsorption mechanism. Conversely, the Purolite® S910 Resin was characterized only by the presence of chelating sites, and the model fitted the experimental behavior well. Thus, the Pb^{2+} adsorption behavior was represented by the Langmuir-Freundlich model, which includes surface heterogeneity in its mathematical expression (Liu et al, 2008; Foo et al., 2010). The Langmuir – Freundlich isotherm is expressed by the following equation:

$$q_e = q_{\max} \frac{K \cdot (C_e)^b}{1 + K \cdot (C_e)^b} \tag{7}$$

where q_e is the adsorbed amount of Pb^{2+} in µg/g, q_{max} is the maximum adsorbable amount in µg/g, C_e is the equilibrium solution concentration in µg/L, K is the equilibrium constant in L/g and b is a heterogeneity parameter. This isotherm was more suitable for describing the heterogeneous adsorption mechanism of the lead onto clinoptilolite (Gunay et al., 2007). Table 4.2 reports the optimized parameters for the clinoptilolite and S910 isotherms, along with statistical parameters indicating the goodness of fit.

	Clinoptilolite			Purolite S910 resin		
	Pb^{2+}	Cd^{2+}	Ni^{2+}	Pb^{2+}	Cd^{2+}	Ni^{2+}
K_{Na+} (L/g)	0.017±0.001	(2.86±0.592)E-08	(4.13±0.797)E-08	(2.34±1.00)E-06	(3.72±0.90)E-06	(6.22±2.04)E-07
q_{max} (ug/g)	46000±3300	54000±2600	43000±1800	33000±2200	49000±2800	48900±1900
B	2.25±0.217	-	-	-	-	-
R^2	0.988	0.990	0.987	0.923	0.953	0.948

***Table 4.2**. Isotherm parameters of Pb^{2+}, Cd^{2+} and Ni^{2+} and onto a) Purolite S910 resin and b) clinoptilolite*

The results indicated that the Purolite® S910 Resin did not show major differences in the affinity constant between the selected heavy metals, with a slightly lower value for Cd^{2+} than for Ni^{2+} and Pb^{2+}. These results suggested that the stability of each amidoxime (the active chelating group of the Purolite® S910 Resin (www.purolite.com) complex was fairly similar among the heavy metals.

4.4.3 Effect of ionic strength

Figures 4.7, 4.8, and 4.9 display the experimental isotherms for the adsorption of Pb^{2+}, Cd^{2+} and Ni^{2+} onto clinoptilolite and Purolite® S910 Resin, as obtained at high ionic strength and compared with the corresponding calculated behavior.

a) *b)*

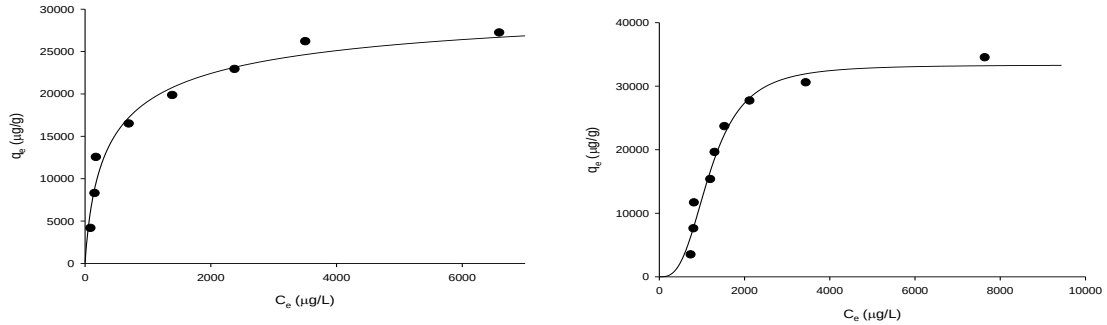

Fig. 4.7. *Pb^{2+} isotherm onto a) Purolite S910 resin and b) clinoptilolite at high ionic strength (comparison between experimental and calculated behavior according to equation (4), panel a, and (5), panel b).*

a) *b)*

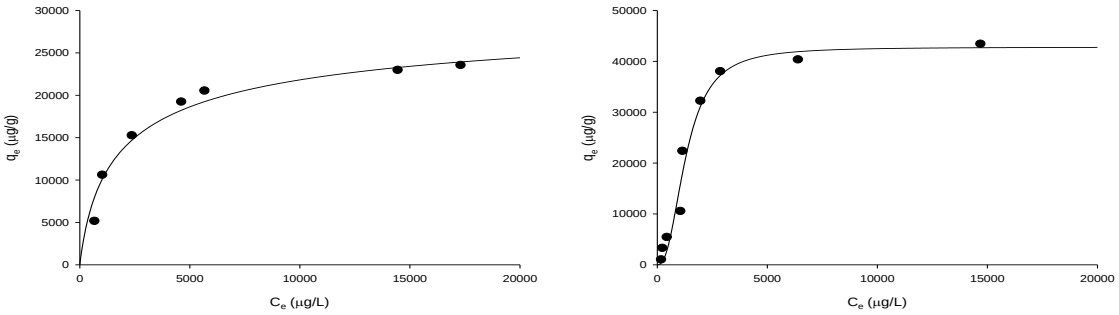

Fig 4.8*. Cd^{2+} isotherm onto a) Purolite S910 resinand b) clinoptilolite at high ionic strength (comparison between experimental and calculated behavior according to equation (4), panel a, and (5), panel b).*

a) *b)*

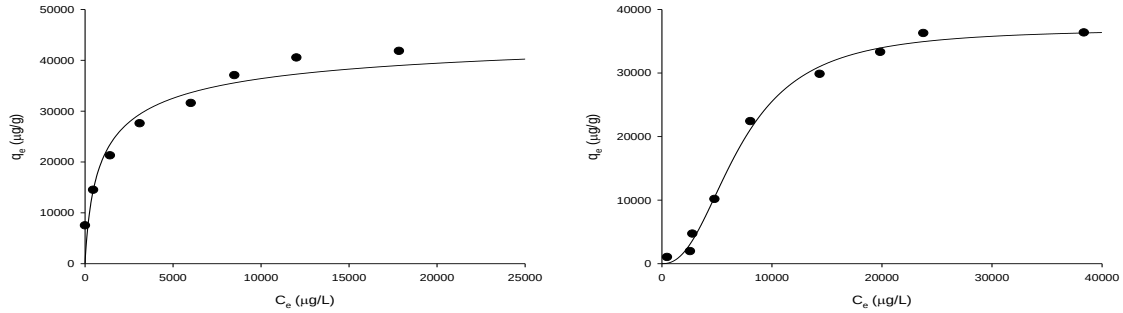

Fig. 4.9*. Ni^{2+} isotherm onto a) Purolite S910 resinand b) clinoptilolite at high ionic strength (comparison between experimental and calculated behavior according to equation (4), panel a, and (5), panel b).*

It is noteworthy to observe that, in the case of clinoptilolite, all of the metal isotherms now exhibited the same behavior, with a change in the adsorption shape at the lower concentration range. This behavior could be interpreted by assuming that the Cd^{2+} and Ni^{2+} adsorption onto ion exchange sites was reduced at higher ionic strengths due to competition from the high Na^{+} concentration, thus making the adsorption contribution onto complexation sites relatively more relevant. Following these speculations, the Cd^{2+} and Ni^{2+} isotherms were better modeled by equation (7). The optimized parameters showed a decrease in the affinity constant and q_{max} value in the case of Pb^{2+}, indicating a competition between Pb^{2+} and Na^{+} for the exchange sites. Concerning the adsorption onto Purolite® S910 Resin, no changes in the adsorption behavior were observed with respect to low ionic strength conditions, and model (6) was still suitable for data representation. As a matter of fact, the Purolite® S910 Resin was characterized by only one adsorption site typology, and the ion competition did not produce modifications to the adsorption mechanism, but rather, only an effect on the adsorption capacity. These observations were confirmed by the optimized values of $K_{Na}{}^{+}$ and q_{max} (Table 4.3). Comparing these values to the corresponding values at low ionic strength (Table 4.2), a small decrease in the affinity and maximum adsorbable quantity of each heavy metal could be observed.

	Clinoptilolite			Purolite S910 Resin		
	Pb^{2+}	Cd^{2+}	Ni^{2+}	Pb^{2+}	Cd^{2+}	Ni^{2+}
K_{Na+} (L/g)	(8.33±0.53) E-04	(7.64±0.77) E-04	(1.40±0.77) E-04	(9.77±3.13) E-08	(2.03±0.72) E-08	(2.88±1.42) E-08
q_{max} (ug/g)	33400±1800	43000±2600	37000±1100	30000±2100	32000±2500	47800±4100
b	2.97±0.49	2.42±0.58	2.35±0.23	-	-	-
R^2	0.968	0.974	0.995	0.965	0.965	0.948

***Table 4.3**. Isotherm parameters of Pb^{2+}, Cd^{2+} and Ni^{2+} onto a) Purolite S910 resin and b) clinoptilolite at high ionic strength*

Indeed, the Na^{+} competition with Pb^{2+}, Cd^{2+} and Ni^{2+} for chelating sites was usually limited to producing a significant decrease in the K_{Na+} and q_{max} values.

4.4.4 Effect of co-contamination: organic compounds

Figures 4.10, 4.11 and 4.12 show the adsorption isotherms of each metal ion onto each adsorbent material in the presence of benzene at approximately 500 mg/L. In table 4.4 the fitted parameters of each isotherm were reported. The presence of benzene appeared to influence the adsorption mechanism in different ways depending on the ion in question. In the case of Pb^{2+}, the presence of benzene induced an appreciable increase in the maximum adsorbable amount, both for clinoptilolite and Purolite® S910 Resin. On the

contrary, Cd^{2+} and Ni^{2+} caused a decrease in the maximum adsorbable amount for both of the adsorbents, and only a limited effect on the affinity constants.

a) *b)*

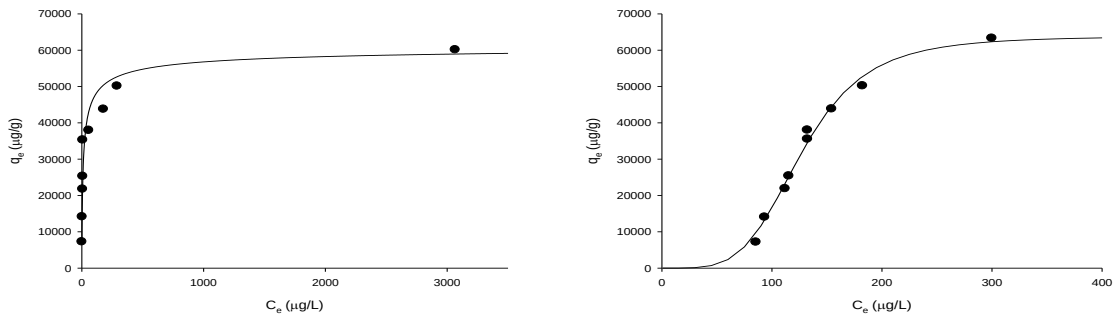

***Fig. 4. 10**. Pb^{2+} isotherm onto a) Purolite S910 resin and a) clinoptilolite in presence of benzene*

a) *b)*

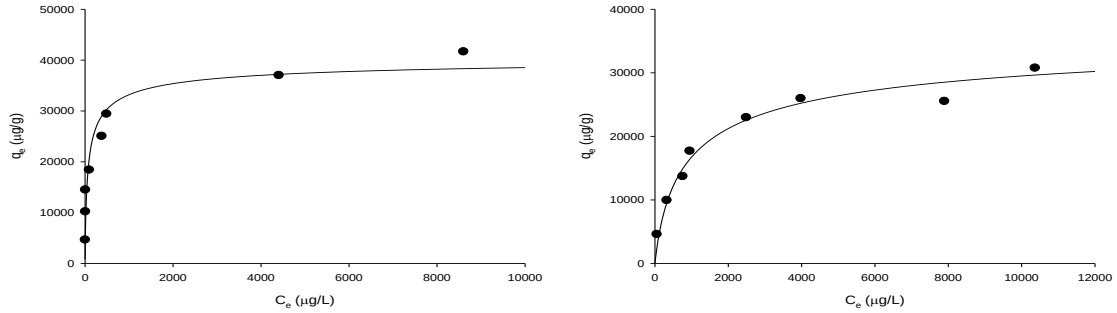

***Fig. 4.11**. Cd^{2+} isotherm onto a) Purolite S910 resin and b)clinoptilolite in presence of benzene*

a) *b)*

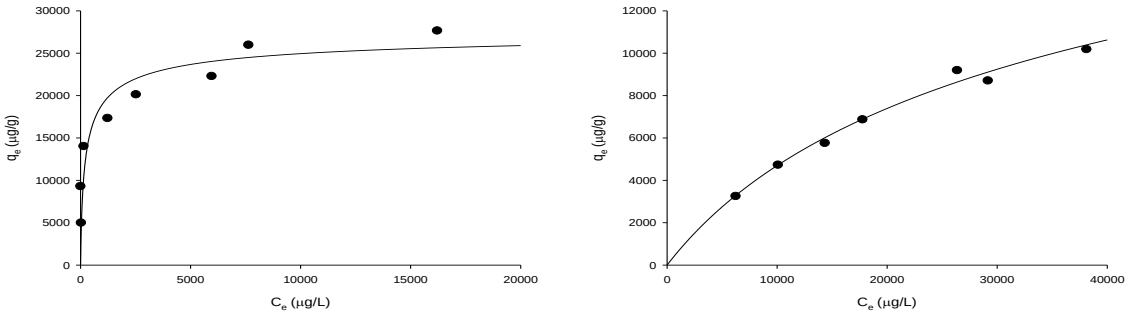

***Fig. 4.12**. Ni^{2+} isotherm onto a) Purolite S910 resin and b)clinoptilolite in presence of benzene*

To better understand the different effects of benzene on metal adsorption, the variation in benzene concentration throughout the adsorption tests was also monitored by measuring its values at the beginning and end of each trial (as reported in Figures 4.13 – 4.15).

a) *b)*

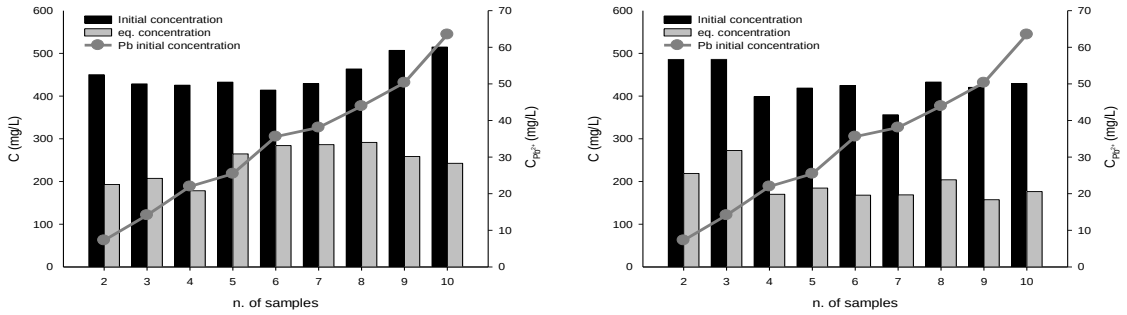

Fig 4.13*. Variation of benzene concentration before (grey) and after (black) a) Pb^{2+}/Purolite S910 Resin and b) Pb^{2+}/clinoptilolite adsorption test. It is also superimposed the corresponding initial concentration of Pb^{2+} for each test.*

a) *b)*

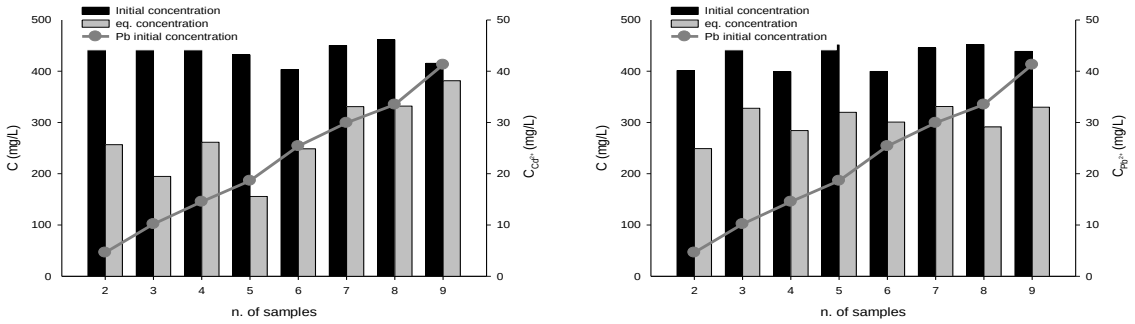

Fig 4.14*. Variation of benzene concentration before (grey) and after (black) a) Cd^{2+}/Purolite S910 Resin and b) Cd^{2+}/clinoptilolite adsorption test. It is also superimposed the corresponding initial concentration of Cd^{2+} for each test.*

a) *b)*

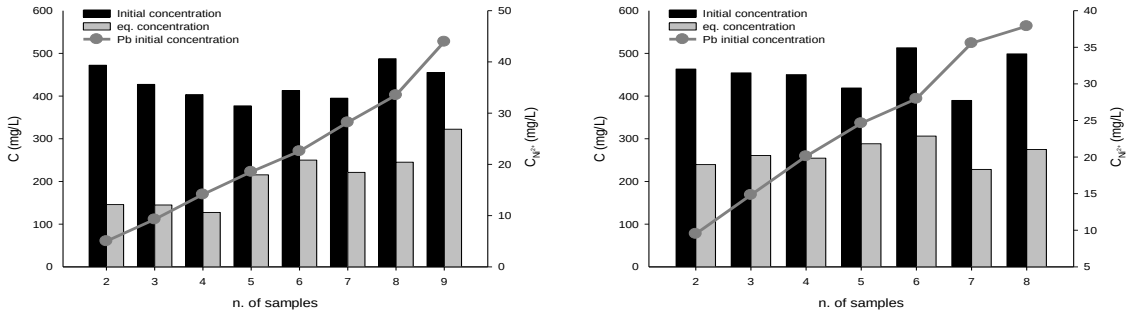

***Fig 4.15**. Variation of benzene concentration before (grey) and after (black) a) Ni^{2+}/Purolite S910 Resin and b) Ni^{2+}/clinoptilolite adsorption test. It is also superimposed the corresponding initial concentration of Ni^{2+} for each test.*

Although the experimental data were quite scattered, different behavior could be observed for Pb^{2+} with respect to Cd^{2+} and Ni^{2+}. The quantity of benzene retained in the Pb^{2+} tests was generally higher, and independent from the increase in initial metal concentration. As reported in the literature (Auel et al., 1968; Gash et al., 1974) Pb^{2+} is capable of forming stable complexes with benzene molecules, and this ability could help in understanding the observed positive effect on its adsorption. On the other hand, no information could be found in the literature on the possible benzene complexation of Cd^{2+} and Ni^{2+}. Our experimental data suggested that Pb^{2+} adsorption could be increased by the simultaneous adsorption of Pb^{2+} ions and benzene Pb-complex (with the general formula $[Pb(C_6H_6)_x]^{2+}$) onto the selected adsorbents.

	Clinoptilolite			Purolite S910 Resin		
	Pb^{2+}	Cd^{2+}	Ni^{2+}	Pb^{2+}	Cd^{2+}	Ni^{2+}
K_{Na+} (L/g)	0.0080±0.0002	3.46±1.06E-08	8.20±2.59E-10	(2.11±0.79) E-06	(5.07±2.32)E-07	(2.18±1.12)E-07
q_{max} (ug/g)	64000±2600	38700±2500	28600±3300	62000±4300	41300±3000	28000±2000
b	4.34±0.42	-	-	-	-	-
R^2	0.989	0.974	0.987	0.920	0.931	0.921

Table 4.4*. Isotherm parameters of Pb^{2+}, Cd^{2+} and Ni^{2+} with a) Purolite S910 resin and b) clinoptilolite in presence of benzene.*

4.4.5 Heavy metal adsorption isotherms: MSA

Figure 4.16 shows the experimental adsorption results for Pb^{2+} and Cd^{2+}, as target heavy metals, onto MSA. Unlike with clinoptilolite and Purolite® S910 Resin, the adsorption isotherm in the adopted experimental range showed linear behavior and a significantly lower removal capacity. This Henry-type isotherm usually describes the adsorption process at low solute concentration and/or low affinity for the surface (and consequently low surface coverage) (Giles C.H. et al., 1973a; Giles C.H. et al., 1973b). The low metal removal capacity was consistent with the MSA's siliceous nature, with a general low affinity for metals, and the observed adsorption could be ascribed to the presence of alumina as a binder in the bulk structure of the MSA, which offered more suitable adsorption sites for the heavy metal removal (Rahmani et al., 2010). Despite the presence of the alumina, the performance of the MSA at heavy metal removal was not comparable

to the that of clinoptilolite and Purolite® S910 resin, which appeared to be better and more suitable for heavy metal uptake.

a) *b)*

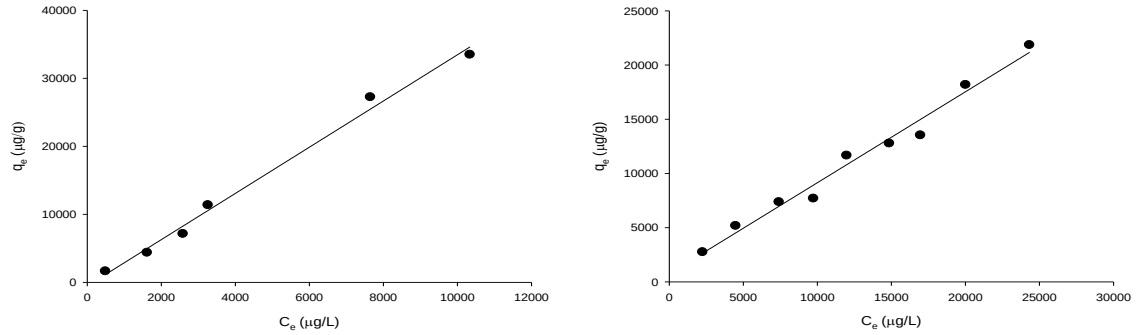

Fig. 4.16. *Adsorption isotherm of a) Pb^{2+} and b) Cd^{2+} onto MSA.*

4.5 Conclusion

In this study, clinoptilolite and Purolite® S910 Resin showed significantly high performances in metal ion adsorption from the liquid phase, although they displayed extreme conditions such as high ionic strength and potential competition of dissolved organic contaminants. These results experimentally demonstrated the potential use of these materials for full scale application in the removal of heavy metals from contaminated water released by petrochemical activities (production water and contaminated groundwater). A new adsorption model was developed to account for

exchange/complexation mechanisms, and, together with the Langmuir-Freundlich model, was used to represent and compare the experimental heavy metal adsorption onto clinoptilolite and Purolite® S910 Resin.

Clinoptilolite showed a significantly higher affinity for the Pb^{2+} ion compared to the other heavy metal ions, whereas Purolite® S910 Resin displayed no evident affinity preference in terms of adsorption rate and adsorption capacity for the different metals. This behavior was consistent with the different removal mechanisms, mostly ion exchange in the case of clinoptilolite (with a small contribution from surface complexation) and only complexation due to a strong functional group in the case of the synthetic resin. The effect of ionic strength on clinoptilolite adsorption was significant only for lead, whereas only Cd removal was negatively affected by the synthetic resin. The effect of dissolved benzene was positive only for Pb removal, especially in the case of Purolite® S910 Resin, indicating the potential co-adsorption of free lead and Pb-benzene complexes, whereas Cd and Ni adsorption was reduced for both adsorbents.

MSA's heavy metal uptake appeared quite limited, especially compared to that of clinoptilolite and Purolite® S910 Resin. In this regard, the potential modification of the MSA structure seems quite promising (Alothman and Apblett, 2009). Specific silanizations using aliphatic chains with cationic exchange terminal groups could represent a valid strategy with which to improve MSA's capability for heavy metal uptake, producing an adsorbent capable of simultaneously and effectively removing high concentrations of dissolved organics and heavy metals from contaminated water.

4.6 References

Abu Lail L., Bergendahl J.A., Thompson R.W., 2010. Adsorption of tertiary-butyl ether on granular zeolites: batch and column studies. Journal of Hazardous Materials 178, 363 – 369.

Adebajo M.O., Frost R.L., Kloprogge J.T., Carmody O., Kokot S., 2003. Porous materials for oil spill cleanup: a review of synthesis and absorbing properties. Journal of Porous Materials 10, 159 – 170.

Ahmadun F.R., Pendashteh A., Abdullah L.C., Biak D.R.A., Madaeni S.S., Abidin Z.Z., 2009. Review of technologies for oil and gas produced water treatment. Journal of Hazardous Materials 170, 530 – 551.

Akgul M., Savak N., Karabakana A., Dumanli A., Yurum Y., 2008. Adsorption of Bovine serum albumin (BSA) on clinoptilolite. Journal of Biology and Chemistry 36, 21-29

Alothmana Z.A., Apblettb A.W., 2009. Preparation of mesoporous silica with grafted chelating agents for uptake of metal ions. Chemical Engineering Journal 155 (2009) 916–924

Altare C.R., Bowman R.S., Katz L.E., Kinney K.A., Sullivan E.J., 2007. Regeneration and long-term stability of surfactant-modified zeolite for removal of volatile organic compounds from produced water. Microporous and Mesoporous Materials 105, 305 – 316.

Anderson M.A., 2000. Removal of MTBE and other organic contaminants from water by sorption on high silica zeolites. Environmental Science and Technology 34, 725 – 777.

Auel T., Amma E.L., 1968. Metal ion-aromatic complexes. VI. Benzene π-complexes of metals of the fourth and fifth groups. Journal of American Chemical Society 90, 5941–5942

Baeza Alvarado M.D., Olguin M.T., 2011. Surfactant-modified clinoptilolite-rich tuff to remove barium and fulvic acid from mono- and bi-component aqueous media. Microporous and Mesoporous Materials 139, 81 – 86.

Borai E.H., Harjula R., Malinen L., 2009. Efficient removal of cesium from low-level radioactive liquid waste using natural and impregnated zeolite minerals. Journal of Hazardous Materials 172, 416 – 422.

Bowman R.S., 2003. Applications of surfactant-modified zeolites to environmental remediation. Microporous and Mesoporous Materials 61, 43 – 56.

Braschi I., Gatti G., Bisio C., Berlier G., Sacchetto G., Cossi M., Marchese L., 2012. The role of silanols in the interactions between methyl tert-butyl ether and high-silica faujasite Y: an infrared spectroscopy and computational model study. Journal of Physical Chemistry C 116, 6943 – 6952.

Canepari S., Carunchio V.,Castellano P., Messina A., 1998. Complex formation equilibria of some b-amino-alcohols with lead(II) and cadmium(II) in aqueous solution. Talanta 47, 1077–1084.

Caputo D., Pepe F., 2007. Experiments and data processing of ion-exchange equilibria involving Italian natural zeolites: a review. Microporous and Mesoporous Materials 105, 222 – 231.

Carati A., Ferraris G., Guidotti M., Moretti G., Psaro R., Rizzo C., 2003. Preparation and characterization of mesoporous silica–alumina and silica–titania with a narrow pore size distribution. Catalysis Today 773, 15–323.

Choi J.H., Kim S.D., Noh S.H., Oh S.J., Kim W.J., 2006. Adsorption behaviours of nano-sized ETS-10 and Al-substituted ETAS-10 in removing heavy metal ions, Pb2+ and Cd2+. Microporous and Mesoporous Materials 87, 163 - 169.

Choi W.W., Chen, Y.K., 1979. The removal of fluoride from water by adsorption, Journal of the American Water Works Association 71 (10), 562 – 570.

Cooper C., Burch R., 1999. Mesoporous materials for water treatment processes. Water Research 33 (18), 3689 – 3694.

Corma A., 1997. From microporous to mesoporous molecular sieve materials and their use in catalysis. Chemical Reviews 97, 2373 – 2419.

Davila Jimenez M.M., Elizade Gonzalez M.P., Mattusch J., Morgenstern P., Pérez Cruz M.A., Reyes Ortega Y., Wenrich R., Yee Madeira H., 2008. In situ and ex situ study of the enhanced modification with iron of clinoptilolite-rich zeolitic tuff for arsenic sorption from aqueous solutions, Journal of Colloid and Interface Science 322, 527 – 536.

Diaz Nava C., Olguin M.T., Solache Rios M., 2002. Water defluoridation by Mexican heulandite-clinoptilolite. Separation Science and Technology 37 (13), 3109 – 3128.

Foo K.Y., Hameed B.H., 2010. Insights into the modeling of adsorption isotherm systems. Chemical Engineering Journal 156, 2–10.

Garcia Basabe Y., Ruiz Salvador A.R., Maurin G., De Menorval L.C., Rodriguez Iznaga I., Gomez A., 2012. Location of extra-framework Co2+, Ni2+, Cu2+ and Zn2+ cations in

natural and dealuminated cliptilolite. Microporous and Mesoporous Materials 155, 233 – 239.

Gash A. G., Rodesiler P. F., Amma E. L., 1974. Metal Ion-Aromatic Complexes. XV. Synthesis, Structure, and Bonding of π-C6H6Pb(AlC14)2 *C6H6. Inorganic Chemistry 13, 2429-2434

Germanus A., Kärger J., Pfeifer H., Samulevič N.N., Zďanov S.P., 1985. Intracrystalline self-diffusion of benzene, toluene and xylene isomers in zeolites Na-X. Zeolite 5, 91-95

Giles C.H., Giles C.H., D'Silva A.P., Easton I. A., 1974. A general treatment and classification of the solute adsorption isotherm. I. Theoretical. Journal of Colloid and Interface Science 47, 766–778

Giles C.H., Smith D., Huitson A., 1974. A general treatment and classification of the solute adsorption isotherm. I. Theoretical. Journal of Colloid and Interface Science 47, 755–765

Gunay A., Arslankaya E., Tosun I., 2007. Lead removal from aqueous solution by natural and pretreated clinoptilolite: Adsorption equilibrium and Kinetics. Journal of Hazardous Materials 146, 362–371.

Hedstroem A., 2001. Ion-exchange of ammonium in zeolites: a literature review. Journal of Environmental Engineering 127 (8), 673 – 681.

Hrubesch L.W., Coronado P.R., Satcher J.H. Jr., 2001. Solvent removal from water with hydrophobic aerogels. Journal of Non-crystalline Solids 285, 328 – 332.

Huttenloch P., Stroehl K., Czurda K., 2001. Sorption of Nonpolar Aromatic Contaminants by Chlorosilane Surface Modified Natural Minerals. Environmental Science and Technology 35, 4260-4264

Kaftan O., Acikel M., Eroglu A., Shahwan T., Artok L., Ni C., 2005. Synthesis characterisation and application of a novel sorbent, glucamine-modified MCM-41, for the removal / pre-concentration of boron from waters. Analytica Chimica Acta 547, 31 – 41.

Khan F.I., Husain T., Hejazi R., 2004. An overview and analysis of site remediation technologies. Journal of Environmental Management 71, 95 – 122.

Krisnandi Y.K., Lachowski E.C., Howe R.F., 2006. Effects of ion exchange on structure of ETS-10. Chemistry of Materials 18, 928 – 933.

Le Tuan Pham A., Sedlak D., Doyle F.M., 2012. Dissolution of mesoporous silica supports in acqueous solutions: implications for mesoporous silica-based water treatment processes. Applied Catalysis B: Environmental 126, 258 – 264.

Lee J.W, J.W. Lee, Shim W.G., Suh S.H., Moon H., 2003. Adsorption of Chlorinated Volatile Organic Compounds on MCM-48. Journal of Chemical and Engineering Data 48, 381-387.

Leusch F., Bartkow M., 2010. A short primer on benzene, toluene, ethylbenzene and xylenes (BTEX) in the environment and in hydraulic fracturing fluids Griffith University – Smart Water Research Centre.

Li J., Qui T., Wang L., Liu C., Zhang Y., 2007. Synthesis and characterisation of imidazole-functionalised SBA-15 as an adsorbent of hexavalent chromium. Materials Letters 61, 3197 – 3200.

Li J., Wang L., Qi T., Zhou Y., Liu C., Chu J., Zhang Y., 2008. Different N-containing functional groups modified Mesoporous adsorbents for Cr(VI) sequestration: synthesis, characterisation and comparison. Microporous and Mesoporous Materials 110, 442 – 450.

Li S., Tuan V.A., Noble R.D., Falconer J. L., 2003. MTBE adsorption on all-silica beta zeolite, Environmental Science and Technology 37, 4007 – 4010.

Liu A.M., Hidajat K., Kawi S., Zhao D.Y., 2000. A new class of hybrid Mesoporous materials with functionalised organic mono-layers for selective adsorption of heavy metal ions. Chemical Communications, 1145 – 1146.

Liu Y., Liu Y.J., 2008. Biosorption isotherms, kinetics and thermodynamics. Separation and Purification Technology 61, 229–242.

Lopes C.B., Pereira E., Lin Z., Pato P., Otero M., Silva C.M., Rocha J., Duarte A.C., 2011. Fixed-bed removal of Hg2+ from contaminated water by microporous titano-silicate ETS-4: experimental and theoretical breakthrough curves. Microporous and Mesoporous Materials 145 (1 – 3), 32 - 40.

Martucci A., Pasti L., Nassi M., Alberti A., Arletti R., Bagatin R., Vignola R., Sticca R., 2012. Adsorption mechanism of 1,2-dichloroethane into an organophilic zeolite mordenite: a combined diffractometric and gas chromatographic study. Microporous and Mesoporous Materials 151, 358 – 367.

Meininghaus C.S.W., Prins R., 2000. Sorption of volatile organic compounds on hydrophobic zeolites. Microporous and Mesoporous Materials 35 – 36, 349 – 365.

Mercier L., Pinnavaia T.J., 1998. Heavy metal ion adsorbents formed by grafting of a thiol functionality to Mesoporous silica molecular sieves: factors affecting Hg(II) uptake. Environmental Science and Technology 32, 2749 – 2754.

Misaelides P., 2011. Application of natural zeolites in environmental remediation: a short review. Microporous and Mesoporous Material 144, 15 – 18.

Mureseanu M., Cioatera N., Trandafir I., Georgescu I., Fajula F., Galarneau A., 2011. Selective Cu2+ adsorption and recovery from contaminated water using mesoporous hybrid silica bio-adsorbents. Microporous and Mesoporous Materials 146, 141 – 150.

Nikolakis V., 2005. Understanding interactions in zeolite colloidal suspension: A review. Current Opinion in Colloid & Interface Science 10, 203-210.

Otero M., Lopes C.B., Coimbra J., Ferreira T.R., Silva C.M., Lin Z., Rocha J., Pereira E., Duarte A.C., 2009. Priority pollutants (Hg2+ and Cd2+) removal from water by ETS-4 titano-silicate. Desalination 249, 742 – 747.

Perego C., Bagatin R., Tagliabue M., Vignola R., 2013. Zeolites and related mesoporous materials for multi-talented environmental solutions. Microporous and Mesoporous Materials 166, 37 – 49.

Ranck J.M., Bowman R.S., Weeber J.L., Katz L.E., Sullivan E.J., 2005. BTEX removal from produced water using surfactant-modified zeolite, Journal of Environmental Engineering 131, 434 – 441.

Reynolds J.G., Coronado P.L., Hrubesch L.W., 2001a. Hydrophobic aerogels for oil spill cleanup – synthesis and characterisation, Journal of Non-crystallyne Solids 292, 127 – 137.

Reynolds J.G., Coronado P.L., Hrubesch L.W., 2001a. Hydrophobic aerogels for oil spill cleanup -intrinsic absorbing properties, Energy Sources 23, 831 – 843.

Richardson J.P., Nicklow J.W., 2002. In situ permeable reactive barriers for groundwater contamination. Soil and Sediment Contamination 11 (2), 241 – 268.

Rossner A., Knappe D.R.U., 2008. MTBE adsorption on alternative adsorbents and packed bed adsorber performance, Water Research 42, 2287 – 2299.

Sachse A., Merceille A., Barrè Y., Grandjean A., Fajula F., Galarneu A., 2012. Macroporous LTA-monoliths for in-flow removal of radioactive strontium from aqueous effluents: application to the case of Fukushima. Microporous and Mesoporous Materials 164, 251 – 258.

Samantya S., Yueksel U., Yueksel M., Kabay N., 2007. Removal of fluoride from water by metal ions (Al3+, La3+, ZrO2+) loaded natural zeolite. Separation Science and Technology 42 (9), 2033 – 2047.

Scherer M.L., Richter S., Valentine R.L., Alvarez P.J.J., 2000. Chemistry and microbiology of permeable reactive barriers for in situ groundwater clean up. Critical Reviews in Environmental Science and Technology 30 (3), 363 – 411.

Schick J., Caullet P., Paillaud J.L., Patarin J., Mangold Callarec C., 2011. Nitrate sorption from water on a surfactant-modified zeolite. Fixed bed column experiments. Micropororous and Mesoporous Materials 142, 549 – 556.

Seliman A.F., Borai E.H., 2011. Utilisation of natural chabasite and mordenite as a reactive barrier for immobilisation of hazardous heavy metals. Environmental Science and Pollution Research 18 (7), 1098 – 1107.

Shevchenko N., Zaitsev V., Walcarius A., 2008. Bi-functionalised Mesoporous silicas for Cr(VI) reduction and concomitant Cr(III) Immobilisation. Environmental Science and Technology 42, 6922 – 6928.

Sing K.S.W., Everett D.H., Haul R.A.W., Moscou L., Pierotti R.A., Rouquérol J., Siemieniewska T., 1985. Reporting physisorption data for gas/solid systems with special reference to the determination of surface area and porosity. Pure and Applied Chemistry 57 (4), 603 – 619.

Standecker S., Novak Z., Knez Z., 2007. Adsorption of toxic organic compounds from water with hydrophobic silica aerogels. Journal of Colloid and Interface Science 310, 362 – 368.

Taguchi A., Schueth F., 2005. Ordered Mesoporous materials in catalysis. Microporous and Mesoporous Materials 77, 1 – 45.

Vignola R., Bagatin R., De Folly D'Auris A., Flego C., Nalli M., Ghisletti D., Millini R., Sisto R., 2011a. Zeolites in a permeable reactive barrier (PRB): one year of field experience in a refinery's groundwater. - Part 1: the performances. Chemical Engineering Journal 178, 204 - 209.

Vignola R., Bagatin R., De Folly D'Auris A., Previde Massara E., Ghisletti D., Millini R., Sisto R., 2011b. Zeolites in a permeable reactive barrier (PRB): one year of field experience in a refinery's groundwater - Part 2: zeolite characterization. Chemical Engineering Journal 178, 210 - 216.

Villaescusa L.A., Marquez F.M., Zicovich Wilson C.M., Camblor M.A., 2002. Infrared investigation of fluoride occluded in double- four-member rings in zeolite. Journal of Physical Chemistry B 106, 2796 – 2800.

Voeroesmarty C.J., Mc Intyre P.B., Gessner M.O., Dudgeon D., Prusevich A., Green P., Glidden S., Bunn S.E., Sullivan C.A., Reidy Liermann C., Davies P.M., 2010. Global threats to human water security and river biodiversity. Nature 467, 555 – 561.

Wang S., Peng Y., 2010. Natural zeolites as effective adsorbents in water and wastewater treatment. Chemical Engineering Journal 156, 11 – 24.

Weitkamp J., 2000. Zeolite and catalysis, Solid State Ionics 131, 175 – 188.

Xu Y., Nakajima T., Ohki A., 2002. Adsorption and remova of arsenic (V) from drinking water by aluminium-loaded Shirasu-zeolite, Journal of Hazardous Materials B92, 275 – 287.

Xue X., Li F., 2008. Removal of Cu(II) from aqueous solution by adsorption onto functionalised SBA-16 Mesoporous silica. Microporous and Mesoporous Materials 116, 116 – 122.

Yoshitake H., Yokoy T., Tatsumi T., 2002. Adsorption of chromate and arsenate by amino-functionalised MCM-41 and SBA-1. Chemistry of Materials 14, 4603 – 4610.

Zadaka Amir D., Nasser A., Nir S., Mishael Y.G., 2011. Removal of methyl tertiary-butyl ether (MTBE) from water by polymer-zeolite composites. Microporous and Mesoporous Materials 151, 216 – 222.

Zhao G.X.S., Lee J.L., Chia P.A., 2003. Unusual adsorption properties of microporous titano-silicate ETS-10 toward heavy metal lead. Langmuir 19, 1977 – 1979.

Zhu L., Zhang C., Liu Y., Wang D., Chen J., 2010. Direct synthesis of ordered N-methylimidazolium functionalized Mesoporous silica as highly efficient anion exchanger of Cr(VI). Journal of Material Chemistry 20, 1553 – 1559.

CHAPTER 5

NEW MATERIAL FOR AROMATIC HYDROCARBONS REMOVAL: BATCH TESTS

Water management is expected to be a major issue in decades to come, due to increasing water scarcity. Aromatic hydrocarbons are frequently present as contaminants in water coming from sites devoted to petroleum extraction or processing (Veil et al., 2004). Their removal to acceptable levels is requested in order to avoid adverse effects on environment and health. Especially in case of massive contamination, bulk removal operations have to be coupled with polishing. For this purpose adsorption technology could represent a good solution especially using mesoporous material as adsorbent. Indeed, mesoporous material thanks to their pore size are able to uptake large amount of contaminants from water. Their physic-chemical properties such as the pore size, surface hydrophobicity (Wang et al., 2011) or functionality can be modified by synthetic or post synthetic via in order to be effective towards a lot of different pollutants or environmental conditions (Moura et al., 2011; Hara et al., 2012; Kim et al., 2011).

In this chapter will be described the study about a set of different mesoporous materials, tested to understand the best material for hydrocarbons removal from water. This set is composed of seven materials: MSA (extruded and particle forms), MCM-41, (siliceous and silica-alumina), Zeolite Y (silica-alumina and de-aluminated), SBA-15, Silice Grace® and ZSM-5. MSA is the new synthetic material and it was tested both in particle and extruded shapes. Silice Grace® is the commercial material and it was used as reference material to understand if the adsorption performances of MSA would be suitable for market standard. MCM-41 is also used as reference material of the state of art being the most studied mesoporous material for adsorption purposes

(Qin et al., 2007; Wu et al., 2012; Parida et al., 2012). The other materials of this study were Zeolite Y, ZSM-5 and SBA-15. The adsorption performances of each material were experimentally investigated under the kinetic (adsorption kinetic) and thermodynamic (adsorption isotherms) point of view and varying the ionic strength of the solution. Batch tests for adsorption kinetic and isotherms were lead out using toluene as target contaminant and the experimental data have been elaborated applying mathematical models for all the experimental conditions.

5.1 Materials and methods

All the mentioned materials were thermally activated at 550 °C for 8 hours. This treatment was necessary to guarantee the removal of template residuals and impurities (Banat et al., 2003). After, the materials were kept in a dessicator to preserve them from humidity adsorption until their utilization. MSA is the material to test for water clean-up and it was synthesized by eni S.p.A. in two different shapes: extruded and particle (Perego et al., 1999). The first is a composite material composed of powdered MSA merged in alumina and calcium carbonate to gain the extruded shape. The particle MSA instead is the synthesized material without any post-synthetic modifications. MCM-41 and Zeolite Y both in siliceous and silica-alumina composition were bought from Sigma Aldrich®, whereas SBA-15 was bought from ACS® and Silica gel was bought from Grace® (for simplicity, this last will be mentioned in the text as Silica Grace®). Toluene aqueous solution for batch test was prepared adding 0,5 mL of pure toluene into 500 mL of deionized water, keeping on stirring for twenty-four hours before utilization. For kinetic study nine solutions of toluene at the same concentration were prepared and inserted into vials of 21 mL adding in each vial 21 mg of material. All the vials were set on the rotative stirrer and removed at definite times : 30, 60, 120, 180, 240, 300, 360, 420 and 1440 minutes. After the stirring all the solutions were analyzed. A single sample of starting solution was immediately analyzed to know the initial concentration. As concerns batch tests for adsorption isotherms, eight solutions of

different concentration were prepared for dilution of the same starting solution used for kinetic test. Also in this case, 21 mL of each solution were inserted into the vial and 21 mg of the material were added afterwards. A little amount of each starting solution was sampled and analyzed in order to know the initial toluene concentration. The vials were then kept on stirring and after twenty four hours an aliquot of liquid phase was sampled for the analysis. All the samples were analyzed by a Shimadzu® Total Organic Carbon analyzer. In table 5.1 the instrumental operating condition are reported.

OPERATIVE PARAMETERS	VALUE
Gas Carrier Pressure	300-600 kPa
Gas Carrier rate	140 ml/min
Oven Temperature	680 °C
Injection number	3
Number of Syringe wash	2

Table 5.1 Operative parameters of TOC-CSN Shimadzu ®

The same experimental plan was repeated increasing ionic strength solution up to 0,5 M by adding K_2SO_4 in order to reproduce the seawater salinity.

Textural characterizations of materials were also lead out by physical adsorption of N_2 at -196 °C. Through the application of BET isotherm to experimental data of N_2 adsorption, information about surface area, pore volume (Gurvitsch method) and pore size distribution (NDLFT method) were obtained (Ravikovitch et al., 2000; Neimark et al., 2009). Regeneration studies are performed on extruded and granulated MSA and MCM-41. This last has been used as reference

material for evaluating the regeneration performances of the two MSA. Preliminary tests were carried out to draw up the best regeneration protocol. All the three material were kept in contact with an aqueous toluene solution of about 400 mg/L for twenty-four hours. Successively, the materials were separated from liquid solution and kept again for 24 hours in contact with the same toluene solution. This phase was necessary to stress materials and to have high amount of adsorbed toluene. After, the materials were put in oven for 1 hours at different temperatures for regeneration. Adsorption tests were repeated on regenerated materials to verify the effectiveness of the regeneration. The lower temperature at which the adsorption performances were similar before and after regeneration was choice as the best regeneration temperature. After having fixed the regeneration temperature the adsorption isotherms of toluene onto extruded and granulated MSA and MCM-41 were performed. Isotherms were made on unloaded materials, on loaded materials and regenerated materials. The unloaded materials are the materials without any contact with toluene, loaded materials are hold in contact with toluene solution and finally regenerated materials are the materials after regeneration.

5.2 Data evaluation: Kinetic and thermodynamic models

The kinetic and thermodynamic data of toluene adsorption were interpreted on the basis of mathematical models, using Micromath® Scientist 1.0. Regarding kinetic data, a new simplified model was developed for toluene adsorption onto mesoporous material assuming the Langmuir adsorption isotherm at equilibrium condition. Indeed, the attempt to develop the rigorous model considering the non Langmuir type isotherm (as will be mentioned ahead) was not achieved. An adsorption reaction between adsorbing species in the liquid phase and active sites on mesoporous surface was hypothesized according to the following equation:

$$A_{liq} + S_{sol} \underset{k_{deads}}{\overset{k_{ads}}{\leftrightarrows}} AS_{sol} \quad (1)$$

Where *A* is the adsorbing liquid, *S* is the active site and *AS* is the adsorbate-adsorbent complex. An equilibrium has to be considered for toluene adsorption, characterized by two distinct kinetic rate constants both of the first order, for adsorption and deadsorption (k_{ads} and k_{deads}) reaction; by this way the kinetic equation becomes:

$$\frac{dC_A}{dt} = -k_{ads}C_A + k_{deads}C_{AS} \quad (2)$$

C_A is the adsorbing species concentration in mg/L, C_{AS} is the adsorbed species concentration in (mg/g) and t is the time in minutes. Afterwards, it was necessary to introduce an approximation, aimed to substitute a known expression to C_{AS} term. Indeed, considering the mass balance of active sites, it is possible to gain a new expression for C_{AS}:

$$C_{A_0} - C_A = C_{AS} \cdot M \quad (3)$$

$$C_{AS} = \frac{C_{A_0} - C_A}{M} \quad (4)$$

In this expression C_{A0} is the starting concentration of species A (in mg/L) and M is the solid-liquid ratio (in g/L, it expresses the amount of solid adsorbent, dispersed in a specific volume of liquid) equal to 1 g/L due to the experimental conditions. This expression is valid only assuming the number of the active sites widely bigger than the adsorbed molecules. After this replacement, some algebraic operations and integrating between C_{A0} and C_A and between t=0 and t, the kinetic equation for toluene adsorption can be written as follows:

$$C_A = \frac{k_{deads}}{M \cdot k_{ads} + k_{deads}} \cdot C_{A_0} - \left[C_{A_0} \cdot \left(\frac{k_{deads}}{M \cdot k_{ads} + k_{deads}} - 1 \right) \right] \cdot e^{\frac{-M \cdot k_{ads} + k_{deads}}{M} \cdot t} \quad (5)$$

The value of k_{ads} and k_{deads} were thus gained applying the non-linear regression of this equation to the experimental data of C_A and t.

Thermodynamic data of adsorption isotherms were interpreted using the isotherm adsorption model proposed by Lee et al. (Lee et al., 2004). Usually, adsorption isotherms of mesoporous materials are typical isotherms included in the IV, V or VI groups of the IUPAC classification, but this classification is related to adsorption isotherm of gas compounds onto mesoporous solids (IUPAC 1985; IUPAC 1994). The model proposed by Lee et al. (Lee et al., 2004) is a two-steps adsorption isotherm model and it is a combination of the Langmuir and Langmuir-Freundlich models, in which the Langmuir equation describes the first part and the Langmuir-Freundlich equation describes the second part of the isotherm:

$$q_e = q_{max} \cdot \left(\frac{K_p \cdot C_e}{1 + K_p \cdot C_e} + \frac{K_q \cdot (C_e)^m}{1 + K_q \cdot (C_e)^m} \right) \quad (6)$$

where q_e is the adsorbed amount of toluene or benzene in mg/g , q_{max} is the maximum adsorbable amount in mg/g, C_e is the equilibrium solution concentration in mg/L, K_p is the Langmuir constant in L/g, K_q is the Langmuir-Freundlich constant in L/g and m is a generic parameter indicating the heterogeneity of the adsorption mechanism. This equation represents the typical isotherm of non-polar compounds adsorbing onto mesoporous materials. In fact, mesoporous materials usually show a two-steps mechanism: the first step, to which corresponds the first term of equation, involves the coverage of mesoporous surface by the monolayer formation of adsorbed species, the second step (represented by the second term) is successive to the monolayer formation and describes the pore's filling (Lee et al., 2004).

5.3 Results and discussion

5.3.1 Pore distribution study

Figure 5.1 shows the distribution of the specific pore volume as function of the pore width for the examined materials.

Extruded MSA

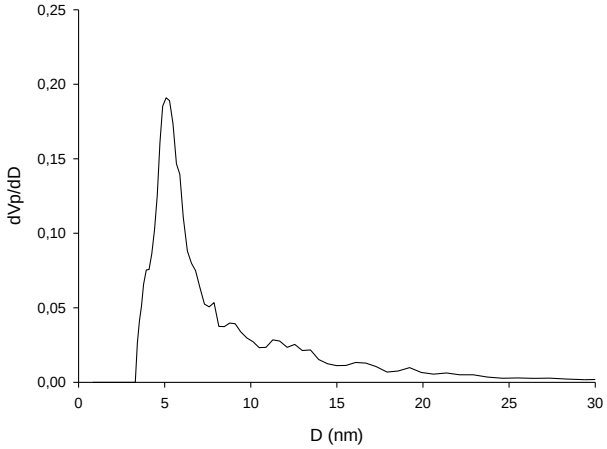

MCM-41 (Si/Al=100)

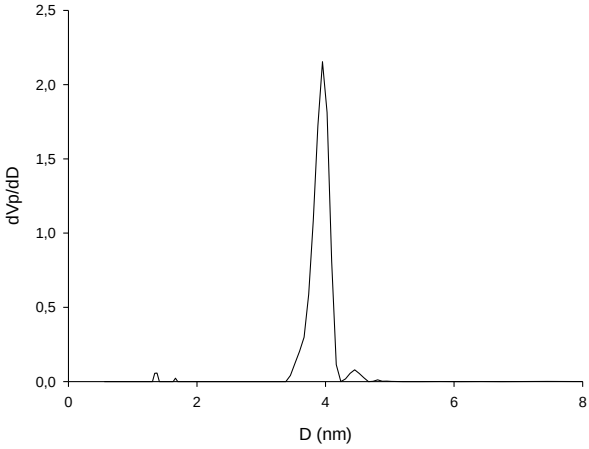

MSA

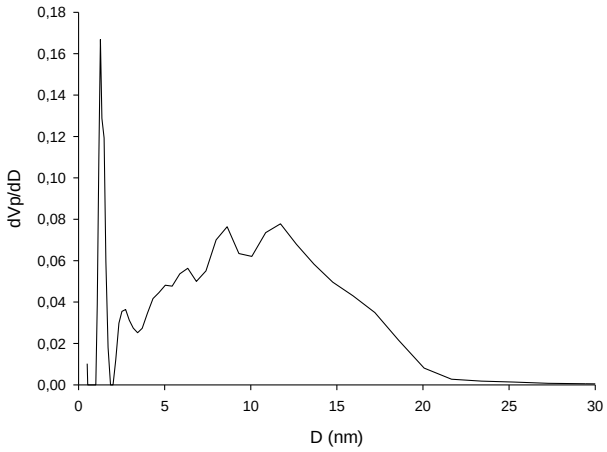

SBA-15

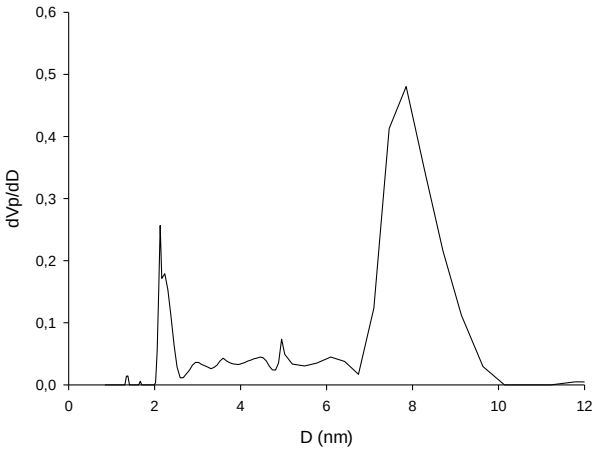

MCM-41

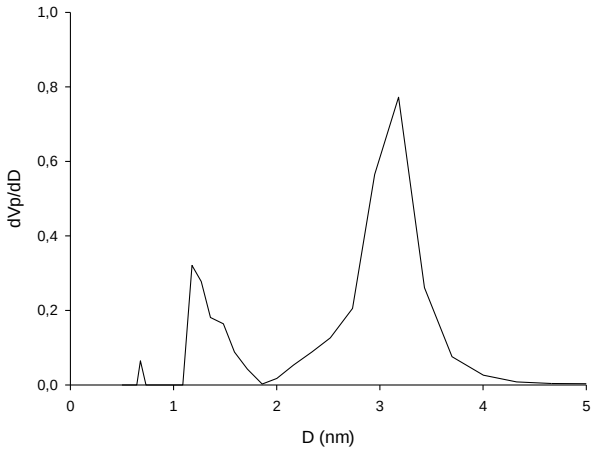

Silica Gel

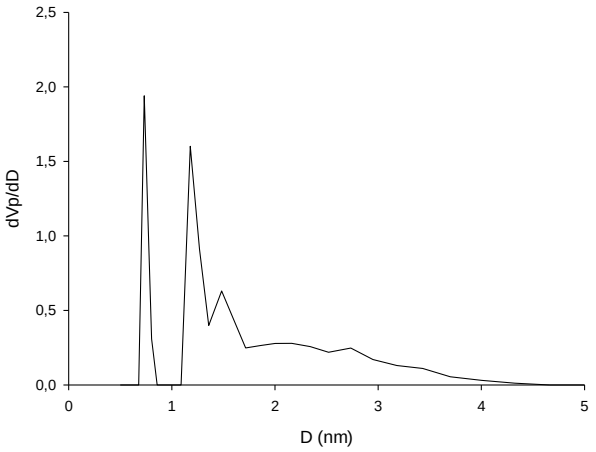

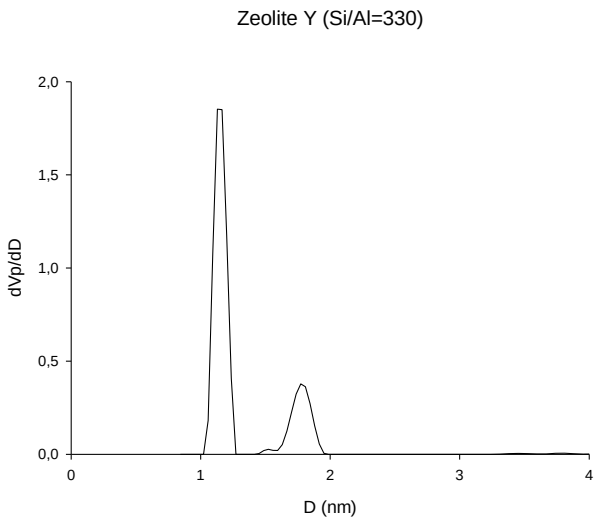

Figure 5.1 Pore size distribution of investigated materials.

These graphs highlight the coexistence of pores with different diameters in the material structure. MCM-41 shows a tri-modal distribution system centred at 6,7 Å, 12 Å and 31 Å respectively, and the majority of pores is included in the last mode. Adding aluminium to the crystal framework, as for Al-MCM-41 (Si/Al=100), the number of modes is reduced to one, centred at 39 Å. Granulated MSA is the one having a bimodal distribution of pores width. The first mode, centred at 12,8 Å, represents a little amount of the total pores, the majority of which are part of a larger distribution that goes from 20 Å to 215 Å (160 Å is the weighted average of the mode). Granulated MSA has the largest pores of the studied material set. Extruding granulated MSA led to reduce the bimodal distribution to one tailed mode centred at about 51 Å. SBA-15 is very singular, characterized by two different modes linked by few pores whose dimensions are intermediate between them. SBA-15 is a mesoporous material (pore diameter larger than 20 Å), whose mesopores are linked together by a microporous channel system (Pollock et al., 2011). Thence, the first mode (21 Å) represents this microporous system whereas the second bigger mode is attributable to the mesopores (about 80

Å). Silica Gel Grace® and Zeolite Y show the majority of their pore dimensions below 20 Å, especially Zeolite Y that can be considered as a microporous material. Information about pore distribution are very important for interpreting the behaviour of material in adsorption applications. The size of pores may have an important role for adsorption performances as regards pollutants concentration or their physical form (dissolved, dispersed or emulsion) (Serna-guerrero and Sayari, 2007).

Table 5.2 resumes the textural and chemical properties of the studied materials.

Material	Average Pore width (Å)	Surface area (m^2/g)	Si/Al	Crystalline phase
Extruded MSA	51	490	∞	amorphous
MCM-41	45	793	∞	Amorphous, hexagonal pores
Al-MCM-41	48	873	100	Amorphous hexagonal pores
Granular MSA	116	850	∞	amorphous
SBA-15	80	508	∞	Amorphous hexagonal pores
Silica Grace	21	703	∞	amorphous
Zeolite Y	11-18	773	330	sodalite

Table 5.2 Textural and chemical characteristics of adsorbent materials.

5.3.2 Kinetic study

Figure 5.2 reports kinetic data of toluene adsorption on all the materials in each of the two explored conditions.

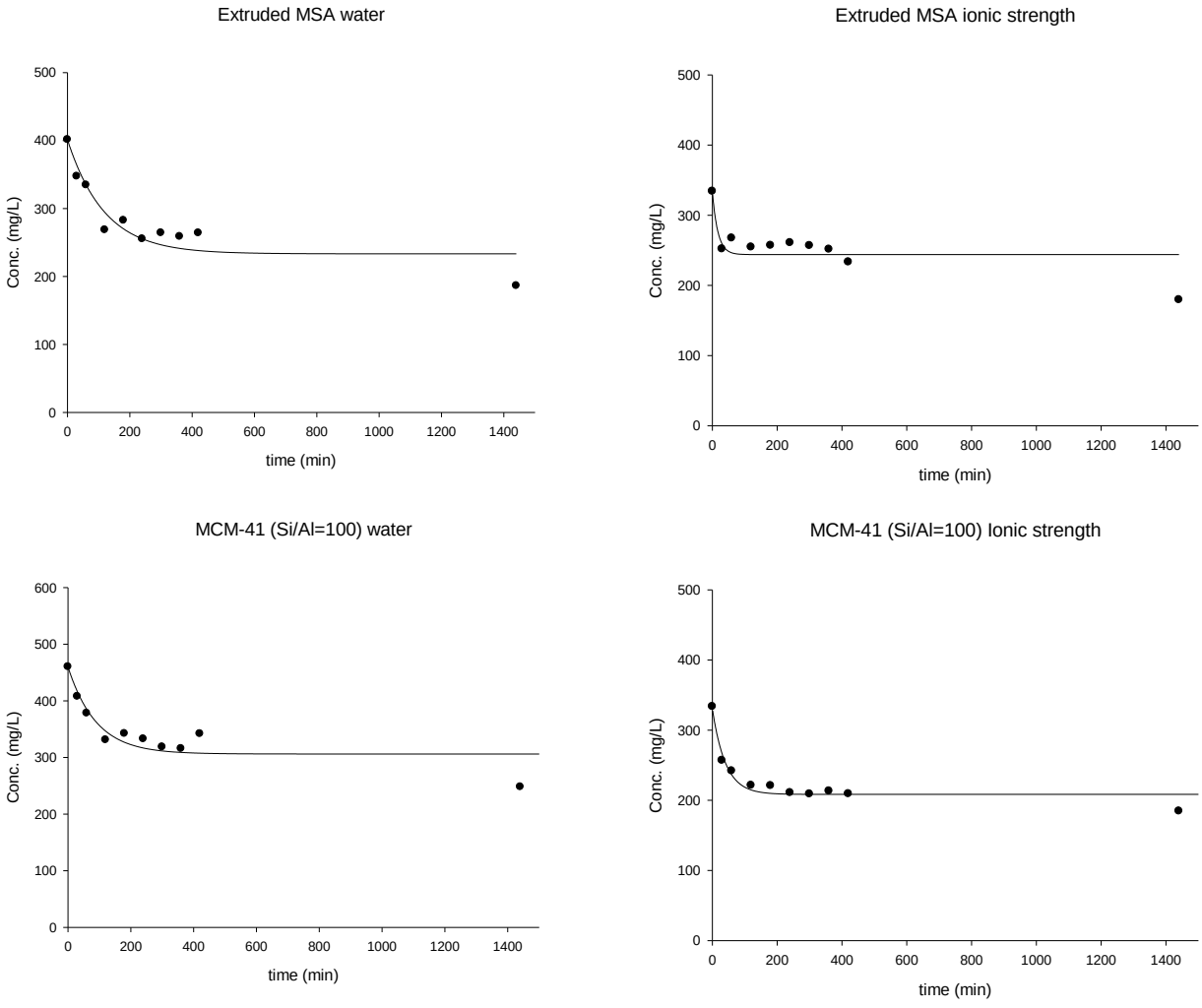

MCM-41 toluene water

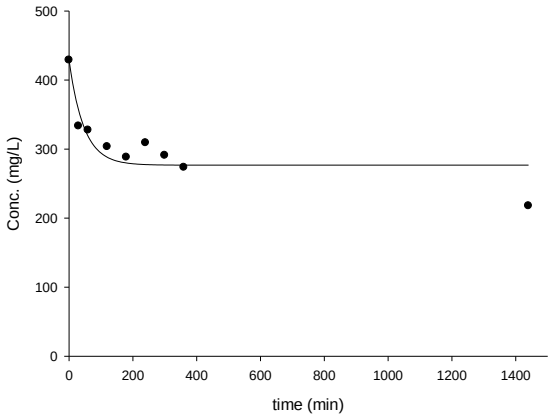

MCM-41 toluene Ionic strength

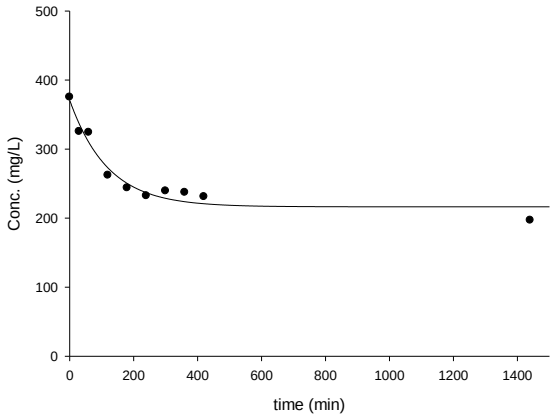

MSA toluene water

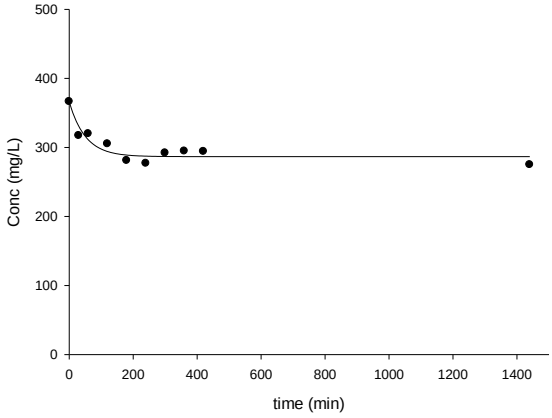

MSA toluene Ionic strength

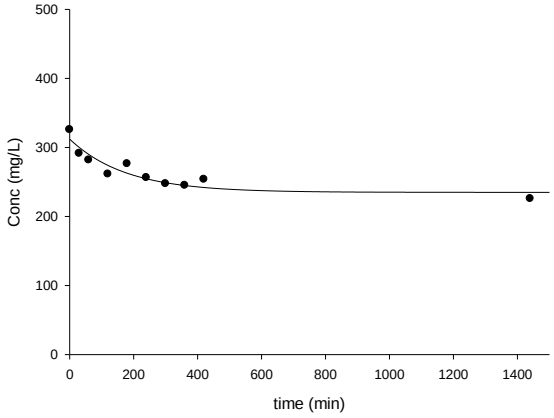

SBA-15 tolene water

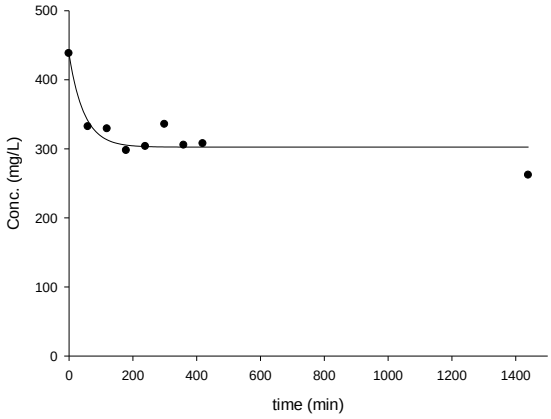

SBA-15 toluene Ionic strength

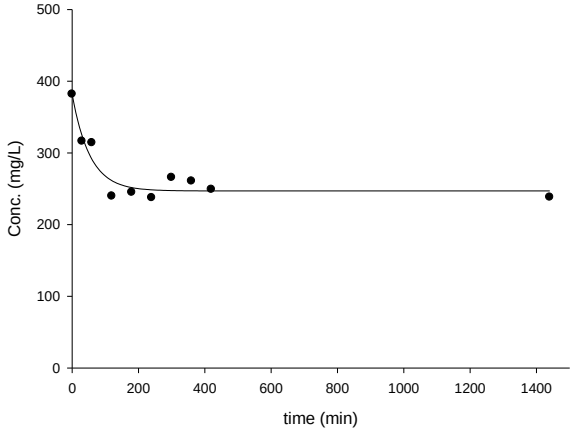

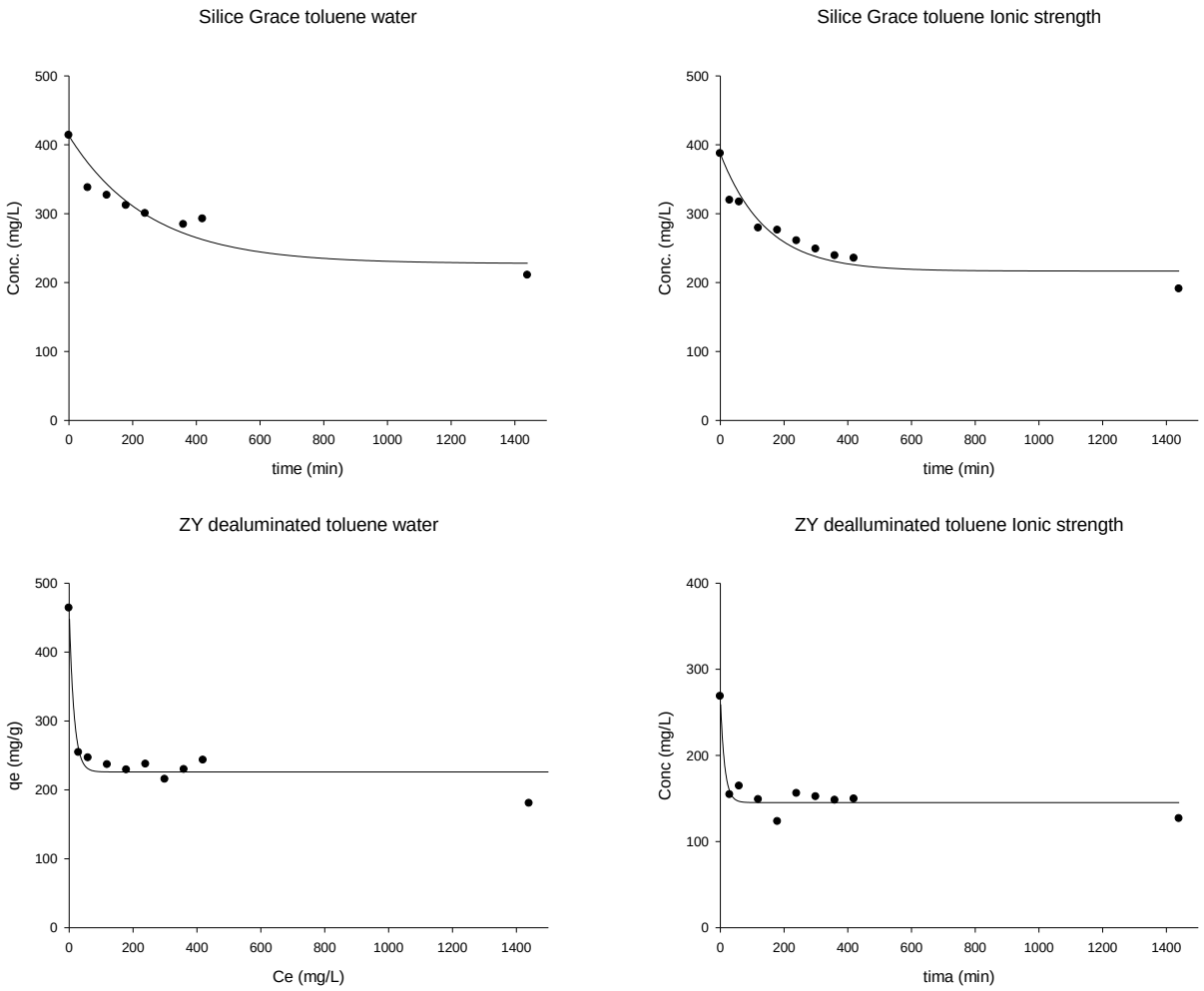

Figure 5.2 Adorption kinetic of toluene onto the investigated materials in water (left panels) and in high ionic strength solution (right panels).

Quantitative removal of the pollutant can be noted within twenty-four hours for all the examined materials. On average, the uptake of toluene is between 40 % and 50 % of the initial concentration, except for granulated MSA and Zeolite Y. The first shows only 25 % of toluene removal, whereas Zeolite Y gives the best performances, exhibiting a toluene removal of 61 % of the initial concentration.

As previously seen, granulated MSA shows the most of pore's diameters centred at about 160 Å and Zeolite Y presents the most of them at about 11 Å, whereas the pore's width of the other

materials take place between them. These considerations joint to results of figures 5.3 and 5.4, which illustrate the relevant influence of the pore width on the toluene removal. When the space to occupy is limited, as for zeolite Y or silica gel, toluene molecules cover materials surface and fill out pore volume more efficiently. Indeed, the plot of the removal percentage versus the pore width of each material (Fig 5.3) shows a good correlation between these two parameters, confirming that the increase of the pore width brings to a decrease of the removal efficiency of toluene within 24 hours. The increase of ionic strength does not bring to changes of data trend (figure 5.3), but the removal efficiency within 24 hours of some materials seems to be influenced.

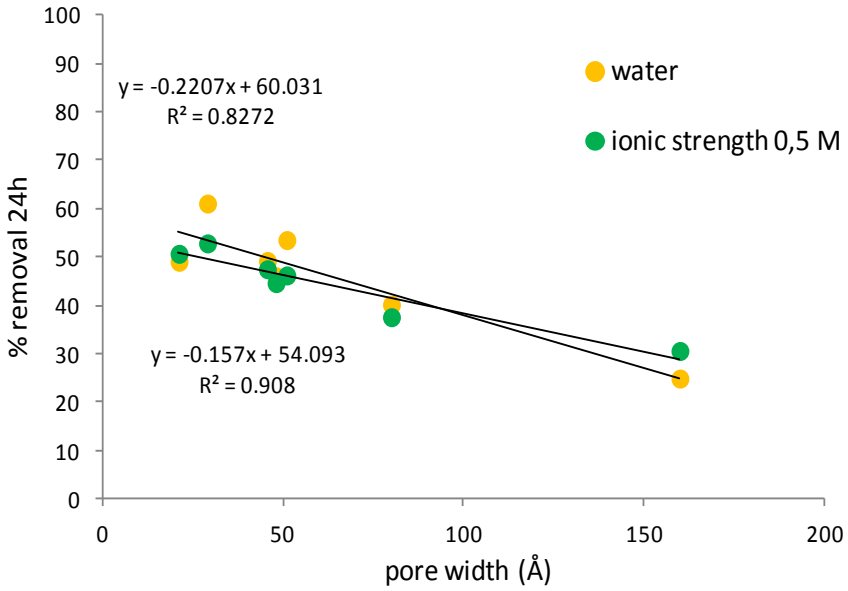

Figure 5.3 Correlation between percentage of toluene removal within 24h and pore width of materials

The effect of high ionic strength on toluene removal by MCM-41, Al-MCM-41, SBA-15 is not significant, while zeolite Y and extruded MSA show a removal decrease and granulated MSA an increase, increasing the water salinity. To explain this behaviour a double effect of surface

chemical composition and pore width of materials might be considered. Zeolite Y is an aluminium-silicate with low Al content, but shows intrinsic basicity as well (due to the few Al atom in its framework) besides it is the material with the smallest pore diameter. At high ionic strength the great number of ions can occupy both the space and surface of pores, interfering with toluene adsorption.

Extruded MSA is a composite material constituted by powdered MSA extruded in cylindrical shape by means of Al_2O_3 binders. It presents large domain of silica surrounded by an alumina matrix. In this case, ions interact with the alumina matrix not interfering with the toluene adsorption but with its diffusion through the bulk material. In both cases, at high ionic strength a reduction of pollutant adsorption is observed. On the contrary, granulated MSA shows an opposite behaviour. The high ionic strength seems to support the toluene removal. This is an high siliceous material with very large pore size and in this case the huge number of ions does not create obstacles inside the pores. The absence of Al in the framework or as binder produces an "hydrophobic" environment suitable for organic molecules. In this case the high ionic strength enhances the suitability of the hydrophobic surface of granulated MSA for toluene adsorption. For these reasons the high salinity of solution promotes the toluene removal from water.

The same considerations can be made about the adsorption and desorption rate constants. The kinetic model (6) developed during this work was applied to experimental data. Through the non linear regression of these data, the values of k_{ads} and k_{deads} of all the materials in both conditions were estimated. The results are reported in table 5.3.

k_{ads} e k_{deads} (min^{-1})	Extruded MSA	Granulated MSA	MCM-41	Al-MCM-41	SBA-15	Silica Gel	Zeolite Y
k_{ads}	0.0035	0.0040	0.0077	0.0037	0.0066	0.0018	0.034
k_{deads}	0.0049	0.0144	0.014	0.0074	0.014	0.0022	0.032
k_{ads}/k_{deads}	0.372	0.326	0.714	0.613	0.545	0.795	0.829
k_{ads} (I=0,5M)	0.016	0.0014	0.0035	0.0092	0.0066	0.0031	0.034
k_{deads} (I=0,5M)	0.043	0.0043	0.0049	0.015	0.0121	0.0039	0.041
k_{ads}/k_{deads} (I=0,5M)	0.714	0.278	0.550	0.500	0.471	0.818	1.063

Table 5.3 Fitted parameters of adsorption kinetic of toluene onto materials in water and high ionic strength solution

Figure 5.4 shows the plot of k_{ads} and k_{deads} ratio versus the pore diameter. The k_{ads} / k_{deads} ratio gives an idea of the extent of the adsorption reaction. In this way the influence of pore diameter and salinity on adsorption rate is evaluated rather than the adsorption efficacy (within 24 hours).

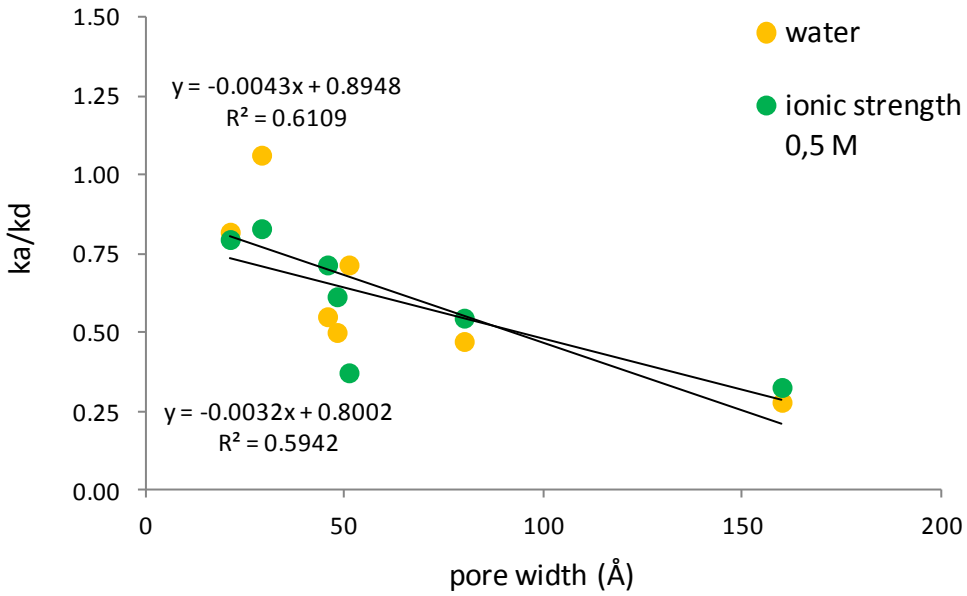

Figure 5.4 Correlation between percentage of toluene removal within 24h and pore width of materials

A similar trend to that seen for removal efficiency is observed for kinetic rate constant ratio, both in water and saline solution. Pore width rules upon the constant rate: materials with smaller pore diameters (Zeolite Y) are faster than those with larger pores (such as granulated MSA). The ionic strength has the same effect observed for removal efficiency; It depresses the adsorption rate of toluene on Zeolite Y and extruded MSA and enhances the adsorption rate on granulated MSA.

5.3.3 Isotherm study

The adsorption process was studied at equilibrium conditions both in water and high ionic strength. Fig. 5.5 shows the adsorption isotherms of the materials and highlights their general ability to remove toluene in both the investigated conditions.

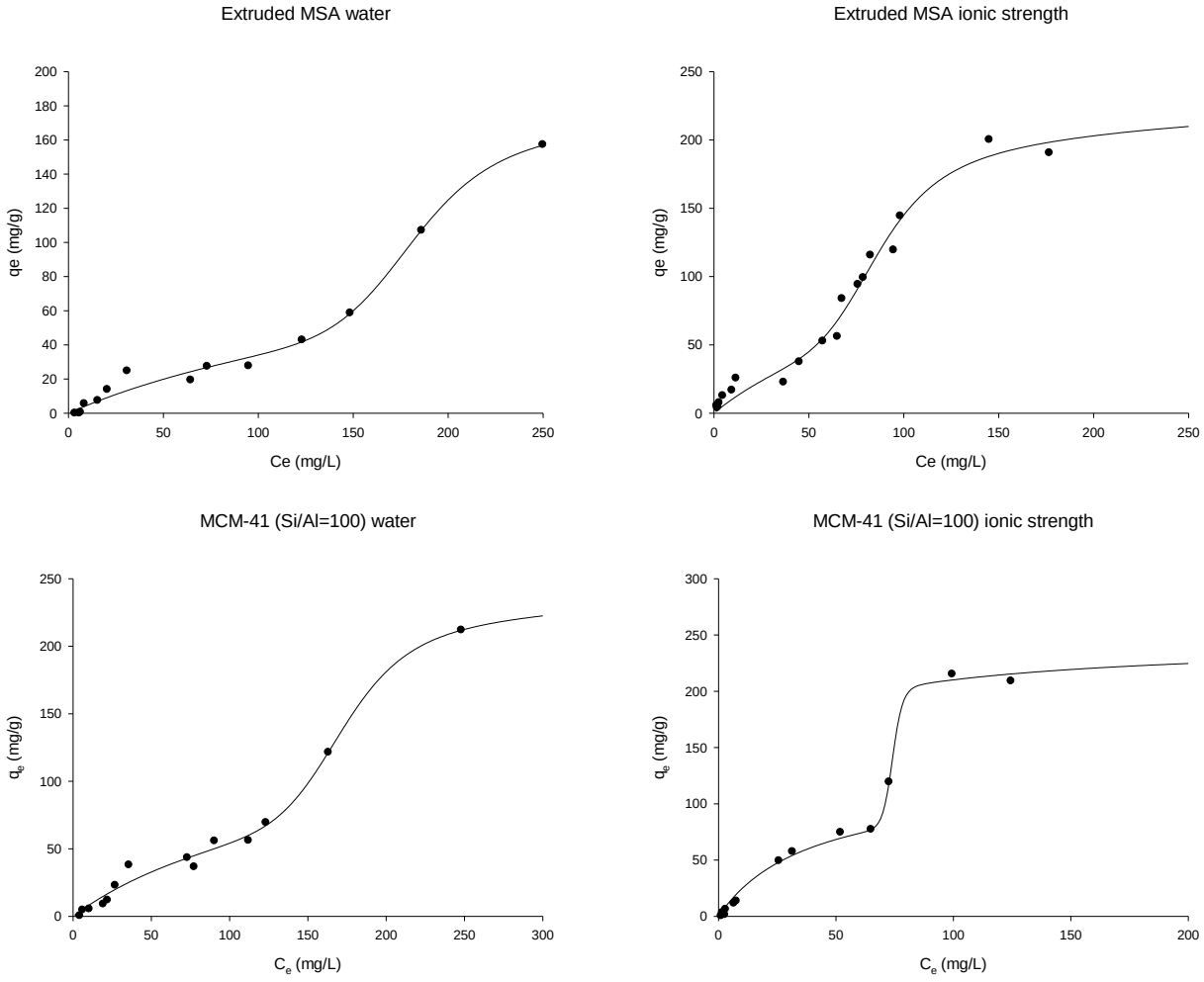

MCM-41 toluene isotherm water

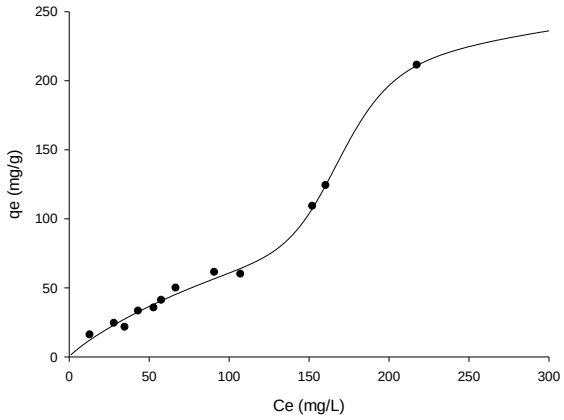

MCM-41 toluene isotherm ionic strength

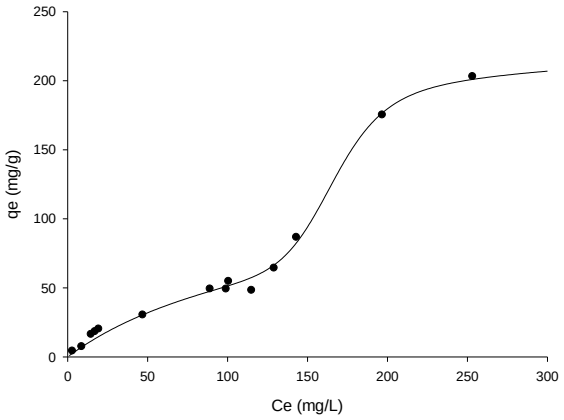

MSA toluene isotherm water

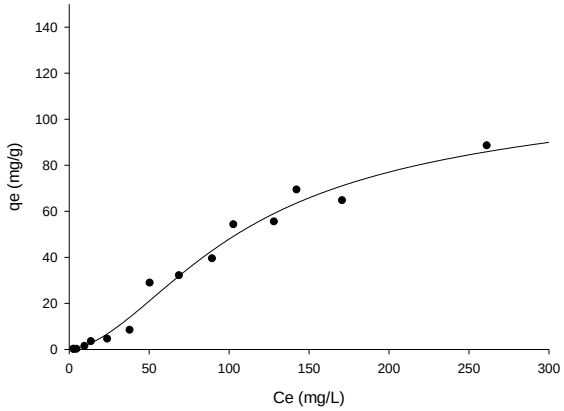

MSA toluene isotherm ionic strength

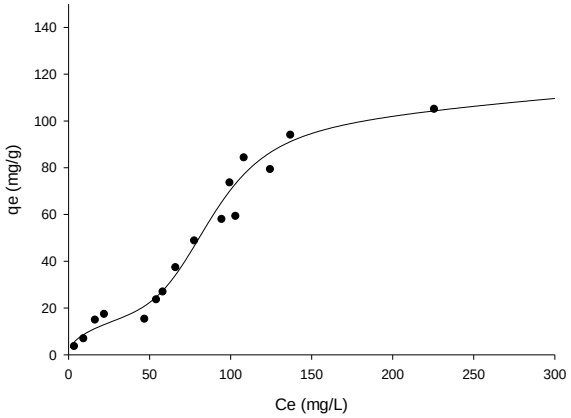

SBA-15 toluene isotherm water

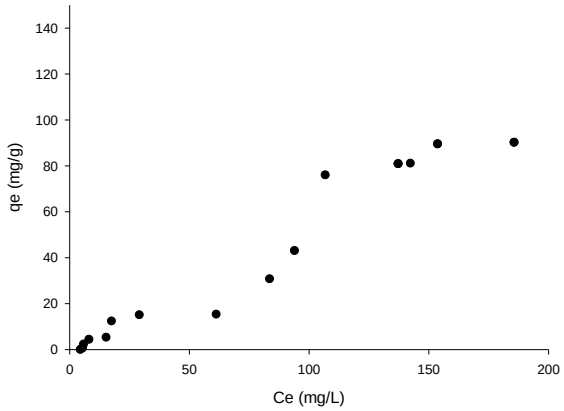

SBA-15 toluene isotherm ionic strength

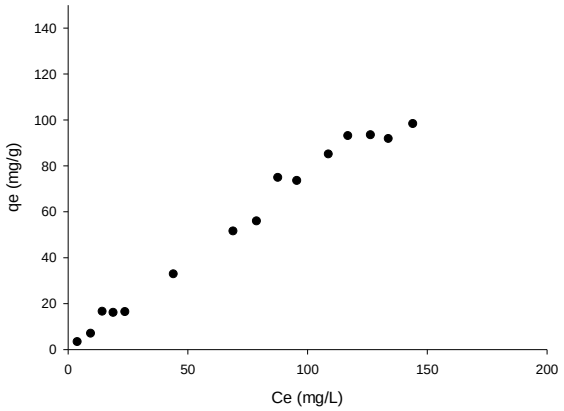

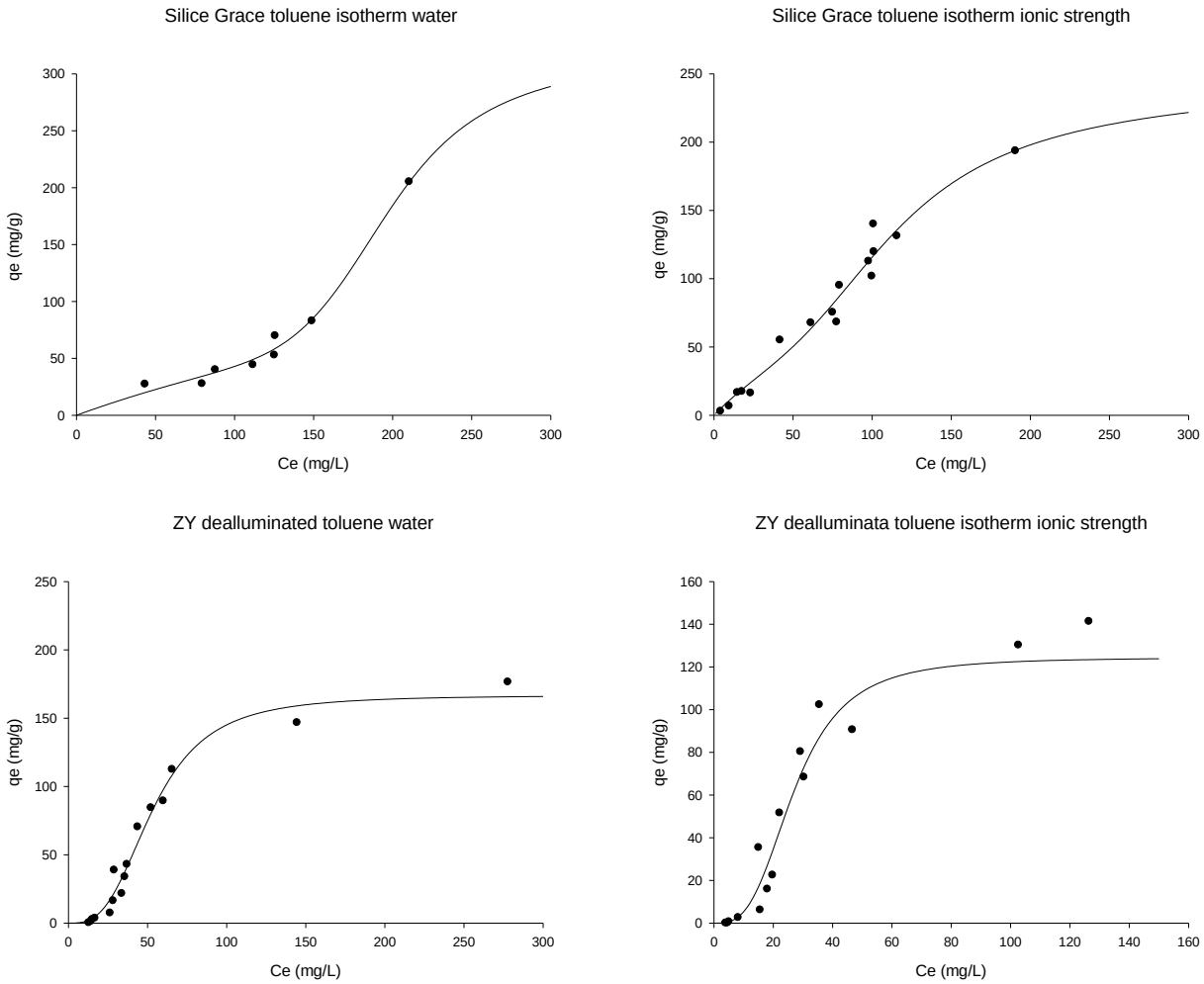

Figure 5.5 Adorption kinetic of toluene onto the investigated materials in water (left panels) and in high ionic strength solution (right panels).

Isotherm data were fitted by equation model (6) for all material, but Zeolite Y.

Zeolite Y is a microporous material with large micropore width and it usually shows an S-type isotherm (Laborde-Boutet et al., 2006). Thence, the Langmuir-Freundilich model seems to be a good choice for describing toluene adsorption onto Zeolite Y. Equation (7) reports the expression of this model:

$$q_e = q_{max} \cdot \left(\frac{K_p \cdot (C_e)^b}{1 + K_p \cdot (C_e)^b} \right) \quad (7)$$

Where Q_e is the toluene adsorbed concentration in mg/g, q_{max} is the maximum toluene adsorbable concentration in mg/g, K_p is the affinity constant in L/g, C_e is the equilibrium concentration of toluene in solution and n is the heterogeneity parameter.

Table 5.4 and 5.5 report the fitted parameters of all the K constants and q_{max} both in simple water solutions and high ionic strength solutions. These parameters were used to understand the influence of ionic strength towards adsorption performances by means of the analysis of the variation of K_p values. K_p is the first affinity constant of the isotherms (6) and (7) and it expresses the affinity of toluene for material surface.

	K_p (L/g)	K_q (L/g)	q_{max} (mg/g)	n
MSA estruso	0.00460	0.00549	213	8.7
MSA granulare	0.00079	0.01007	166	1.9
MCM-41	0.00701	0.00578	285	8.7
Al-MCM-41	0.00642	0.00581	270	8.4
SBA-15	0.0100	0.0103	110	19.6
Silica grace	0.00241	0.00515	420	7
Zeolite Y	0.0187	-	170	3

Table 5.4 *Fitted parameter of adsorption isotherms of toluene onto the materials in water solution*

	K_p (L/g)	K_q (L/g)	q_{max} (mg/g)	n
MSA estruso	0.01156	0.00935	247	5.5
MSA granulare	0.01103	0.01058	123	5.2
MCM-41	0.00697	0.00600	250	10.5
Al-MCM-41	0.02520	0.01349	245	35
SBA-15	0.0208	0.0119	120	4.8
Silica grace	0.00924	0.00885	262	3.2
Zeolite Y	0.0369	-	124	3.1

Table 5.5 *Fitted parameter of adsorption isotherms of toluene onto the materials in high ionic strength solution*

Figure 5.6 shows the comparison between K_p values for simple water solution and K_p values for saline water solution of all the investigated materials (0,5M of ionic strength).

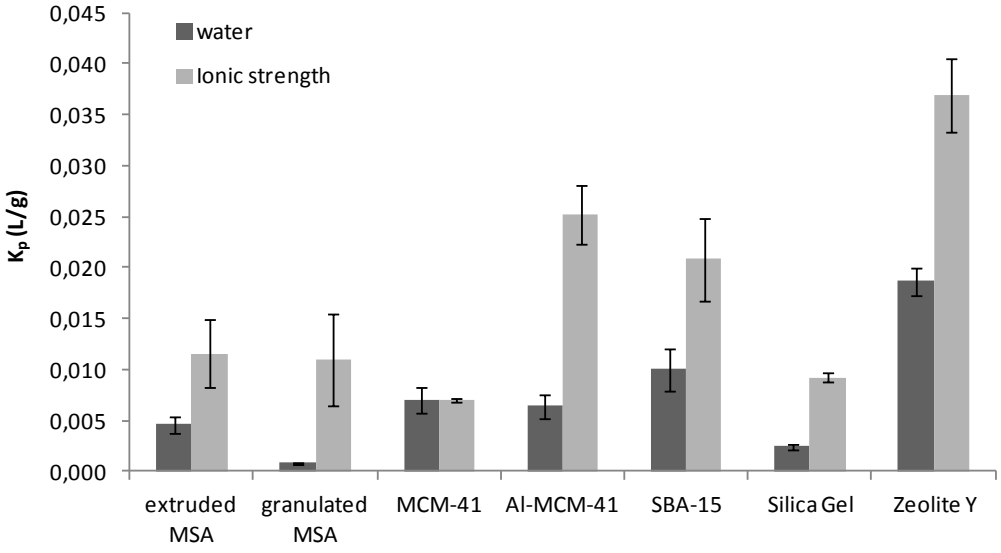

Figure 5.6 *Comparison between K_p value of isotherm in water and high ionic strength conditions.*

The increase of ionic strength brings to a dramatic growing of the K_p value that means a growing of the toluene affinity constant for materials surface. This is due to the chemical-physical phenomenon called salting-out: when an hydrophobic molecule such as toluene is in hydrophilic environment such as a solution at high saline concentration there is the tendency of the molecule for looking for more comfortable environment. In this case the comfortable environment is the hydrophobic siliceous surface of the tested materials, causing the increase of K_p. The effect of ionic strength on q_{max} is diametrically opposite, it decreases when the ionic strength of solution increases, as shown in Fig. 5.7.

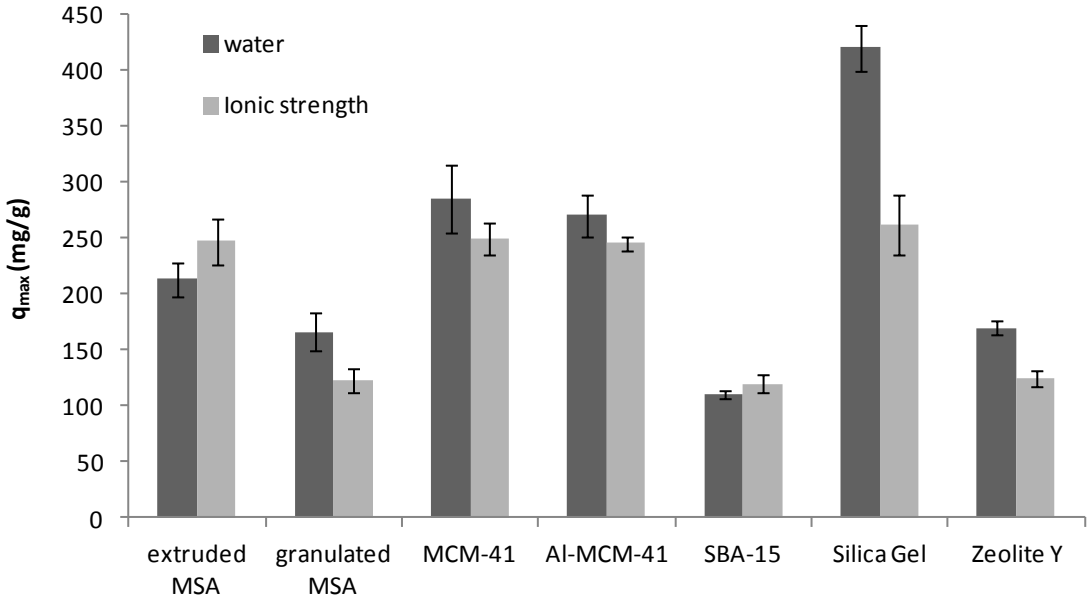

Figure 5.7 *Comparison between q_{max} value of isotherm in water and high ionic strength conditions.*

Extruded MSA is the only material whose q_{max} value increases whit the increasing of ionic strength. Q_{max} expresses the amount of adsorbed toluene when its equilibrium concentration tends towards infinitive or, in other words, the maximum amount of toluene that 1g of adsorbent material is able to adsorb. For microporous materials q_{max} is strictly linked to the internal surface, being the adsorption essentially a superficial phenomenon. For mesoporous material instead q_{max} is linked both to the internal surface and volume of pores. Thence, emptier is the internal space of the pores more toluene can adsorb and stack inside it. These considerations highlight that at high ionic strength the great number of ions can occupy space in lieu of toluene molecules, determining the observed q_{max} decrease.

Extruded MSA does not show this general depression of q_{max} with the increase of ionic strength. This material is the only composite material of the studied set and it is composed of an hydrophilic matrix of alumina that surrounds little hydrophobic domains of silica (art ingh). In this case, the ions do not occupy the pore volume of silica domains preferring the interaction with the hydrophilic surface of the alumina. In this way there are not any interferences between toluene and ions and this brings to an increase of the q_{max} value. Figure 5.8 reports the correlation between micropore volume of materials and the value of q_{max} related to the first plateau of the isotherms.

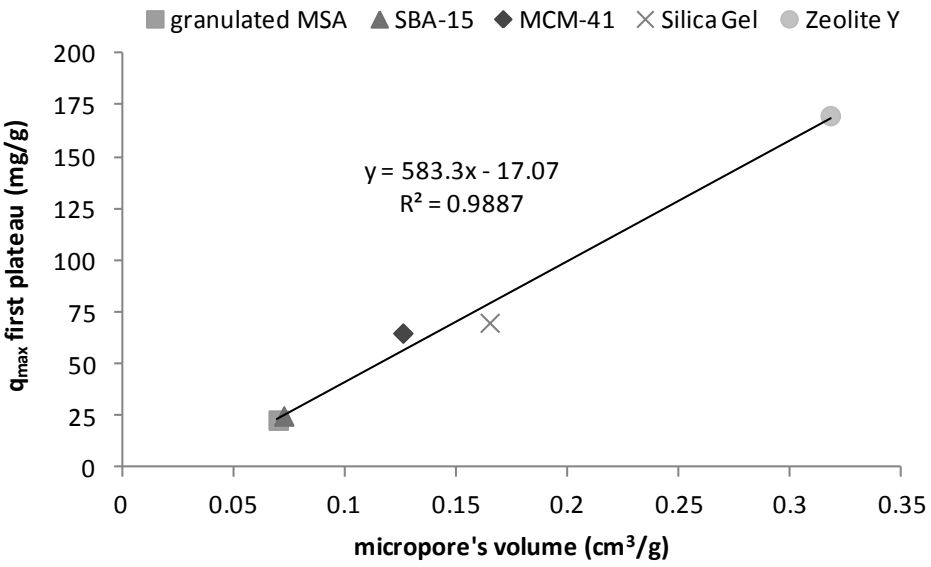

Figure 5.8 *Correlation between q max of first plateau and micropore's volume of Granulated MSA, SBA-15, MCM-41, Silica Gel and Zeolite Y*

This correlation can be made for all the material, except for extruded MSA and Al-MCM-41 because they do not have micropores as indicated in Figure 5.1. Figure 5.8 shows the strong dependence of the amount of toluene adsorbed in the first part of the isotherm and micropore dimensions. For Zeolite Y the q_{max} of the first plateau correspond to the overall $q_{max,}$ being zeolite Y a microporous material. For the adsorbents showing the q_{max} dramatically lower than the Zeolite Y's one, the q_{max} value of the first plateau represents only a part of the overall q_{max}. This means that pores of microporous materials (such as zeolite Y) are all readily filled during the adsorption of high concentrated compounds, whereas mesoporous material can virtually adsorb compounds at low and high concentrations using alternatively micropores and mesopores, depending on the applied conditions. Indeed, Figure 5.1 can give an idea about the potentiality of mesoporous material in the adsorption of organics from water. For instance, only the micropores of granulated MSA (the same consideration can be made for the other mesoporous materials) are filled after the

adsorption of toluene from the initial concentration of 400 mg/L, leaving its mesopores empty and thence ready to further molecules.

It was then hypothesized for toluene an adsorption mechanism that first provides the microporous surface coverage and after the filling of pores. To understand how many toluene molecules are stacked up into the pores it might be useful to compare the q_{max} value (that expresses the amount of toluene into the pores) with a virtual q_{max} calculated as the product of the micropores' volume and the toluene bulk density. In this way, calculated q_{max} represents the amount (in mg/g) of toluene packed into the pores considering that the distance between two adjacent molecules is equal to the distance existing between the same molecules in the liquid toluene. Thence, the calculated q_{max} becomes both an indicator of the maximum degree of molecules' stacking and a term for comparison to establish how much toluene molecules are stacked into the pores, in real adsorption conditions.

Figure 5.9 reports the graph of q_{max} of the first plateau (that is related to micropores' filling) versus calculated q_{max} for all the materials and also shows the linear correlation between these two parameters. The slope of the line could be called *stacking factor* and gives an idea of the actual stacking of toluene molecules. In this case toluene molecules are stacked for almost 60% of their capacity.

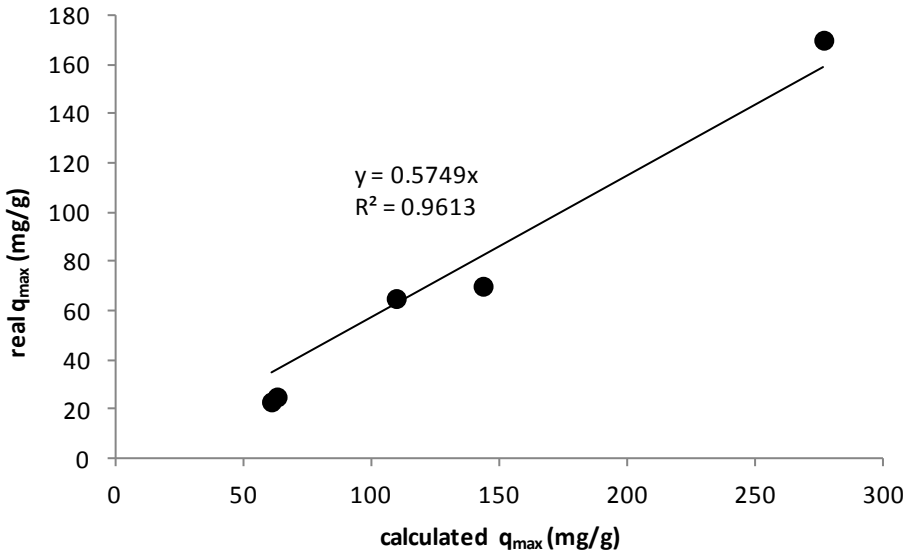

Figure 5.9 *correlation between real q_{max} and calculated q_{max} of the first plateau of isotherms.*

5.3.4 Regeneration study

Figure 5.10 shows the results of the preliminary tests performed for regenerating the studied materials. In the histograms is reported the percentage of toluene adsorbed after regeneration by heating materials versus the temperature of regeneration. Tests are performed at 60°C, 80°C and 100°C and the percentages of adsorbed toluene at these temperatures of regeneration are compared to the percentages of adsorbed toluene on materials kept at 550°C. This last represents the temperature at which the materials have been previously activated (Perego et al., 1999).

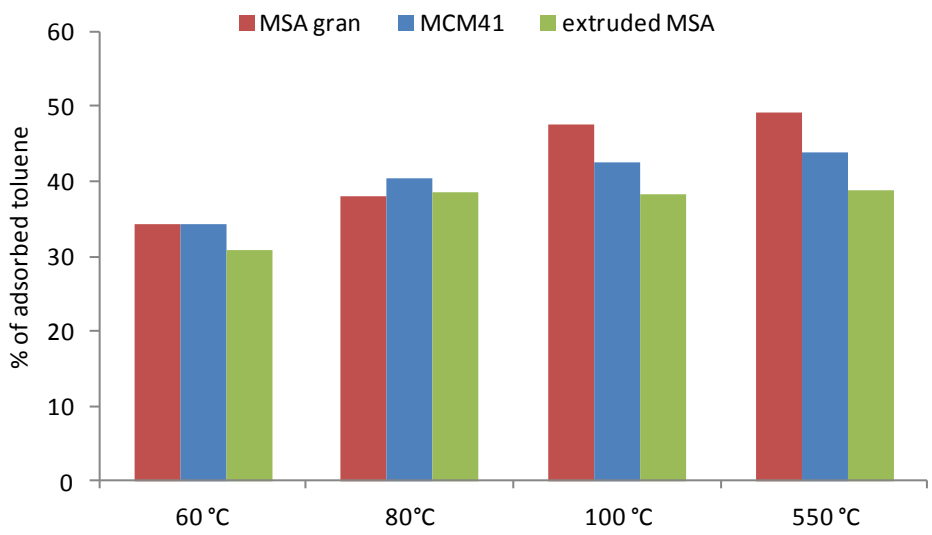

Figure 5.10 Percentage of adsorbed toluene onto granulated MSA, extruded MSA and MCM-41 after regeneration at 60°C, 80°C, 100°C and 550°C.

The graph of figure 5.10 highlights that the amount (%) of adsorbed toluene after regenerating materials at 100°C for 1h is the same than that at 550°C. For this reason the experiments of adsorption isotherm on regenerated materials are performed using 100 °C as regeneration temperature.

Figures 5.11 displays the isotherms of granulated MSA, extruded MSA and MCM-41. The adsorption performances get worse on loaded (kept in contact with toluene) granulated MSA and MCM-41 and they remain the same for extruded MSA.

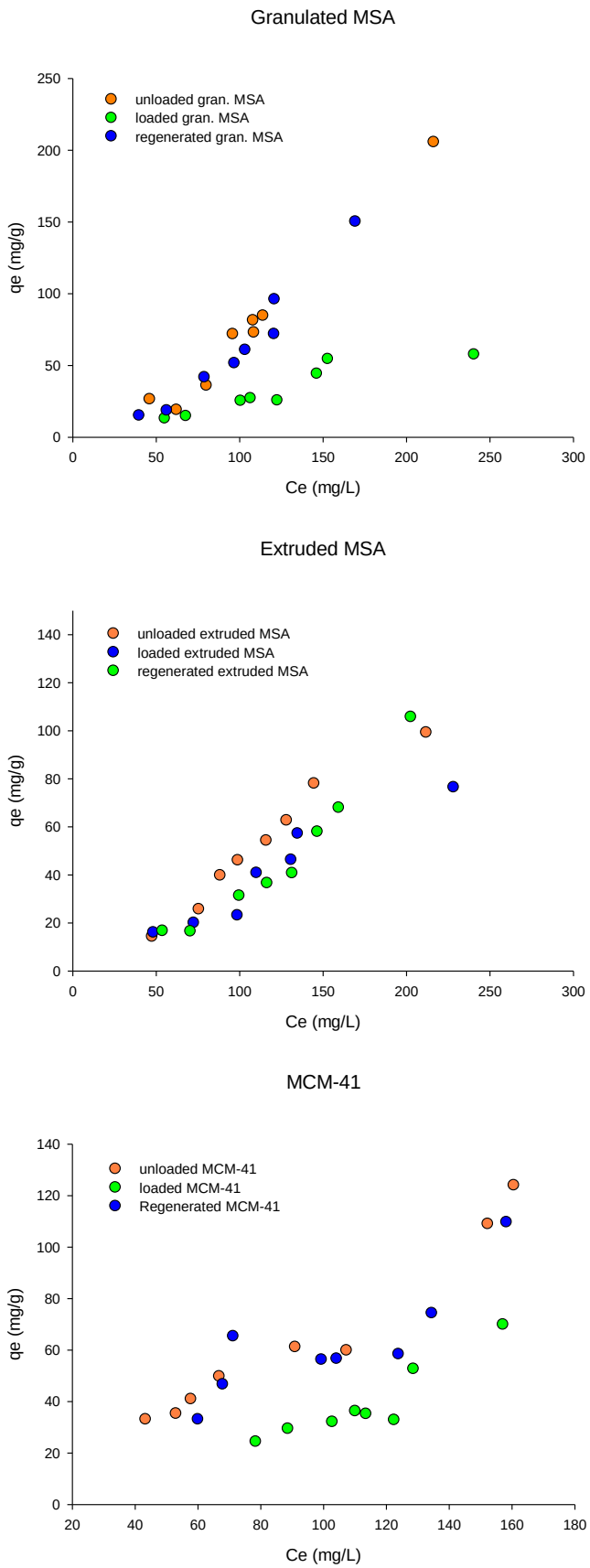

Figure 5.11 *Adsorption isotherms of toluene onto unloaded, loaded and regenerated granulated MSA extruded MSA and MCM-41*

This different behaviour can be again ascribed to the different distribution of pore dimensions that characterizes each material. Granulated MSA and MCM-41 have both micropore and mesopore system and, as seen in the previous section, under the applied initial concentration of toluene, their micropores are firstly filled by toluene molecules. On the other hand, extruded MSA is devoid of pores below 20 Å of diameter and the adsorption of toluene is all due to its mesopores. In the range of the initial toluene concentration of 40 – 400 mg/L, the mesopores are far from being filled by toluene, remaining a wide space for further molecules. For this reason the isotherm of loaded extruded MSA is similar to that of unloaded one. Only the point at high initial toluene concentration seems to be affected by the presence of previous adsorbed molecules, maybe due to the covering or partial filling of mesopores by toluene at these concentrations.

5.4 Conclusion

This study underlines the importance that mesoporous materials can play in the adsorption processes for water remediation. They are good adsorbent for dissolved hydrocarbons and the huge internal empty space is suitable to host also oil drops that are usually present in the real wastewaters derived from petrochemical activities (Viel et al., 2004). The role of pore distribution is crucial for adsorption performances of these materials. Materials with pore width below 2 nm (microporous material) such as Zeolite Y and Silica Gel are suitable for dissolved pollutants at moderate concentration. Mesoporous material with more than one pore width domain can act simoultaneously as adsorbent for dissolved hydrocarbons thanks to their micropores system and as sponge for dispersed hydrocarbons or oil drops hosting them in their mesopores system. The high ionic strength of solution seems to not depress the adsorption performances of the materials and in some cases it represents an advantage increasing the amount of adsorbed toluene. Finally regeneration study has highlighted how thermal regeneration of MSA is simple and already

effectiveness at 80 °C – 100 °C. The facility of regeneration and the relative low temperature required for removing the adsorbed pollutants may represent an important advantage in terms of cost-effectiveness.

5.5 References

Banat F., Sameer Al-Asheh, Leema Al-Makhadmeh. Evaluation of the use of raw and activated date pits as potential adsorbents for dye containing waters. Process Biochemistry Volume 39, Issue 2, 31 October 2003, Pages 193–202

Cícero P. Moura, Carla B. Vidal, Allen L. Barros, Luelc S. Costa, Luiz C.G. Vasconcellos,Francisco S. Dias, Ronaldo F. Nascimento Adsorption of BTX (benzene, toluene, o-xylene, and p-xylene) from aqueous solutions by modified periodic mesoporous organosilica. Journal of Colloid and Interface Science 363 (2011) 626–634.

IUPAC Recommendations Pure Appl. Chem. 1985, 57, 604

IUPAC Recommendations Pure Appl. Chem. 1994, 66, 1739

Kenji Hara, Saiko Akahane, Jerzy W. Wiench, Breina R. Burgin, Nobuhiro Ishito, Victor S.-Y. Lin, Atsushi Fukuoka and Marek Pruski. Selective and Efficient Silylation of Mesoporous Silica: A Quantitative Assessment of Synthetic Strategies by Solid-State NMR. J. Phys. Chem. C 2012, 116, 7083−7090

Kim Yong-ho, Byunghwan Lee, Kwang-Ho Choo, Sang-June Choi Selective adsorption of bisphenol A by organic–inorganic hybrid mesoporous silicas Microporous and Mesoporous Materials 138 (2011) 184–190

Laborde-Boutet C., G. Joly, A. Nicolaos, M. Thomas and P. Magnoux. Selectivity of Thiophene/Toluene Competitive Adsorptions onto NaY and NaX Ind. Eng. Chem. Res., 2006, 45 (20), pp 6758–6764

Lee J.W., Wang Geun Shim, Hee Moon. Adsorption equilibrium and kinetics for capillary condensation of trichloroethylene on MCM-41 and MCM-48. Microporous and Mesoporous Materials 73 (2004) 109–119

Neimark AV, Lin Y, Ravikovitch PI, Thommes M. Quenched solid density functional theory and pore size analysis of micro-mesoporous carbons. Carbon 2009;47:1617-28.

Parida K., Krushna Gopal Mishra and Suresh Kumar Dash. Adsorption of Copper(II) on NH2-MCM-41 and Its Application for Epoxidation of Styrene Ind. Eng. Chem. Res. 2012, 51, 2235–2246

Perego C., S. Amarilli, A. Carati, C. Flego, G. Pazzuconi, C. Rizzo, G. Bellussi Mesoporous silica-aluminas as catalysts for the alkylation of aromatic hydrocarbons with olefins Microporous and Mesoporous Materials 27 (1999) 345–354.

Pollock Rachel A. , Brenna R. Walsh, Jason Fry, I. Tyrone Ghampson, Yuri B. Melnichenko, Helmut Kaiser, Roger Pynn, William J. DeSisto, M. Clayton Wheeler and and G. Frederick Size and Spatial Distribution of Micropores in SBA-15 using CM-SANS Chem. Mater. 2011, 23, 3828–3840.

Qingdong Qin, Jun Ma., Ke Liu Adsorption of nitrobenzene from aqueous solution by MCM-41 Journal of Colloid and Interface Science 315 (2007) 80-86.

Ravikovitch PI, Vishnyakov A, Russo R, Neimark AV. Unified approach to pore size characterization of microporous carbonaceous materials from N2, Ar and CO2 adsorption isotherms. Langmuir 2000;16:2311-20.

Serna-guerrero Rodrigo and Abdelhamid Sayari. Mesoporous Silica. 7. Adsorption of Volatile Organic Compounds Environ. Sci. Technol. 2007, 41, 4761-4766.

Shengping Wang, Yun Shi, Xinbin Ma, and Jinlong Gong Tuning Porosity of Ti-MCM-41: Implication for Shape Selective Catalysis ACS Appl. Mater. Interfaces 2011, 3, 2154–2160

Veil John A., Markus G. Puder, Deborah Elcock, Robert J. Redweik, Jr A white paper describing Produced water from production of crude oil natural gas and coal bed methane U.S. Department of Energy National Energy Technology Laboratory

Wu X., K.N. Hui, K.S. Hui, S.K. Lee, W. Zhou, R. Chen, D.H. Hwang, Y.R. Cho, Y.G. Son. Adsorption of basic yellow 87 from aqueous solution onto two different mesoporous adsorbents. Chemical Engineering Journal 180 (2012) 91– 98

CHAPTER 6

NEW MATERIAL FOR HYDROCARBONS AND HEAVY METALS REMOVAL: STRUCTURAL CHARACTERIZATION.

In this chapter the attention is focused on the host-guest interactions, the morphological features and the structural modifications that occurs during the adsorption process onto the MSA material, using different spectroscopic and analytical techniques. The thermal behavior of the loaded and unloaded material and is also studied. SEM images and EDX analysis of the two materials have confirmed their amorphous nature and their elemental composition while XRD spectra of virgin and loaded MSA displayed the appearance of some reflection peaks after the adsorption of benzene and toluene; A Le Bail refinement using these peaks indicated a monoclinic structure for these molecules when adsorbed onto the MSA. FT-IR measurement were performed to know the type of interaction that occur between material surface and adorbed compounds. FT-IR spectra collected on loaded and unloaded MSA highlighted the interaction of water with the free silanol groups while the aromatic hydrocarbons probably adsorb through different active sites: the Lewis acid sites. Indeed, intrinsic acidity measurements by Pyridine adsorption showed the presence of a fairly good number of these acid sites. Finally the thermal behavior of loaded MSA samples with different contaminants have shown the strong influence of water on the desorption temperature of pollutants from MSA.

6.1 Experimental section

6.1.1 Materials

The mesoporous material was developed and synthesized by eni S.p.A. (Belussi et al., 1993; Belussi et al., 1994). MSA adsorbents were synthesised via sol-gel in alkali-free medium using $Si(OC_2H_5)_4$ (Dynasil-A, Nobel), $Al(sec\text{-}OC_4H_9)_3$ (Sigma-Aldrich®), tetrapropylammonium hydroxide (TPA-OH, Sachem), alcohol (R-OH) selected among C_2H_5OH or $n\text{-}C_3H_7OH$ (Aldrich). All preparations were performed at the same molar ratios: TPA-OH/SiO_2 = 0.09, H_2O/SiO_2 = 8 and alcohol/SiO_2 = 8. A typical synthesis preparation is described: $Al(sec\text{-}OC_4H_9)_3$ was dissolved in $Si(OC_2H_5)_4$ at 60 °C. The obtained homogeneous solution was cooled at room temperature, and then the required alcohol and TPA-OH in aqueous solution were added in sequence. Monophasic clear solutions were obtained, and then transformed in homogeneous compact gel without separation of phases. The SiO_2/Al_2O_3 (SAR) molar ratio and the selected alcohol are reported in Table 1 for each preparation. After 15 hour ageing at room temperature, the gels were dried at 100 °C and calcined 8 h in air at 550 °C. MSA samples textural characterisation was carried out by nitrogen adsorption at -196 °C on Micromeritics ASAP 2010 apparatus. Before determination of adsorption-desorption isotherms the samples (~ 0.2 g) were outgassed for 16 h at 350 °C under vacuum. The MSA synthesized and studied in this work was amorphous with a low degree of long-range order in terms of pore disposition. The extruded MSA was obtained by a post-synthetic modification of particle MSA, extruding the MSA particles into cylindrical shape, using Al_2O_3 as binder. In table 6.1, the main physical characteristics of the particle and extruded MSA are shown. Apparent specific surface area (A-SSA, Brunauer Emmett and Teller method), specific pore volume (V_p, Gurvitsh rule) and mean pore size (D_p,

non-local density functional theory algorithm) were evaluated from the acquired isotherms. Before water treatment experiments, materials were sifted between 0.12 and 0.5 mm and calcined at 550 °C for 8 h.

Adsorbent	SAR	A-SSA (m^2/g)	Alcohol	Vp (ml/g)	Dp (Å)
Extruded MSA	∞	487	C_3H_7OH	1.06	51
Particle MSA	∞	233	C_3H_7OH	0.52	98

Table 6.1. *Textural properties of particle and extruded MSA.*

6.1.2 Adsorption tests

The adsorption tests were carried on both materials using toluene and benzene as target contaminants. Aqueous solutions of these hydrocarbons were prepared at a concentration as high as possible paying attention to not overcome their solubility limit; in this way, we chose to operate at 400 mg /L of toluene and 800 mg/L of benzene. Each solution (50 ml) was kept in contact with 0.05 g of MSA with rotative stirring for twenty four hours to ensure the attainment of the equilibrium state. Tests using an emulsion of diesel oil in water were performed in order to have information about the behavior of the MSA in a situation closer to reality. Afterwards, each sample was filtered and the solid material was analyzed by X-ray diffractometry (XRD), Fourier transformed Infra-Red spectrometer (FT-IR), Thermogravimetric analysis (TGA) and

scanning electron microscopy (SEM). To investigate the nature of the host-guest interaction and the role of the water in the adsorption phenomenon, the same type of analyses were performed on the material before the adsorption tests. Finally, analyses on pure adsorbed contaminants (benzene and toluene) have been made to distinguish which kind of interactions are due to organics, water and water-organic mixture.

6.1.3 SEM

Morphological analyses have been performed using a SEM (Carl Zeiss EVO®50) after and before the adsorption of the contaminants. In addition to this, an EDX probe (Oxford INCA *x*-sight) was used to determine the elemental chemical composition of the mesoporous material and the Si/Al ratio in the extruded one.

6.1.4 XRD

A Panalytical Empyrean and X'Pert Pro XRD diffractometers (Cu Kα, λ=1.54184 Å) were used to analyze the solid samples before and after the adsorption of benzene and toluene. The loaded and unloaded material were finely ground before the analysis. The range 5 to 80 degrees in 2θ angle was investigated and the data was used to perform a Le Bail refinement structure utilizing FullProf® suite. Phase identification was performed by using the Panalytical High Score Plus software package. The refinement was made both on the loaded and unloaded MSA to understand which kind of structure modifications occurred during the adsorption process of the hydrocarbons and which kind of position the organic contaminants assumed into the pore channel. Afterwards

small angle analyses were performed in the range 0 to 5 degrees. This kind of measurement is more suitable to investigate the mesoporous region of the material and the possible changes occurring after the adsorption, as well as the molecule arrangement into the mesopores.

6.1.5 FTIR

The FT-IR analysis was made using a Mattson Genesis II spectrometer. Powder samples of MSA were analyzed before and after the adsorption of benzene and toluene to understand the interaction between the organics and the functional groups present at the solid surface. The spectra were recorded from 400 to 4000 cm^{-1} wave number in terms of transmittance percentage with a resolution of 1 cm^{-1}.

6.1.6 Acidity Measurement

The IR spectrometer was also used to measure the intrinsic acidity of the MSA. The method applied was the Pyridine adsorption and IR detection method described in (Flego et al., 1995). The MSA samples were held in a saturated pyridine environment overnight and then collected, powdered and analyzed by the FT-IR. The peak at 1455 cm^{-1} is indicative of the presence of Brønsted acid sites (such as silanol groups), while at 1545 cm^{-1} there is a peak linked to the absorption of pyridine adsorbed onto the Lewis acid sites (Perego et al., 1999)

6.1.7 TGA

Thermogravimetric analyses were performed on a Perkin Elmer TGA7 thermogravimetric analyzer heating from room temperature to 800 °C at 20°C/min. Also in this case, the analysis was performed on the unloaded MSA and loaded MSA with aqueous and pure contaminant solutions. TGA measurements are suitable to determine the amount of adsorbed contaminant and better temperature for regeneration, besides the strength of the adsorbent-adsorbed bond. To understand the regeneration ability of the MSA and its possible loss in the adsorption performances, we stressed the MSA with ten consecutive cycles of adsorption-regeneration using both toluene and benzene. The regeneration step took place in the same conditions of the MSA synthesis; the material was held in a furnace at the temperature of 550 °C for 8 hours.

6.2 Result and discussion

6.2.1 SEM

SEM images of the extruded MSA were collected to explore its morphological features. In figure 1 a and b, the images are at 200 nm and 10 µm, respectively. At every resolution it is possible to note the amorphous nature of the material.

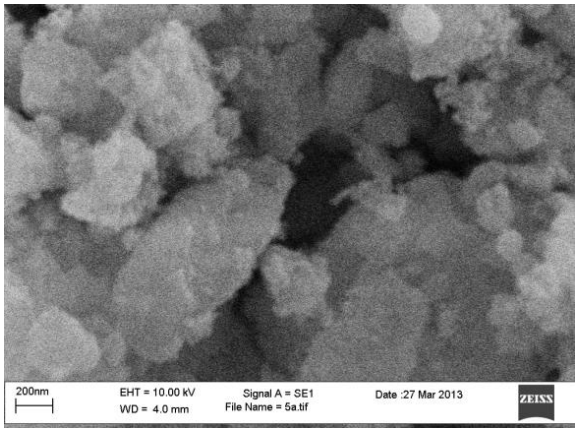

***Fig. 6.1**. Extruded MSA 200 nm.*

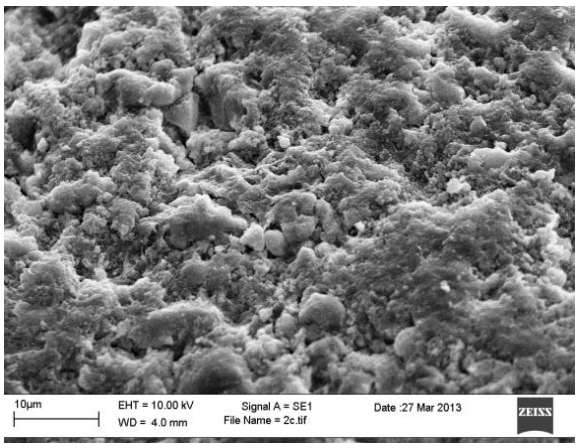

***Fig. 6.2** Extruded MSA 10 µm.*

Table 6.2 shows instead the atomic percentage weight of the main chemical constituent of the mesoporous materials.

Atom	Extruded MSA	Particle MSA
Si (weight %)	23.69	45.6
O (weight %)	44.54	53.8
Al (weight %)	9.90	0.6

Table 6.2 EDX analyses of extruded and particle MSA

As expected, the extruded MSA is also composed of aluminum while the particle MSA inside is poor. The image 6.3a displays a sample of extruded MSA at 30 µm of resolution; the same image is rebuilt in terms of aluminum and silicon atoms (figure 6.3b). The green color is indicative of the Al atom and the blue is specific for the silicon atom. It is very clear how the surface of the extruded MSA is not homogenous as expected: little aluminum domains are surrounded by a silicon matrix. This surface heterogeneity may represent a criticality during the adsorption process.

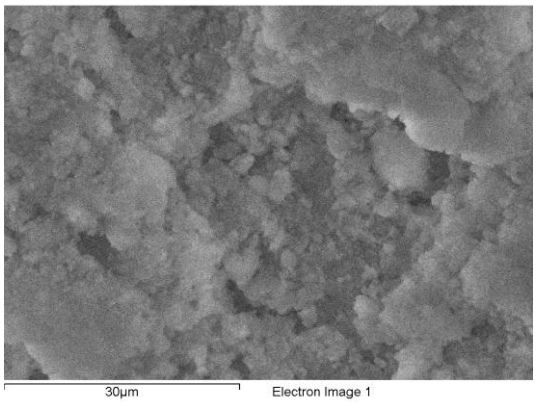

Fig 6.3a *SEM image of extruded MSA at 30 µm.*

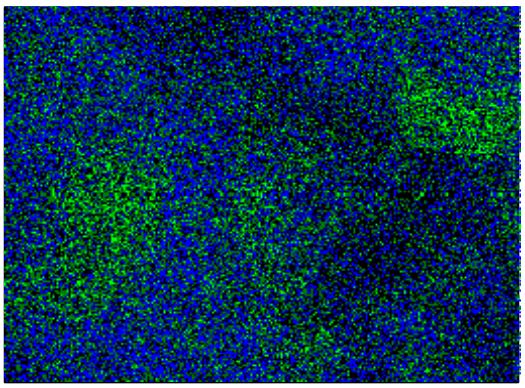

Fig 6.3b. *Reproduction of extruded MSA in terms of Al atoms (green) and silicon atom (blue).*

The dehydroxylated silicon content is the main factor in the adsorption of organic contaminants; the presence of areas rich in hydrophilic aluminum enclosed in a silica active matrix might create a "cold" spot not suitable for removing hydrophobic hydrocarbons. SEM images (Figures 6.4 and 6.5) of the particle MSA were also

collected at 200 nm and 2 µm of resolution to gain an idea of the surface morphology of this material. The images show the presence of a smooth surface at higher and lower resolution very different from the extruded MSA one. The extrusion process is probably responsible for the alteration of the particle MSA surface.

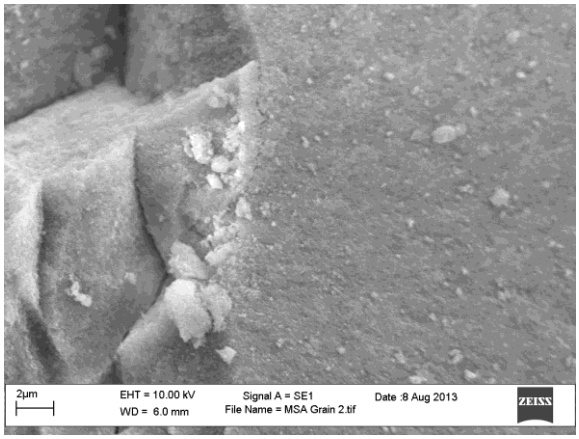

Fig. 6.4 *Particle MSA 2 µm.*

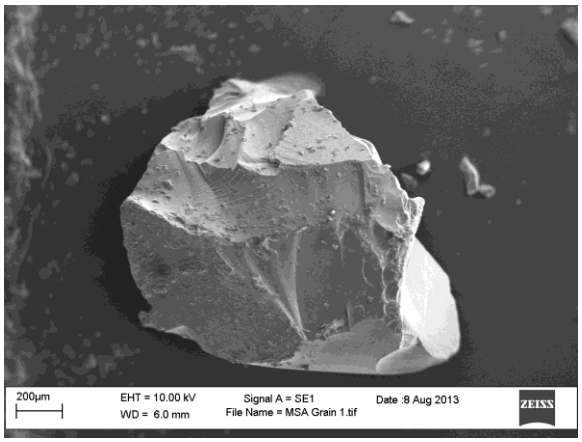

Fig. 6.5 *Particle MSA 200 nm.*

The EDX analysis in table 6.2 confirms the siliceous nature of these materials; the higher percentage of aluminum content in the extruded MSA is mainly due to the use of alumina as binder during the extrusion process.

6.2.2 XRD

XRD analyses are reported in Figures 6.6 a-b, 6.7 a-b and 6.8 a-b.

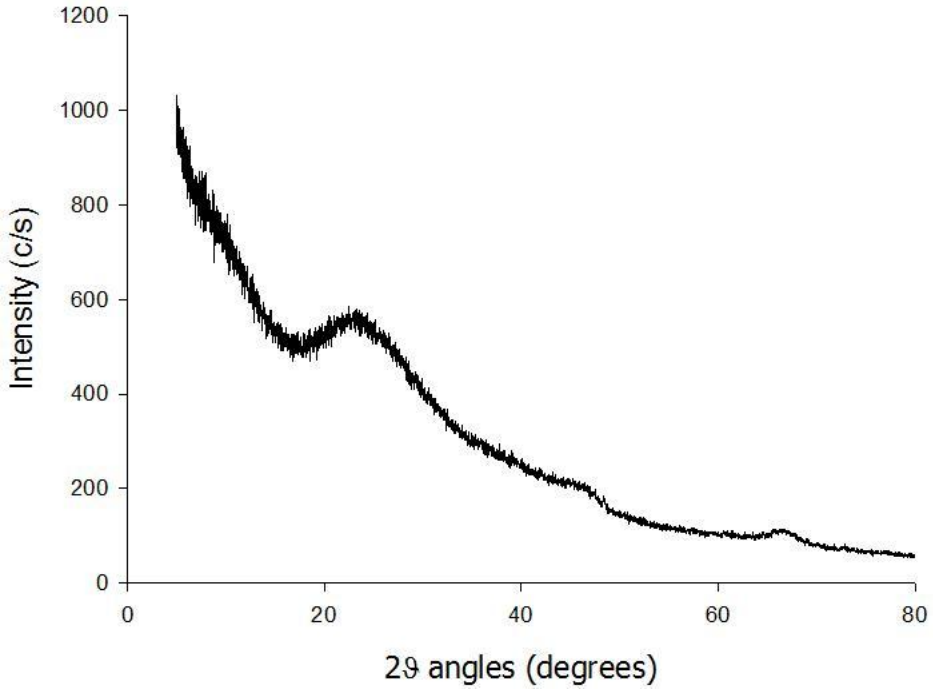

***Fig 6.6a**. XRD spectrum of adsorbed pure toluene and benzene onto extruded MSA.*

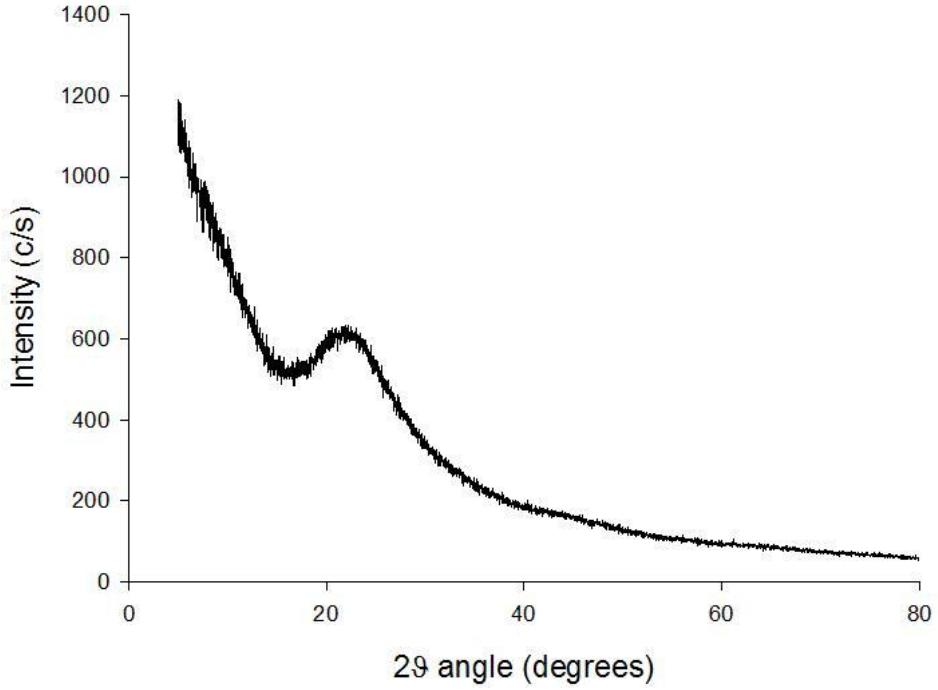

***Fig 6.6b**. XRD spectrum of adsorbed pure toluene and benzene onto particle MSA.*

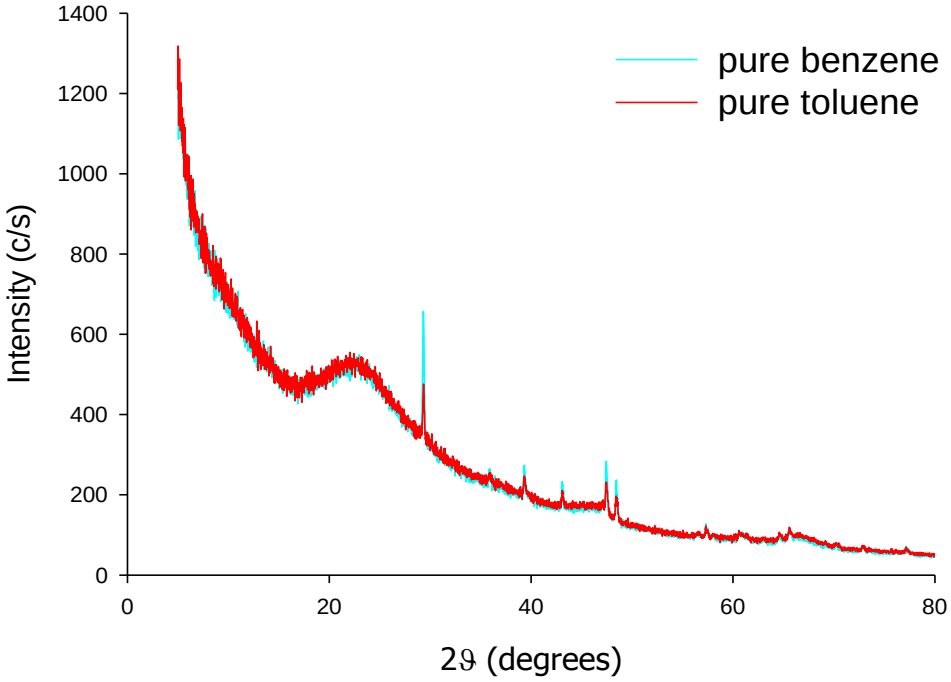

***Fig 6.7a**. XRD spectrum of adsorbed aqueous toluene and benzene onto extruded MSA.*

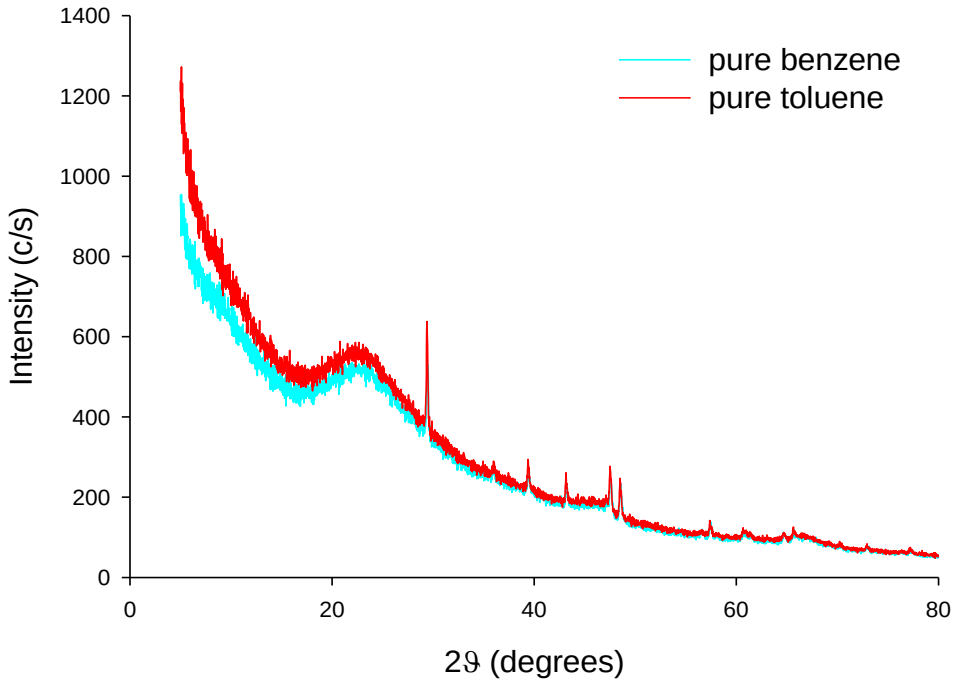

***Fig 6.7b**. XRD spectrum of adsorbed aqueous toluene and benzene onto particle MSA.*

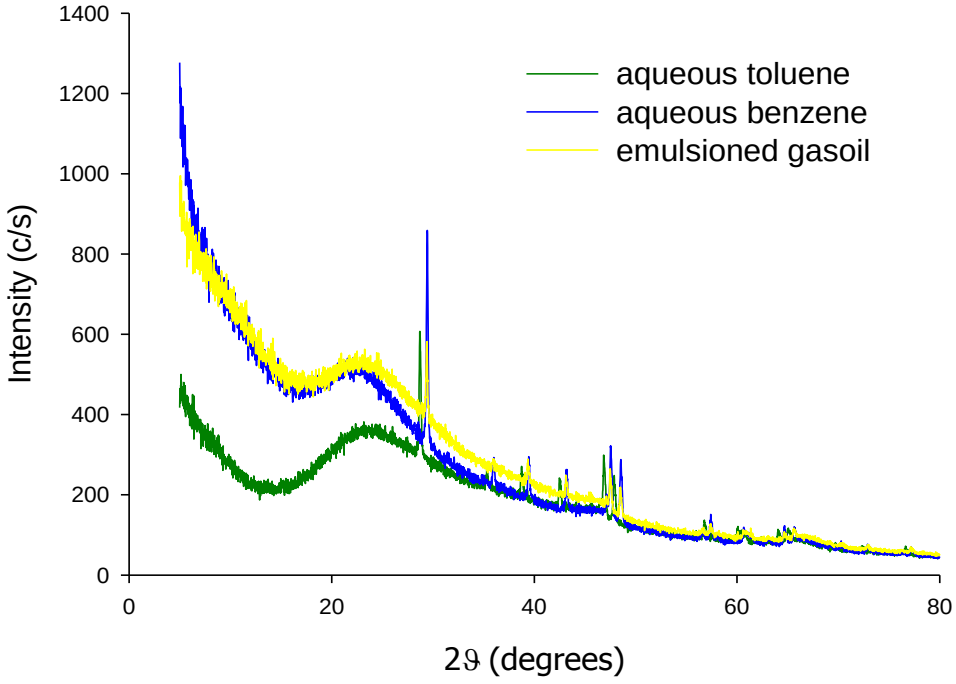

***Fig. 6.8a**. IR spectra of extruded MSA with water contaminants mixture.*

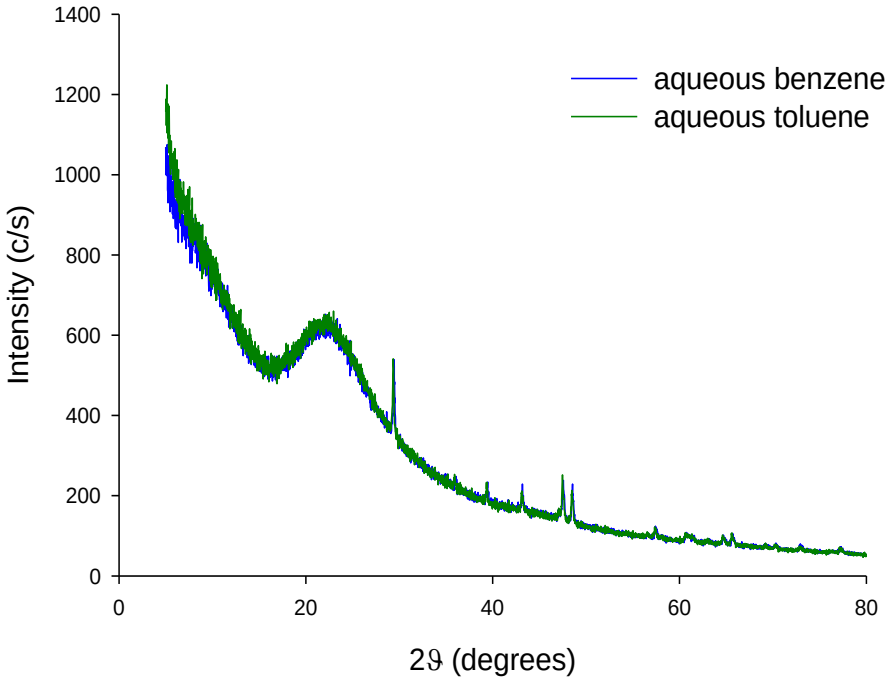

***Fig. 6.8b**. IR spectra of extruded MSA with pure contaminants.*

The image 6.6a shows the XRD spectrum of as-synthesized extruded MSA, while Fig. 6.6b shows the as-synthesized particle MSA. The absence of significant peaks and the presence of a very noisy background confirm the amorphous nature of this material in each of its shapes. Figures 6.7 a-b and 6.8 a-b report the same materials after the adsorption of aqueous and pure contaminants. The adsorption of benzene and toluene both pure and aqueous causes the appearance of some significant peaks. This means that the adsorption process brings the formation of an ordered structure able to diffract the X-rays. Nevertheless, the adsorption of benzene and toluene is not able to modify all the amorphous structure of the MSA into a crystalline one because the required energy to promote such a transformation is higher than the one involved in the adsorption

phenomena. Indeed, the spectrum background still remains noisy, indicative of the persistence of the amorphous phase of the MSA. At this point, we can consider two different hypotheses: benzene and toluene adsorb into the pores following an ordered arrangement or the adsorption of contaminants promotes the crystallization of some little domain of the amorphous phase of the MSA.

As for the first hypotheses, Tables 6.3 and 6.4 report the results obtained using the Le Bail profile matching software (FullProf®) to investigate the crystal system and parameters. After benzene and toluene adsorption, we always find a monoclinic crystal structure with the β angle value between 90° and 110°. By this regard, it is known that toluene and benzene crystallize with an orthorhombic structure in bulk conditions and a value of β close to 90°, as in our case, and that the monoclinic structure is very similar to the orthorhombic one. Thus, benzene and toluene could organize themselves in a distorted orthorhombic arrangement inside the pore channel of the MSA. However, they do not crystallize in the pore; indeed many works in the literature explain how molecules confined in pores and channels crystallize at lower temperatures than the bulk ones (Jackson and McKenna, 1990; Aksnes and Kimtys, 2004; Sliwinska-Bartkowiak et al., 2001). These previous studies investigated the crystallization of adsorbed molecules from the gas phase and not from liquid phase hence they do not elucidate what role the water plays during these phenomena. The hydrophobicity of organic molecules may represent a powerful driving force for the stacking of benzene and toluene into the pore using a monoclinic system. This system can be considered a distorted orthorhombic system, and it is maybe the only allowed one by the dimension of the pores and the most suitable to guarantee the minimum contact between water and aromatics in the mesoporous channels. In this way, the adsorbed and stacked aromatic

hydrocarbons act in the pores as a metastable phase able to reflect X-rays but not able to crystallize due to the confinement in the pores (Christenson, 2001).

	a (Å)	b (Å)	c (Å)	α (°)	β (°)	γ (°)	V (Å^3)	cell type
Aqueous toluene	5.2363	5.2905	4.7128	90.00	104.268	90.00	126.5293	P 2/m
Aqueous benzene	8.095	4.9894	3.1842	90.00	107.766	90.00	122.4	P 2/m
Pure toluene	4.704	10.2444	4.189	90.00	93.05	90.00	201.5791	P 2/m
Pure benzene	8.1033	2.4994	6.3778	90.00	107.74	90.00	123.0312	P 2/m
Emulsioned diesel fuel	7.6621	16.1359	4.205	90.00	110.459	90.00	487.0874	P 2/m

Table 6.3 *Crystal structure parameters of load extruded MSA.*

	a (Å)	b (Å)	c (Å)	α (°)	β (°)	γ (°)	V (Å^3)	cell type
Aqueous toluene	6.3721	7.6357	4.5685	90.00	107.887	90.00	211.5395	P 2/m
Aqueous benzene	5.1883	3.8239	4.3529	90.00	105.73	90.00	83.1242	P 2/m
Pure toluene	13.9934	6.1073	2.6036	90.00	108.804	90.00	210.6351	P 2/m
Pure benzene	8.0978	2.4938	6.3721	90.00	107.722	90.00	122.574	P 2/m

Table 6.4 *Crystal structure parameters of load Particle MSA.*

The second hypothesis is based on the assumption of the presence of some amorphous/crystalline metastable domains originated during the synthesis of the MSA. During the synthesis of mesoporous material, a large amount of template is used in order to create big surfactant clusters necessary for the formation of pores with the chosen dimension. Indeed, around it the silicon and oxygen atoms arrange to form the mesoporous structure. After this phase, the surfactant is eliminated by calcination.

However, it is possible that some template molecules did not take part to the clusters formation and around them silicon and oxygen atoms arranged to form the solid structure. In this case, the elimination of the template brings micropores. In addition to this, the reaction conditions of temperature, pressure, and contact time do not allow the direct formation of microporous crystalline structure, leaving metastable domains (Carati et al., 2003). In this sense, the adsorption of benzene and toluene could promote the transition of the metastable amorphous domain into microcrystalline ones. To experimentally investigate this hypotheses, additional XRD spectra were acquired and compared with the database of the International Centre for diffraction Data. A positive match with the diffraction peaks of Cristobalite, a polymorph of silica (Parise et al., 1994) was found thus supporting the possible transition from amorphous to microcrystalline phase of some MSA domain.

In order to investigate adsorption behavior in more realistic conditions, additional tests were performed with emulsioned diesel fuel and extruded MSA as adsorbent, being the material used in full scale application. Experimental results after the adsorption have shown appearance of the same diffraction peaks as observed in the previous single component toluene and benzene test. Diesel fuel is a complex mixture of aliphatic and aromatic hydrocarbons and, in the emulsified form, the interaction with MSA surface could happen through different mechanisms, such as adsorption of the different soluble components from the aqueous phase and possible uptake of the dispersed phase. Thus, the occurrence of these peaks is hardly interpreted on the basis of single components adsorption and arrangements into the MSA pores, and it seems more reasonably associated to structural changes that occur in the solid phase.

6.2.3 FT-IR

Figures 6.9 a-b show the comparison between the IR spectra of the extruded MSA before and after the adsorption of benzene and toluene in aqueous medium.

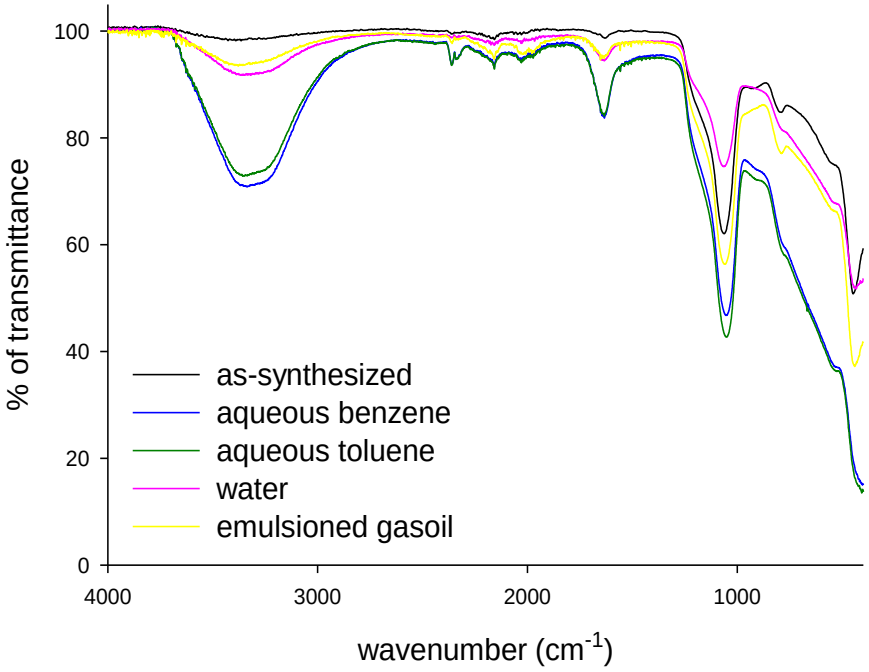

Fig. 6.9a*. IR spectra of extruded MSA with water contaminants mixture.*

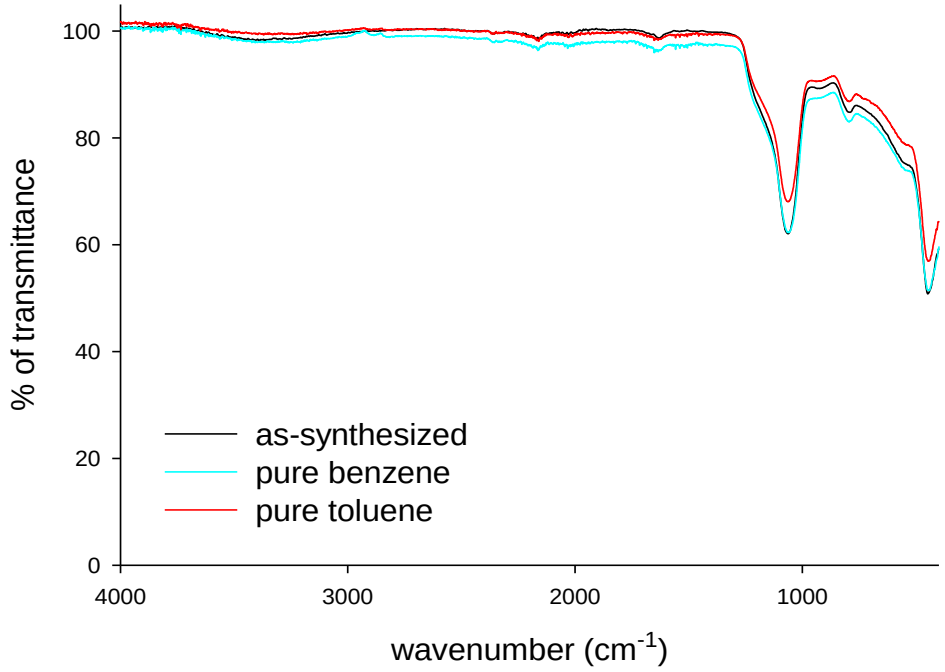

***Fig. 6.9b**. IR spectra of extruded MSA with pure contaminants.*

Regarding the spectra of the as-synthesized MSA (MSA without any kind of treatment), we can observe in the region between 4000-1300 cm^{-1} the absence of most relevant peaks. In this region, there are only very small and broad peaks: one at 3700-2875 cm^{-1} and one at 1630 cm^{-1}. The first mentioned peak is due to the –OH stretching of the few, free and isolated silanol groups present at the MSA surface and to the little amount of adsorbed atmospheric water. The same atmospheric water is responsible for the peak at 1630 cm^{-1} (Parida et al., 2006). It can also be noted a triplet of peaks very weak in intensity in the region between 2390-1960 cm^{-1}, but due to their low intensity, it is hard to distinguish them from the background noise. However, they are probably due to the stretching of the few Si-H bonds (Koropecki et al., 1991; Lucovsky, 1979). In the region

from 1300 to 400 cm^{-1}, the so-called finger print region, there is a strong peak at 1050 cm^{-1} and three weaker peaks at 920-910, 795 and 438 cm^{-1}. The stronger one is typical of the asymmetric Si-O-Si stretching bond in the SiO_4 tetrahedron, while the peak at 438 cm^{-1} is due to the rocking of Si-O bond (Parida et al., 2006). At 795 cm^{-1} we can observe the bending of the silanol group, while the IR absorption at 920-910 cm^{-1} is probably due to the stretching of the strained siloxane bridges (Inaki et al., 2002). This spectrum underlines the poor presence of silanol groups on the MSA surface confirming its hydrophobic nature. The same kind of IR spectrum was observed for the MSA held in contact with pure water; the only visible difference is the increase of the bending and stretching peaks of the silanol groups and hydrogen bond of the –OH groups. After the adsorption of aqueous benzene, aqueous toluene and the emulsioned diesel fuel, many changes occur. At first a very large and intense peak appears between 3700-2700 cm^{-1} typical of the -OH stretching of the adsorbed water molecule as well as the peak at 1630 cm^{-1} which increases in intensity due to a higher presence of water molecules after the adsorption. In the finger print region, we can observe an increasing in the absorption of the Si-O-Si asymmetric stretching in the case of aqueous contaminants but not in the case of pure water. This may be explained by considering the interaction between the hydrocarbon-water mixture and the siliceous surface of the MSA that could produce a major stretching of the Si-O-Si bond. The bending of silanol at 800 cm^{-1} seems to disappear in the spectrum of aqueous benzene, aqueous toluene and water while in the case of diesel fuel emulsion it remains much the same as the as-synthesized MSA one. This may be explained observing the IR spectra of extruded MSA with pure contaminants instead of the aqueous mixture in figure 6.9b. In these spectra, we can note that the peak at 800 cm^{-1} still remains the same. Apparently only the aqueous solution of contaminants and the pure water are able to modify the bending of silanol

groups; on the contrary, the pure contaminant and the diesel fuel are not able to do this. Hence it can be deduced that water molecules interact with the silanol group while the aromatic hydrocarbons adsorb onto the MSA using different adsorption sites. The hypothesis on the type of these second adsorption sites would involve the presence of the Lewis acid sites present on the mesoporous channel surface. These sites are characterized by point defection such as electron vacancies or empty orbitals (strong acid sites) and unbalanced charge as in the case of the strained siloxane bridge in which the asymmetry of the bridge can produce a partial positive charge delocalization on one Si atom (Inaki et al., 2002). The aromatic system, rich in electron lone pairs, is the better candidate to interact with Lewis acid sites in comparison to water molecules (in which there are only lone pairs on the oxygen atom). Therefore, it is quite possible that hydrocarbons are removed from water by means the Lewis acid sites. Perego et al. (1999) reported the synthesis and the acidity measurements of an MSA with a Si/Al ratio of 100. In this work, we used a MSA with a Si/Al ratio of infinity, but it is possible to note that already at Si/Al= 100 most of the acidic sites were the Lewis ones reinforcing the hypothesis of the contaminants adsorption through this kind of site. Performing the same acidity measurements of Perego et al. (1999) through the Pyridine adsorption followed by IR detection has confirmed our speculation about the presence of the Lewis and Brønsted sites on the MSA surface. The results are presented in Figure 6.10 in which the IR signal of the extruded MSA is superimposed on the particle MSA one and the wavenumber axes is restricted to 2000-1200 cm^{-1} range to better visualize the absorption peaks.

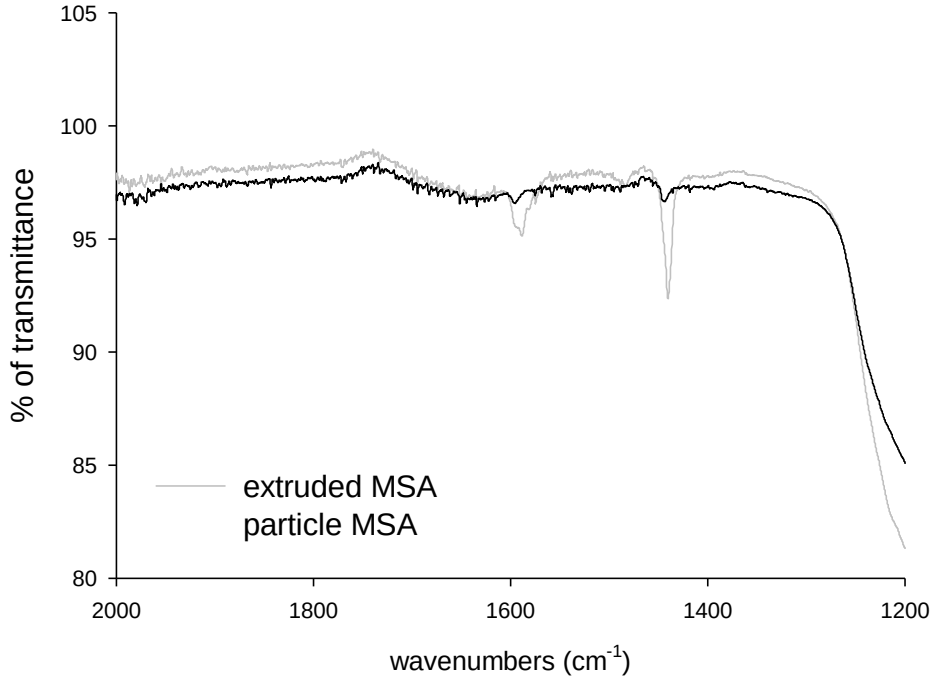

***Fig. 6.10**. IR spectra of particle MSA (grey) and extruded MSA (black) with Pyridine (2000-1200 cm^{-1} range).*

The well-known peak that appears at 1455 cm^{-1} ca is the peak absorption of pyridine adsorbed onto Lewis sites and at 1545 cm^{-1} the peak of pyridine onto Brønsted sites (Perego et al., 1999). In addition, the MSA the peak at 1455 cm^{-1} is higher than the one at 1545 cm^{-1} suggesting a wide abundance of the Lewis acid sites compared to the Brønsted ones.

Figures 6.11 a-b show the IR spectra of the particle MSA before and after the adsorption test with pure contaminants and their aqueous solutions.

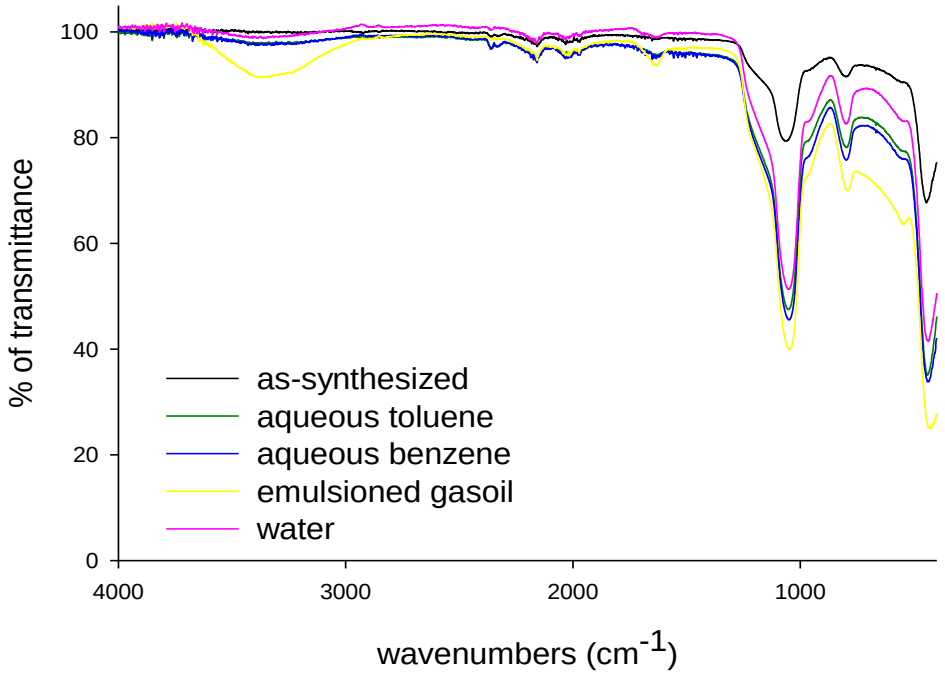

***Fig. 6.11a**. IR spectra of particle MSA with water contaminants mixture.*

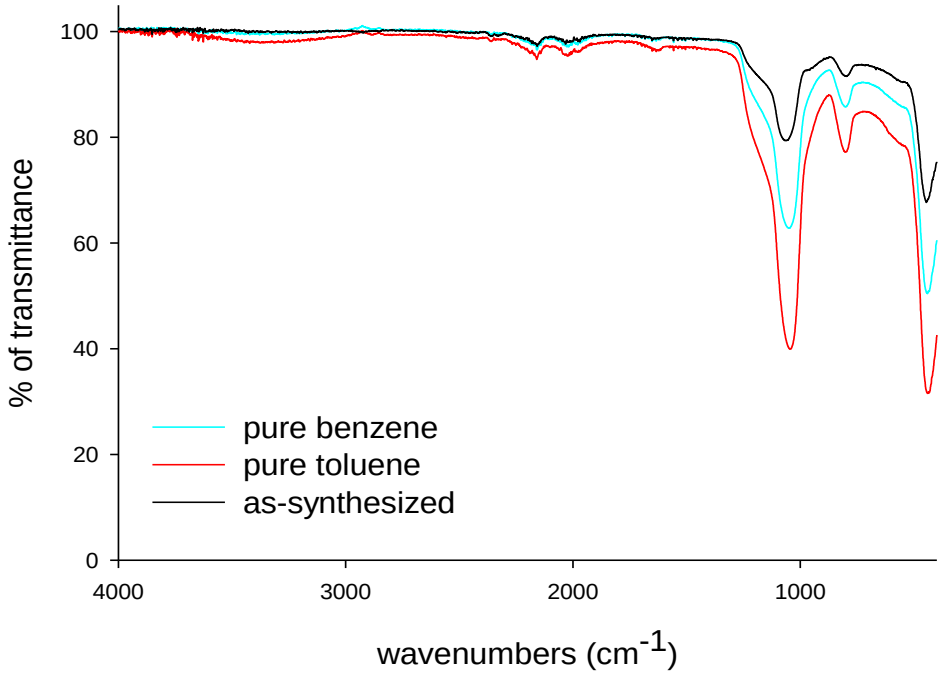

***Fig 6.11b**. IR spectra of particle MSA with pure contaminants.*

It is possible to distinguish the same peaks observed in the extruded MSA. The most important difference is in the finger print region during the adsorption of the aqueous contaminants. The process of extrusion with Al_2O_3 binder may have modified the structure of the tetrahedral silicon ring. In addition, the higher peak intensity corresponding to the silanol and water wavenumbers suggests a major interaction of the extruded MSA in comparison to the particle MSA, probably due to the hydrophilic binder contained in the former. The particle MSA spectra with pure contaminants do not show any new absorption peaks after the adsorption confirming the poor interaction between pure hydrocarbons and silanol groups. Also, particle MSA acidity measurements were performed highlighting the same two peaks at 1545 and 1455 cm^{-1} ca typical of Brønsted and Lewis acid sites, respectively. The intensity of these peaks was less strong than the extruded MSA one, suggesting an increase of the number of acid sites maybe due to the presence of Al_2O_3 (binder) in the solid matrix. (Figure 6.10).

6.2.4 TGA

Figures 6.12a and 6.12b show the TGA analysis of the particle MSA and extruded MSA both with aqueous and pure contaminants. A test using emulsioned diesel fuel was carried out on extruded MSA to study its thermal behavior in an application very similar to a real one. A comparison of the weight loss of the two types of MSA between pure and aqueous aromatics displays the important role of water. Indeed, water is the most retained compounds and represents above a third of the total weight loss of both the materials. In addition, the extruded MSA seems to capture a major amount of

compounds and water, suggesting a possible role of the Al_2O_3 binder in the retention of water molecules and contaminants. However, emulsioned diesel fuel in the extruded MSA shows higher weight loss probably linked to the presence of several different compounds adsorbed onto the MSA besides water molecules. Figures 6.13a and 6.13b report the derivative form of the TGA weigh loss graphs. These graphs are really helpful for visualizing the temperature at which there is the maximum loss of the compounds (T_{max}). The knowledge of the T_{max} is very important to understand and fix the optimal regeneration temperature in the application field.

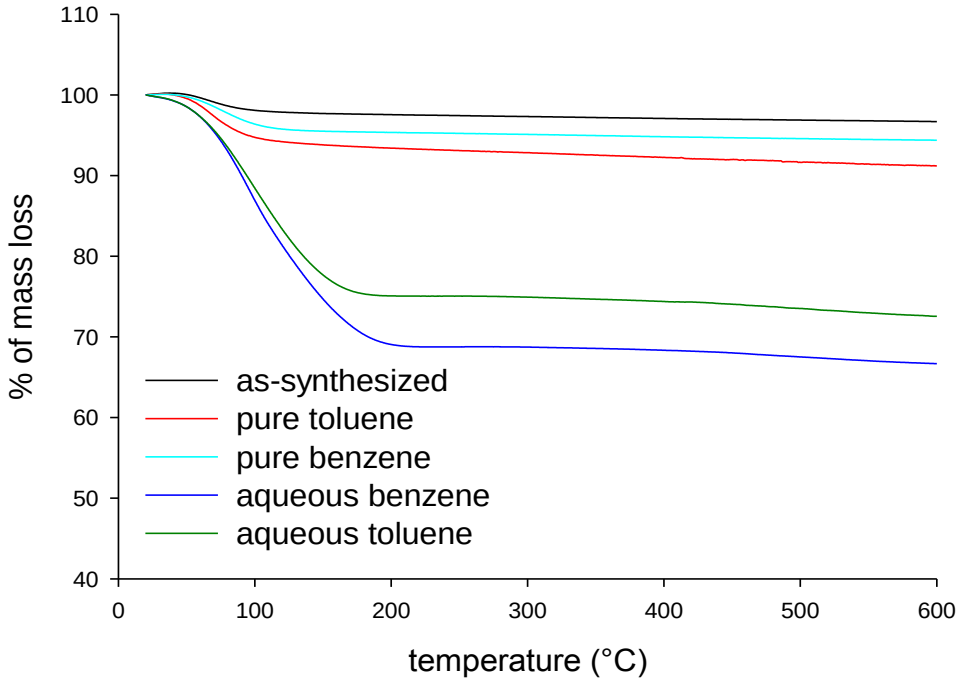

***Fig 6.12a**. Particle MSA TGA weight loss.*

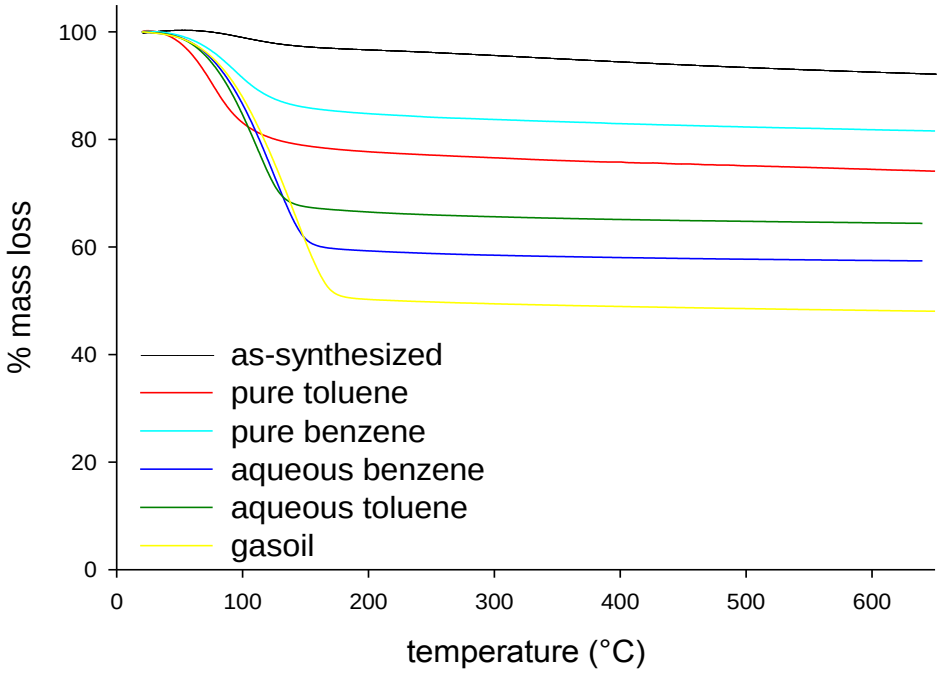

***Fig. 6.12b**. Extruded MSA TGA weight loss.*

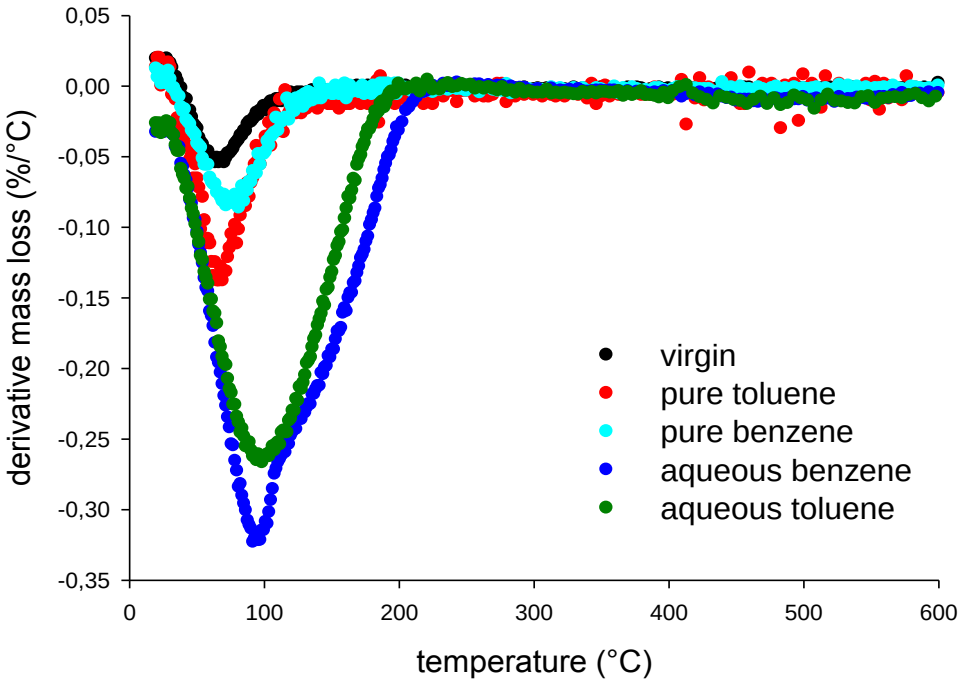

***Fig. 6.13a**. Particle MSA TGA derivative weight loss.*

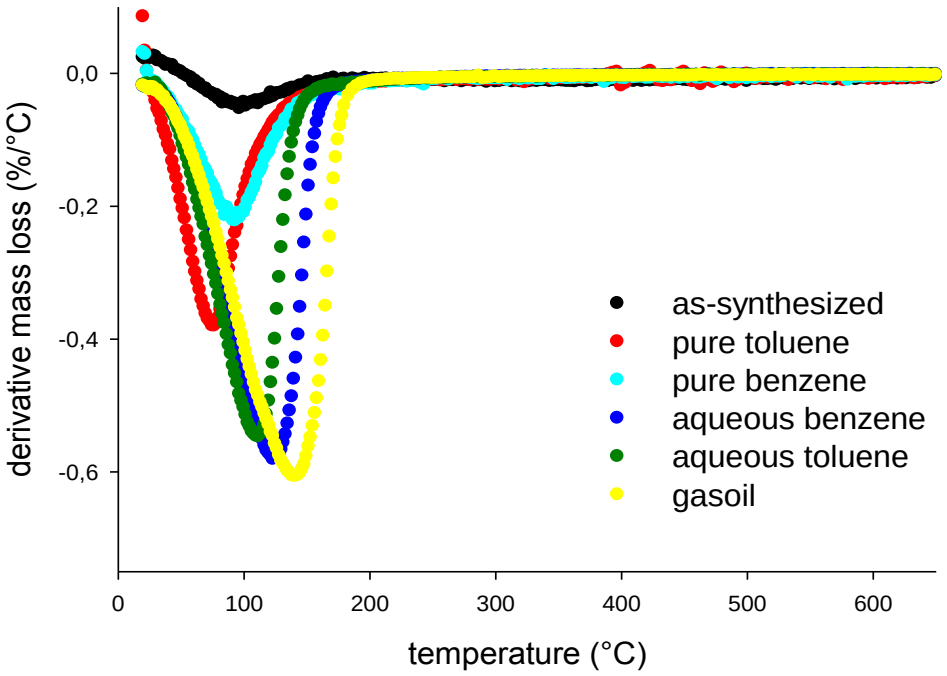

***Fig. 6.13b**. Extruded MSA TGA derivative weight loss.*

In table 6 the values of T_{max} are inserted for each contaminant and material. Observing these values, the role of water and alumina can be noted again in the release temperature of contaminants in all of their chemical forms. There is an increase of the T_{max} values replacing particle MSA with the extruded MSA, and especially for the aqueous contaminants that shows an increase above 20 °C. This suggests an increase in the number of the adsorption sites able to retain water molecules, such as the silanol groups due to the use of alumina as extruding binder.

	Particle MSA T_{max} (°C)	Extruded MSA T_{max} (°C)
Virgin	64	96
Pure toluene	71	76
Pure benzene	78	93
Aqueous benzene	108	128
Aqueous toluene	103	131
Gasoil	-	141

Table 6.5 T_{max} values of contaminants desorption from particle and extruded MSA

The diesel fuel test with extruded MSA shows the highest T_{max} value attributable to the presence of light and heavy hydrocarbons in the diesel fuel less ready to desorb than benzene and toluene.

6.3 Conclusions

The adsorption mechanisms of targeted aromatic hydrocarbons onto MSA were investigated by the combination of different techniques (SEM, XRS, FTIR, TGA). Experimental results were used to discriminate water interaction at the MSA surface and hydrocarbon adsorption. Water molecules seem to adsorb on the MSA surface interacting with silanol groups through hydrogen bonds whereas aromatic hydrocarbons coordinate with the mesoporous surface through the interaction with electron poor

Lewis acid sites. Acidity measurements by Pyridine adsorption confirmed the presence of the Lewis acid sites strengthening our hypothesis. Water is also responsible for the increase in temperatures at which there is the maximum desorption as displayed by the TGA measurements. XRD analysis allowed us to suppose the ability of adsorbed benzene and toluene to organize themselves in a very ordinate structure identified as a monoclinic crystal structure and able to diffract X-rays or, perhaps more realistically, a partial crystallization of silica induced by the adsorbed molecules. Finally, the comparison between the extruded and as-synthesized MSA (particle MSA) highlighted the role of the Al_2O_3 binder. The use of this hydrophilic binder increased the adsorption of water on the MSA due to an increase of the available silanol groups; however, it does not seem to affect the adsorption of the benzene and toluene or produce modifications during the adsorption step.

6.4 References

Aksnes and L. Kimtys, Solid State Nuclear Magnetic Resonance 25 (2004) 146–152.

Bellussi, C. Perego, A. Carati, S. Peratello, E. Previde Massara, G. Perego. Stud. Surf. Sci. Catal. 84 (1994) 85.

Bellussi, C. Perego, S. Peratello, 1993, US Pat. 5342814.

Carati, G. Ferraris, M. Guidotti, G. Moretti, R. Psaro, C. Rizzo, Catal. Today 77 (2003) 315-323

Christenson, J. Phys.: Condens. Matter 13 (2001) 95-133

Flego, I. Kiricsi, C. Perego, G. Bellussi, Catal. Lett. 35 (1995) 125.

Inaki, H. Yoshida,, T. Yoshida, T. Hattori, J. Phys. Chem. B 106 (2002) 9098-9106

Jackson and G.B McKenna, J. Chem. Phys. 93 (1990) 9002-9011

Koropecki, F. Alvarez, R. Arce, J. Appl. Phys. 69 (1991) 7805- 7811

Lucovsky, Solid State Commun, 29 (1979) 571-576.

Parida, S. Dash, S. Patel, B.K. Mishra, Adv. Colloid Interface Sci. 121 (2006) 77-110

Parise, A. Yeganeh-Haeri, D. J. Weidner, J. D. Jorgensen and M. A. Saltzberg J.Appl. Phys. 75 (1994) 1361.

Perego, S. Amarilli, A. Carati, C. Flego, G. Pazzuconi, C. Rizzo, G. Bellussi Microporous Mesoporous Mater. 27 (1999) 345–354

Sliwinska-Bartkowiak G. Dudziak , R. Gras,R.Sikorski , R. Radhakrishnan, K. E. Gubbins, Coll. and Surf. A 187 (2001) 523–529.

CHAPTER 7

CONCLUSIONS AND FINAL EVALUATIONS

This work represent an attempt to develop a new adsorbent material for water remediation and purification able to compete against the existing material such as active carbon or polymeric resins. The MSA is this new material and it was thought as multitalented material for removal of heavy metals and hydrocarbons from water. Under this point of view the adsorption of Pb, Ni and Cd onto clinoptilolite and a commercial resin, Purolite® S910, is investigated. These materials were used as reference material to test the capability of the MSA for heavy removal. From the comparison between the adsorption performances of reference materials and those of MSA is clear how this last has to be improved for heavy metals uptake. Clinoptilolite and Purolite S910 are more selective and powerful adsorbent for Pb, Ni and Cd removal. The functionalization of MSA internal surface with specific ligands such as alkyl chains ending with thiol, hydroxyl or amino group may represent a good solution for improving MSA performances. Regarding hydrocarbons removal the same approach was followed. A set of reference material was tested to compare their adsorption performances to those of the MSA. The new material has shown high adsorption ability in toluene removal from water comparable and in some cases stronger than those of reference materials. The extruded MSA for example is able to bring down the toluene concentration up to 50% of its initial concentration. Nevertheless after toluene adsorption the free pore volume is still significant (as for the other mesoporous

materials) and allows the adsorption of further contaminants. Considering the application of this material to real contaminated water the availability of this big empty space can use to host oil drops and emulsion removing them from water. In this sense MSA can be seen as a sponge that absorb dispersed oil and adsorb dissolved hydrocarbons without causing the pore clogging. Mesoporous material might be used in series with other adsorbent materials. The idea is to set firstly the MSA, for removing the oil drops and the most of contaminants, followed by others adsorbents for polishing the output water. Regeneration study has shown how the MSA is easily regenerable. Between 80 °C and 100 °C all the adsorbed toluene is removed and the MSA showed the same adsorption performances than before. In addition to the kinetic and thermodynamic investigations a structural study about the MSA modifications after hydrocarbons adsorption and the interaction between them and the MSA was carried out. By this study the importance of the dehydroxylation of the MSA surface was highlighted. More dehydroxylated is the material surface more efficient is the uptake of hydrocarbons. A very dehydroylated surface is also very hydrophobic suggesting that hydrophobization brings to improvements of the adsorption performances.